DIAGNOSING HUMAN CONTROL SYSTEM CAPABILITY UTILIZING BANDWIDTH

A thesis presented to the faculty of the Graduate School of

Western Carolina University in partial fulfillment of the

requirements for the degree of Master of Science in Technology

By

Shahab Karimi

Advisor: Dr. Martin L. Tanaka

Department of Engineering & Technology

Committee Members: Dr. Sudhir Kaul, Engineering & Technology
Dr. Paul M. Yanik, Engineering & Technology

April 2016

©2016 by Shahab Karimi

To those strong individuals who smile while

struggling against their physical disability

ACKNOWLEDGEMENTS

I would like to give special thanks to my thesis director, Dr. Martin L. Tanaka, whose guidance and support made all my research possible. I am really grateful that he introduced this fantastic and new topic to me, so that I can have this valuable opportunity to work on it. I gained lots of valueable experiences while working with Dr. Tanaka. His passion for research has always been an encouragement for me, and he's been always willing to support me. I learned a lot in the courses I had with him and also from his valueable advices in our discussions.

I truly appreciate Dr. Norman Peter Reeves for his precious supports in this project. Without Dr. Reeves, this research would not be possible. His idea about using bandwidth to assess human neuromuscular system performance formed the foundation of this thesis project. Moreover, the entire experiments and data collection were performed by Dr. Reeves and his colleagues at Michigan State University. Without those experimental data, the results of this study could not have been realized. In addition, his advice during different steps of this project increaseed my knowledge in application of control and dynamics to the study of human dynamics.

My thanks also go to my committee members, Dr. Sudhir Kaul and Dr. Paul Yanik. I learned lots of useful and beneficial techniques and information about mathematical modeling, dynamics and vibration, classical control and application of linear algebra in the optimization. Without assistance from them, this research would have taken a lot of time. They helped me to have a better understanding of every step of this research.

Finally, I would like to thank my friends and my family members for their endless support.

TABLE OF CONTENTS

LIST OF TABLES vi
LIST OF FIGURES vii
ABSTRACT ix
CHAPTER 1 : INTRODUCTION 1
CHAPTER 2 : LITERATURE REVIEW 3
2.1 Biomechanics, mathematical modeling and optimization 3
2.2 Neuromuscular system and torso movement 7
2.3 Bandwidth and human motor control 10
CHAPTER 3 : METHODS 13
3.1. Movement Tracking Experiment 14
3.2 Mathematical Modeling 20
3.3 Simulation and parameter estimation 25
3.3.1 Mathematical procedure 26
3.3.2 Programming in MATLAB 31
3.4 Analysis and Validation 34
3.4.1 Pre-processing analysis 34
3.4.2 Post-processing validation 39
3.5 Bandwidth and other characteristics of the system 41
3.5.1 Bandwidth calculation technique 41
3.5.2 Other characterstics of models 45
CHAPTER 4 : RESULTS AND DISCUSSION 47
4.1 Experimental results 47
4.2 Parameter estimation results 50
4.2.1 Moment of inertia 50
4.2.2 Effective mass 54
4.2.3 Effective length 58
4.2.4 Delay 61
4.2.5 Stiffness coefficient 66
4.2.6 Damping coefficient 69
4.2.7 Proportional gain 72
4.3 Simulation results 76
4.4 Bandwidth 86
CHAPTER 5 : CONCLUSION 94
Bibliography 98
Appendices 101
Appendix A: Average and standard deviation plot of estimated parameters for each subject's response to different targets (horizontal axis represents the target) 101
1) Moment of inertia 101
2) Rotating mass 102
3) Effective length 104
4) Delay 105
5) Stiffness coefficient 106

6) Damping coefficient 108
7) Proportional gain 109
Appendix B: Average and standard deviation plot of estimated parameters for all of subjects' responses to each target 111
1) Moment of inertia 111
2) Rotating mass 112
3) Effective length 113
4) Delay 114
5) Stiffness coefficient 115
6) Damping coefficient 116
7) Proportional gain 117
Appendix C: Average and standard deviation plot of estimated parameters for all of subjects' responses to each target 118
1) Percentage of overshoot 118
2) Settling time 119
Appendix D: Average and standard deviation values of bandwdith of each subject's response to different targets 120
Appendix E: Mathematical model of responses of subjects 1 and 2 to different targets 121
Appendix F: One series of experimental and modeled response of each subject to different targets 123
Appendix G: MATLAB codes 125

LIST OF TABLES

Table 3.1: The basic information of test subjects 14
Table 3.2: Properties of step functions (input signals) 17
Table 3.3: Identification code for classification of individual step responses 35
Table 3.4: Constraints for *m* , *l* and *i* 39
Table 3.5 : Detail of *"fit percentage"* outputs 41
Table 4.1: Mean of estimated values for parameter *i* (standard deviations in the parenthesis) 51
Table 4.2: Mean of estimated values for parameter *m* (standard deviations in the parenthesis) .. 58
Table 4.3: Mean of estimated values for parameter *l* (standard deviations in the parenthesis) 61
Table 4.4: Mean of estimated values for parameter τ (standard deviations in the parenthesis).... 66
Table 4.5: Mean of estimated values for parameter *k* (standard deviations in the parenthesis) ... 69
Table 4.6: Mean of estimated values for parameter *b* (standard deviations in the parenthesis) ... 72
Table 4.7: Mean of estimated values for parameter *g* (standard deviations in the parenthesis) ... 76
Table 4.8: Mean of percentage of overshoot (standard deviations in the parenthesis)..... 83
Table 4.9: Mean of settling time (standard deviations in the parenthesis) 86
Table 4.10: Mean value of bandwidth frequency (standard deviations in the parenthesis)..... 90

LIST OF FIGURES

Figure 2.1 Borelli's first pictures of human's dynamic 3
Figure 2.2 Winter's schematic physical model by using inverted pendulum 5
Figure 2.3 Different orders of polynomials fitting a series of experimental data 6
Figure 2.4 Huston's proposed physical model for human body 7
Figure 2.5 Tanaka's proposed model for human torso's dynamics 8
Figure 2.6 Davidson's free body diagram of the human model 9
Figure 2.7 Proposed block diagram of the assessed system in davidson's study 10
Figure 3.1 Used set-up for the experimental part of the project 16
Figure 3.2 Human's flexion and extension 16
Figure 3.3 Step function and the returning after that 18
Figure 3.4 Two designed input signals for experiment 19
Figure 3.5 Different responses and corresponded input signals for one subject 20
Figure 3.6 Proposed block diagram in simulink 22
Figure 3.7 Trust-Region-Reflective algorithm procedure 29
Figure 3.8 Group of 40 responses to the input signal of -2 for the subject 1 32
Figure 3.9 Problem in convergence for short period trials 36
Figure 3.10 Model and observed data after convergence 37
Figure 3.11 Model and obsevred data with %fit 40
Figure 3.12 Bode plot and determination of bandwidth 44
Figure 3.13 Step response and characteristics of system 46
Figure 4.1 Each individual response of subject 1 to different targets 48
Figure 4.2 All of the responses of subject 1 to different targets 49
Figure 4.3 Estimation of parameter "i" for subjects 1 and 2 52
Figure 4.4 Estimated values of parameter "i" for different subjects responses to ±2 deg 53
Figure 4.5 Estimation of parameter "m" for subjects 1 and 2 55
Figure 4.6 Estimated values of parameter "m" for different subjects responses to ±4 deg 56
Figure 4.7 Estimated values of parameter "m" for different subjects responses to ±2 deg 57
Figure 4.8 Estimation of parameter "l" for subjects 1 and 2 59
Figure 4.9 Estimated values of parameter "l" for different subjects responses to ±6 deg 60
Figure 4.10 Estimation of time delay for subjects 1 and 2 63
Figure 4.11 Estimated values of time delay for different subjects responses to ±2 deg 64
Figure 4.12 Estimated values of time delay for different subjects responses to ±4 deg 65
Figure 4.13 Estimation of parameter "k" for subjects 1 and 2 67
Figure 4.14 Estimated values of parameter "k" for different subjects responses to ±2 deg 68
Figure 4.15 Estimation of parameter "b" for subjects 1 and 2 70
Figure 4.16 Estimated values of parameter "b" for different subjects responses to ±2 deg 71
Figure 4.17 Estimation of parameter "g" for subjects 1 and 2 73
Figure 4.18 Estimated values of parameter "g" for different subjects responses to ±2 deg 74
Figure 4.19 Estimated values of parameter "g" for different subjects responses to ±6 deg 75
Figure 4.20 Simulated and observed responses of subject 1 and 2 77
Figure 4.21 Simulated and observed responses of subject 3 and 4 78
Figure 4.22 Simulated responses of subjects 1 and 2 80
Figure 4.23 Percentage of overshoot in responses of subjects 1 and 2 82
Figure 4.24 Settling time in responses of subjects to ±2 deg 84

Figure 4.25 Settling time in responses of subjects to ±6 deg..... 85
Figure 4.26 Bandwidth of responses of subjects to ±2 deg 87
Figure 4.27 Bandwidth of responses of subjects to ±4 deg 88
Figure 4.28 Bandwidth of responses of subjects to ±6 deg 89
Figure 4.29 Bandwidth in responses of subjects 1 and 2..... 92
Figure 4.30 Bandwidth in responses of subjects 3 and 4..... 93

ABSTRACT

DIAGNOSING HUMAN CONTROL SYSTEM CAPABILITY BY APPLICATION OF BANDWIDTH CONCEPT

Shahab Karimi, M.S.T.

Western Carolina University (April 2016)

Director: Dr. Martin L. Tanaka

The methods used to quantify bandwidth for a simple engineering system are well established. However, the application of bandwidth to complex systems like human's motor control is more challenging. Conceptually, bandwidth is a measure of how capable a system is to respond to a command and stabilize in a shorter time and with less fluctuations. The goal of this research is to develop new diagnostic methods that can be used by medical professionals to assess the degree of neuromuscular disease and evaluate the effectiveness of treatment. In this study, ten healthy subjects performed twenty tasks, involving tracking trunk angular position in the sagittal plane. Trials consist of a one-dimensional input signal displayed on a screen. Subjects moved their torso to track the target as it moved. Responses were recorded and MATLAB was used to model and simulate each response. Mathematical modeling utilized a nonlinear least squares method to fit the model to experimental data. The optomized model parameters were validated after data fitting. Models were transformed to frequency domain by using Fourier transforms. The bandwidth of the human neuromuscular system controlling trunk motion in sagittal plane was found to be in the range of 0.35 to 0.85 Hz. Bandwidth may be used as a measurable variable to quantify neuromuscular controller capability.

CHAPTER 1 : INTRODUCTION

The methods used to quantify bandwidth for a simple engineering system are well established [1], [2]. However, the application of bandwidth to complex systems like human motor control is more challenging. A simple explanation is that controllers with higher bandwidth are able to respond to the commands more quickly and with less fluctuation. A mathematical definition of bandwidth in signal processing is the range of frequencies over which the magnitude response of the transfer function drops by 3 dB. This drop in amplitude corresponded to a 50% decrease in power [36]. Many different factors influence the human neuromuscular control system, and its response to input commands. Some of these factors include age, physical condition, neurological condition, external environment and body mass distribution [3]. The human neuromuscular control system is even more complicated, because it may also have different responses to the same input signal [4]. Due to the large number of influencing factors and since they are inherently coupled with the system, a large amount of experimental data is needed to understand the influence of each factor on bandwidth.

In order to understand the complexity of human motor control, some researchers have used mathematical models to study the dynamics and statics of the torso [5], [6]. Typically, input commands are presented to the system and the motor control moves the body to track these movement commands. In nonlinear dynamical control systems, the mathematical model is more complex and has higher order [7]. Accordingly, data fitting and optimization procedure for estimation of model parameters take more effort. However, it is essential to have an accurate model for the system in order to determine the bandwidth of the system.

The error between the result from mathematical the model of the system and experimental data is desired to be zero. Thus, the parameters of the nonlinear mathematical model are estimated such that they minimize the error between the model result and experimental data. Although many different data fitting methods have been proposed, focus of this research was on Least Squares method. "Nonlinear least squares" is one of the methods that results in an accurate model. The parameters estimated by this method fit the nonlinear model to the experimental data with a high precision [8].

Modeling and simulation of complex systems like the dynamics and motor control of human takes a massive amount of time. Here, computational methods can be used efficiently. Computational programming can help to increase the speed of the optimization process by using the computational devices [9]. Moreover, simulation of complex systems could be performed by computational methods [10]. MATLAB is one of the most useful tools in modeling, optimization and simulation of complex linear and nonlinear systems. In this study, all of the simulation and parameter estimation processes on the mathematical model have been performed by using MATLAB.

The ultimate goal of this research is to develop new diagnostic methods that can be used by medical professionals to assess the degree of neuromuscular disease and evaluate the effectiveness of treatment. In this research, methods were developed to calculate the bandwidth of the neuromuscular control system, which may be used as a measurable parameter to quantify neuromuscular controller capability.

CHAPTER 2 : LITERATURE REVIEW

2.1 Biomechanics, mathematical modeling and optimization

A brief and clear definition of biomechanics is the application of mechanics principles to study of the function and structures of biological systems such as humans, animals, cells, etc. [11]. The first study in biomechanics was performed by Aristotle and focused on the study of animal movements [12]. After him, there were many other pioneers in this field of science. Da Vinci studied force interaction between muscle and skeletal system [13], Galilei studied the structure of bone which is believed to be the first understanding in biological optimization [13], and Borelli studied the musculoskeletal system of human's [14]. Figure 2. 1 depicts the first figures that Aristotle made to describe the human body's dynamics.

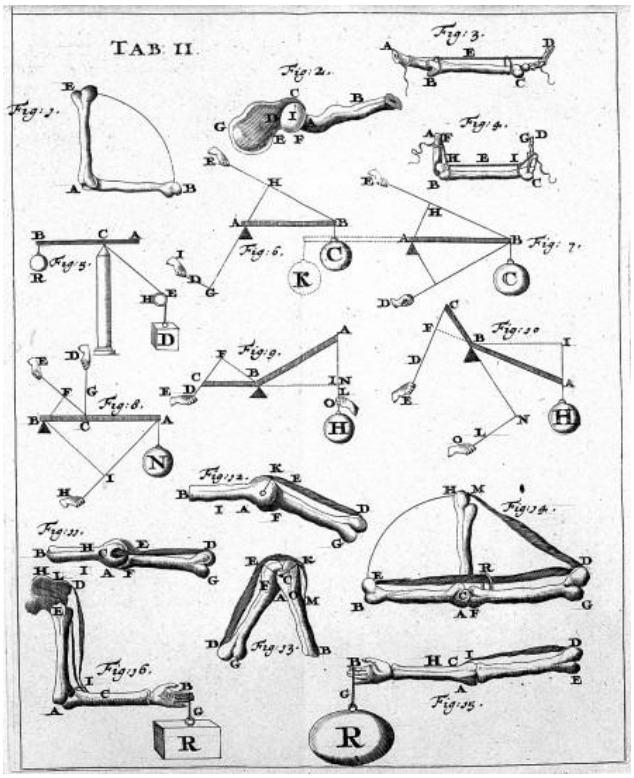

Figure 2.1 Borelli's first pictures of human's dynamic

One of the major subfields of biomechanics is the study of the human body motion. In this subfield, quantitative based methods are applied for the analysis of different human motions [15].

Using dynamics and physics rules of dynamical systems is one of the most helpful tools in the study of human movement. Almost all of the studies in this field have been done by using existing rules in physics of motion and dynamics such as Newton's second law and its results [16]. Mathematical equations are the tools by which the dynamics and physics of motion are represented. The mathematical model is an illustration of a system or phenomena by mathematical concepts [17]. Therefore, the dynamic of human movement can be modeled by a mathematical model based on physical rules.

A broad variety of studies have been conducted on different types of human body movement such as gait, torso movement, lumbar motion, jumping, diving, sport exercises, etc. In 1964, Hanavan presented a mathematical model of the human body [18]. In 1989, Barin found and evaluated a generalized model of human postural dynamics and control in sagittal plane [19]. In 1995, Winter used the mathematical model of an inverted pendulum to model the human balance and posture control [20]. In most of the cases, the dynamic of the human body was modeled to a simple mechanical/physical system, which consisted of one or more lumped mass, to represent the moving part of the body, with bars or rods between them as connectors. Figure 2.2 shows the schematic of an inverted pendulum model that Winter proposed for standing. Mathematical and differential equations were generated for the system. Using mathematical optimization, the model was modified to have the best fir with the experimental data.

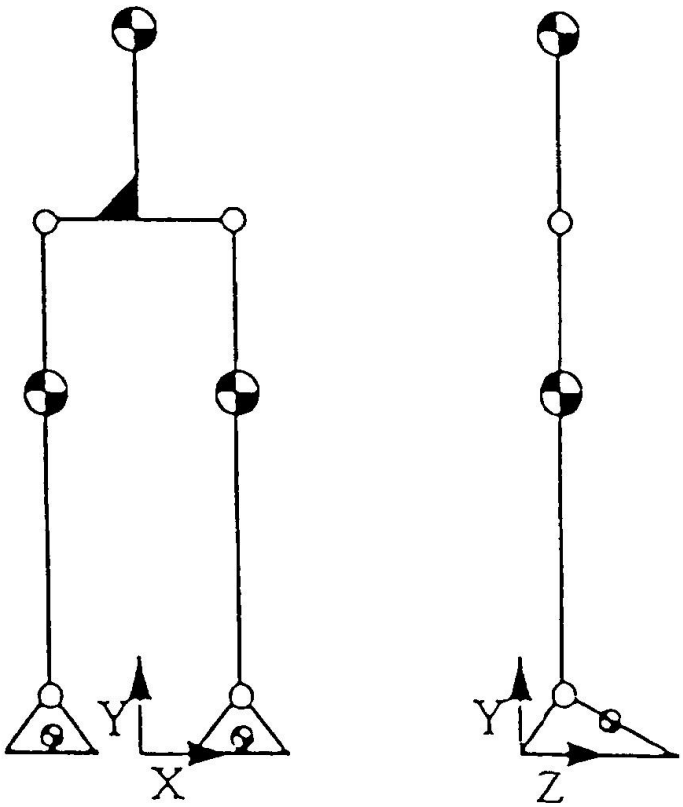

Figure 2.2 Winter's schematic physical model by using inverted pendulum

Any mathematical model that describes the behavior of a dynamical system is supposed to be accurate. That means, its results must fit the experimental data of the system. In other words, the error between the data from the corresponded experiments and the data from the mathematical model should be minimized. In 1982, Vaughan et al. did an mathematical optimization to estimate the human body's segment parameters [21]. They applied an optimization method on kinematic data to identify the mechanical properties of a body segment. In 1990, Zajac et al. did a comprehensive study on mathematical modeling and parameter estimation of the musculoskeletal movement system [22]. They modeled human dynamics mathematically. The mathematical model had different parameters. Each parameter described a specific effect of a different segment of the human body. By utilizing mathematical optimization methods, they tried to minimize the error between mathematical model output and experimental data.

Many different methods have been found for mathematical optimization and parameter estimation. Then "least squares" method of optimization was invented by Gauss in 1806 [23]. This method is used for overdetermined systems of equations. Overdetermined systems contain more equations than the unknowns [24]. In least squares method the overall solution for the system of equations minimizes the sum of the squares of errors between observed data and modeled data [25]. Least Squares' most important application is data fitting or curve fitting [26]. "Nonlinear least squares" method is one of subsets of least squares that have been used in many parameter estimation and optimization research projects. This method is a form of least squares that is used to fit a group of experimental data (observations) with a nonlinear mathematical model that contains a set of parameters [27]. Figure 2. 3 depicts different orders of polynomials (colored lines) fitting a series of experimental data (black dots) [28].

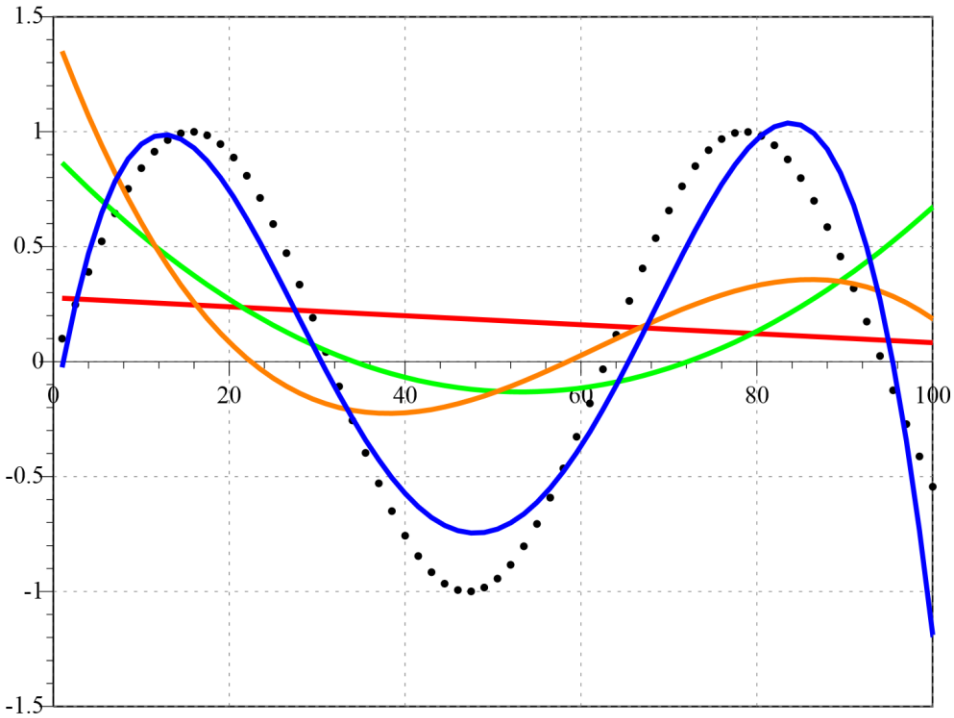

Figure 2.3 Different orders of polynomials fitting a series of experimental data

2.2 Neuromuscular system and torso movement

One of the major motions hapenning in the human body is rotation of the entire upper body in main anatomical planes. The human neural system is the motor controller for motions in the human body [29]. Many researchers have investigated the dynamics of the upper body and torso in humans and its association with the neuromuscular system.

In 1976, Huston et al. studied the dynamics of human body in a full scale. They presented a physical model of human body by ellipsoids, elliptical cylinders and frustrums of elliptical cones [30]. They also analyzed the dynamics of torso and presented a general equation for its motion. Figure 2. 4 shows the physical model they proposed for human body.

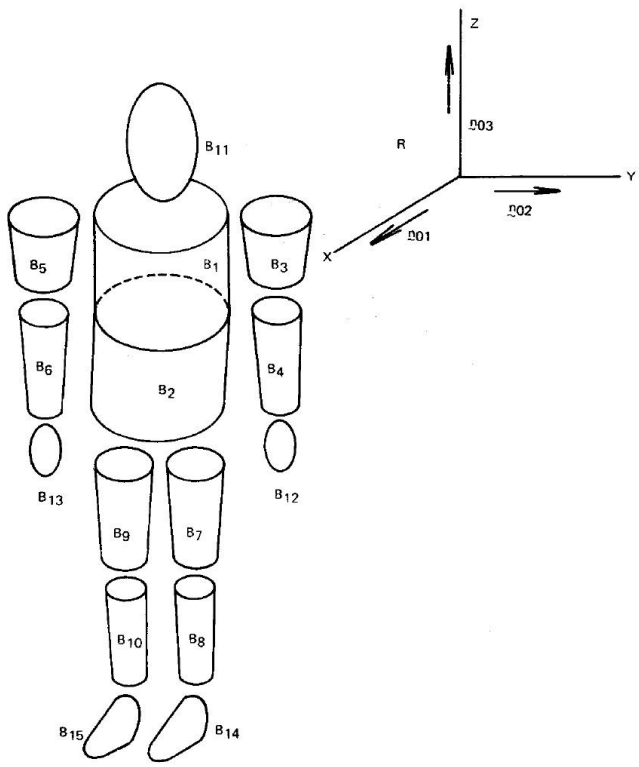

Figure 2.4 Huston’s proposed physical model for human body

Miles presented a comprehensive and simple mathematical model for dynamics of the torso in 1981 [31]. The proposed model by Miles retained all of the intuitive mechanical and dynamical characteristics and properties. Parameter estimation was also performed and the estimated parameters of the model were corroborated by experimental data. In 2007, Tanaka and Granata did a nonlinear analysis on low back stability that was associated with dynamics of the torso. Lyapunov Stability Analysis was applied in this research as a tool for measuring the local stability [32]. In 2010, Tanaka et al. proposed a mathematical model for seated stability [33]. The dynamics and statics of the seated human is associated with the neuromuscular control system and also with dynamics of the trunk and torso. In this study, a Lagrangian approach was used to describe the dynamics of motion and determine the equations of dynamics. Figure 2.5 is the schematic

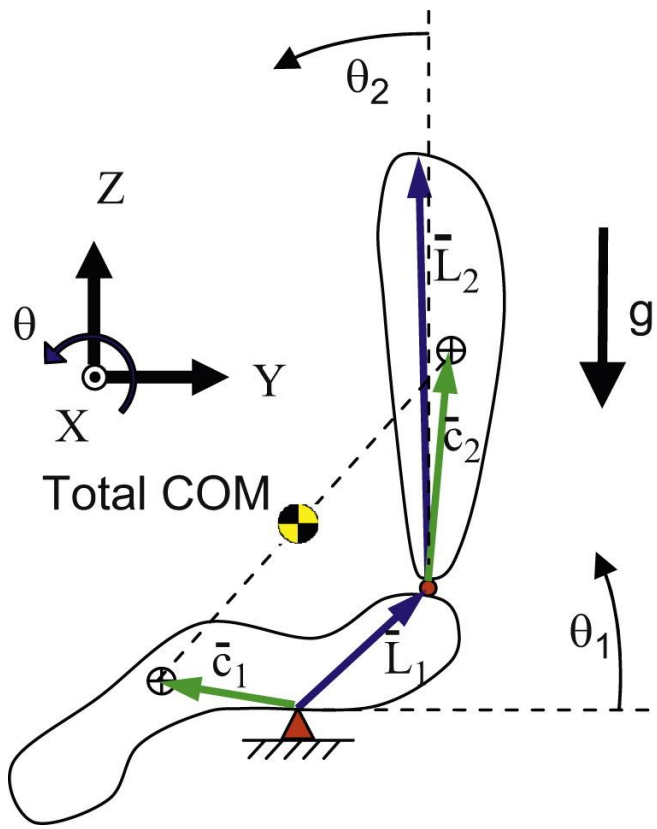

Figure 2.5 Tanaka's proposed model for human torso's dynamics

representation of the proposed mathematical model for this specific type of analysis in this study [33].

In 2011, Davidson et al. assessed human postural response to sagittal plane perturbations with localized muscle fatigue and aging. This study was experimental and simulation based research. The effects of localized muscle fatigue and aging on neural control of balance recovery from a postural perturbation was studied in this research [34]. Figure 2 – 6 depicts the free body diagram of the human model presented in this study.

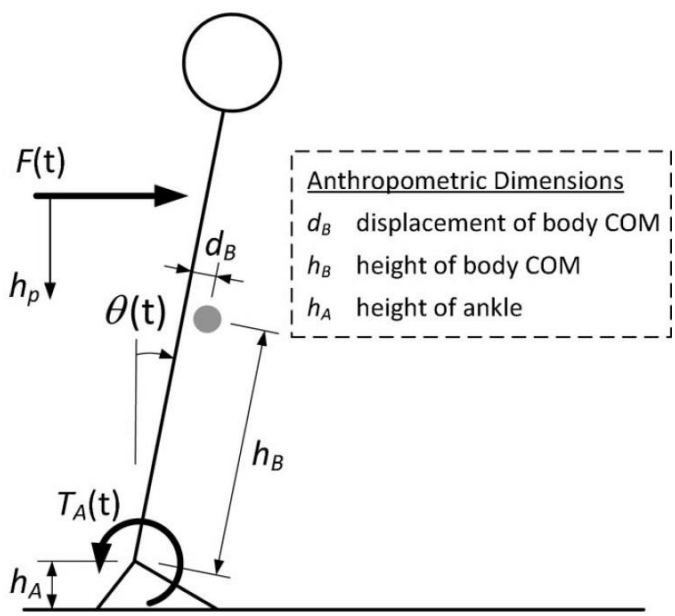

Figure 2.6 Davidson's free body diagram of the human model

Also, Figure 2. 7 shows the proposed block diagram of the system in this study. Figure 2. 7 includes the plant and the neural controller [34].

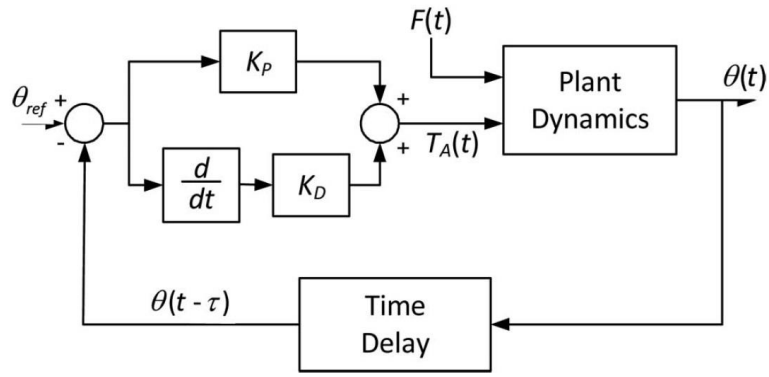

Figure 2.7 Proposed block diagram of the assessed system in davidson's study

In 2013, Reeves et al. investigated the reliability of assessing trunk motor control by application of position and force tracking, and stabilization tasks [35]. The experimental section of this study was similar to the experimental part of this thesis project. A system based approach was applied to study and assess trunk motor control in different human subjects. It was stated that the position and force control tasks for investigation of trunk motor control is deemed reliable [35]. Therefore, the similar experimental task was used to collect necessary data for this thesis project.

2.3 Bandwidth and human motor control

Although the methods used to quantify bandwidth for a simple engineering system are well established, the application of bandwidth to complex systems like human's neuromuscular system is more challenging. A general definition for bandwidth is the difference between the highest and lowest frequencies in a continuous set of frequencies [36]. To say that a system has a certain bandwidth means that the system can process signals with the frequency values within that bandwidth [37]. In 2013, Reeves et al. explained bandwidth as follows [38]:

"Like other physical systems, human motor control has constraints, referred to as bandwidth, which limit the range of frequency over which the system can operate within some tolerated level of error. For instance, a person can track closely a reference signal such as a low-frequency sine wave, but, as the frequency of the sine wave increases, limits in the controller's bandwidth will

result in tracking error. This tracking error occurs as a result of a reduction in amplitude and/or an increase in delay (i.e., phase shift) between the reference and tracking signal."

All of the statements above indicate that a control system with higher bandwidth is capable of responding to commands, changes more quickly and reach the steady state in a shorter period. Hence, the bandwidth is associated with time delay, rise time, settling time and percentage of overshoot of the system's response. Therefore, a system with higher bandwidth has shorter time delay, settling time, rise time, and lower percentage of overshoot. A brief and clear definition for bandwidth of human's neuromuscular system based on the current definitions could be represented as follows: The bandwidth of a human motor control system is a measure of how capable he/she is to respond to a command and stabilize in a shorter period and with a less fluctuation. In this definition, a shorter period refers to a shorter delay, rise time and settling time, and less oscillation refers to smaller percentage of overshoot.

The stated definition of bandwidth above describes it qualitatively. The quantitaive definition of bandwidth is well established and is defined as the range of frequencies over which the magnitude response of the transfer function drops by 3 dB. This drop in amplitude corresponded to a 50% decrease in power [39]. There are some established mathematical methods to determine the bandwidth of simple control systems such as first order or second order transfer functions with one or two numbers of poles and zeros [2].

Basically, the mathematical model is transformed to frequency domain for calculation of bandwidth [2]. The Fourier transform is used to associate the time domain representation of a mathematical domain to the frequency domain [40]. In using Fourier transforms, signals are written as the sum of a set of sinusoidal signal components. Each sinusoidal component is described by a complex function consisted of a real part and an imaginary part. The magnitude of

this complex function is the amplitude of the signal's component [41]. Bandwidth frequency is determined by finding a solution for the equality of this amplitude and amplitude of -3db in logarithmic scale [2].

Calculation of bandwidth and its application to complex systems like a human is more challenging. The human neuromuscular system and its interaction with the musculoskeletal system are a complex and nonlinear. Finding an accurate mathematical model for high order and nonlinear system is a challenging job. It requires a high accuracy optimization process to estimate the parameters of the mathematical model which describes the system precisely. It all causes determination of bandwidth for a complex and high order system such as the human motor control to take an excessive amount of time.

CHAPTER 3 : METHODS

The goal of this study was to determine the bandwidth of the neuromuscualar system controlling torso movement. In this consits of three major components, human subject experiment, mathematical modeling and analysis of models. The subjects used small torso movements to track a target and their movment was recorded. Data collected from the experiment was used to tune the parameters of a mathematical model. Once the model was tuned, a simulation was conducted to determine the system response. The system response was analyzed to calculate the bandwidth and other system characteristics.

An overvew of the entire methods section is shown below.

1. Movement Tracking Experiment — An experiment was performed on human subjects. This expetiment consisted of position tracking tasks and the trials were made up of pseudorandom perturbations. The results of the experiment were used to tune the parameters of the proposed mathematical model.
2. Mathematical Modeling — A proper model had to be proposed to describe the behavor of system. This model consisted of variables and parameters. According to the studied system, the variables are general rotational dynamic variables. Parameters of the model are physical properties of subjects and control properties of the system.
3. Simulation — This level was consisted of estimation of mathematical model's parameters. An optimization process must be performed to find the best values of parameters in order to minimize the difference between model and experimental data.

4. Analysis and Validation — The result of simulation must be compared to the experimental data to see if any change or modification is required in previous levels. This level caused the accuracy of final results increased. Also it prevented additional useless repettition of modeling and simulation.
5. Determination of Bandwidth — After creating the best fit mathematical model for the system, Bandwidth of the system was calculated based on this model. In addition, other control and dynamical characteristics such as cognitive time delay and etc. were determined in this level.

3.1. Movement Tracking Experiment

A movement tracking experiment was performed at Michican State University by Dr. Reeves and his research group. Ten individuals participated in the study. Participants included 5 females and 5 males between the ages of 20 and 58. Human subjects protection training was completed by all investigators and the study was approved by the Institutional Review Board (IRB) at Michigan State University. All of the human subjects were required to be generally healthy and have no issue their back such as low back pain, previous spinal surgery, etc. Physical information of subjects is shown in Table 3.1.

Table 3.1: The basic information of test subjects

Subject No.	Gender	Age	Height (cm)	Weight (Kg)
1	F	37	160	69
2	F	21	164	56.8
3	M	46	179	83.6
4	M	58	165.5	80
5	M	39	174.5	154.6
6	F	20	173.6	62.4
7	M	25	180	71
8	M	24	185.5	85.4
9	F	43	170.2	64.1
10	F	26	165.5	58.1

In the postion tracking experiment participants sat on a chair and string potentiometers were attached to a borad that was strapped to the back. Figure 3-2 depicts the set-up schematically. As the subject moved his/her torso the length of the string potentiometers changed and the from this the angle was calculated. All movment occurred in the saggital plane. The human subjects were strapped to the seat such that an angle of 120 degree was maintained between their hip and knee. A monitor was used to provide visual feedback for subjects. The monitor displayed the input signal and output reponse of the subjects during the experiment. It was placed one meter in front of each subject such that the center of monitor was at the same height as the subject's eyes.

As each subject moved, the string potentiometers changed length causing the output signal indicator on the monitor moved up or down. Participants were instructed to track the target and move their torso to place the output signal indicator on the target. The location of the input signal indicator, shown in figure 3.1, changed on the monitor over time. Subjects were instructed to track the input by flexing or extending their torso. This caused the output indicator moves on the monitor and it provided the subject with visual feedback of his/her current position. Each subject tried to keep the output indicator on the input target. The change of length of the string potentiometers were recorded during each task. The sampling rate of recording was 0.01 seconds which was fast enough for the modeling and simulation process.

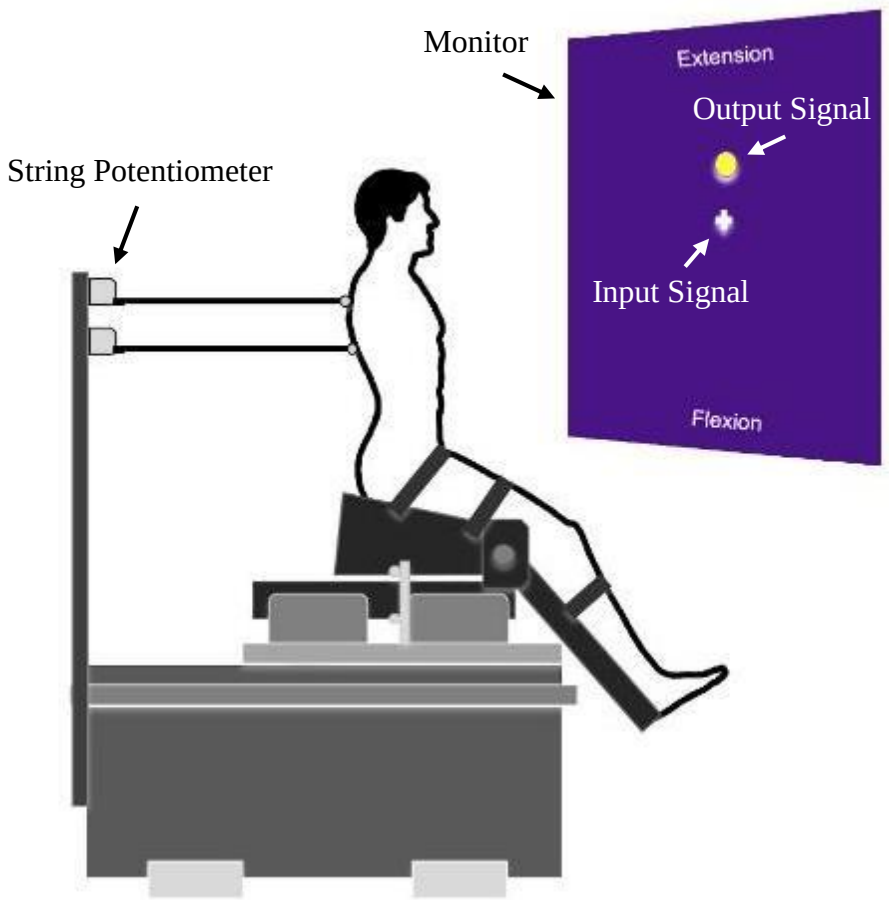

Figure 3.1 used set-up for the experimental part of the project

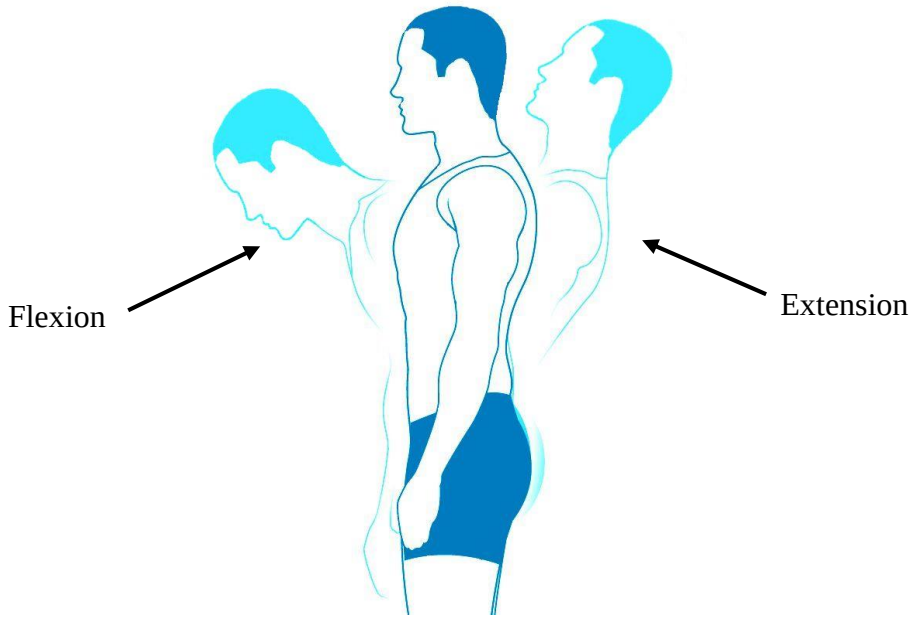

Figure 3.2 human's flexion and extension

Flexion describes a bending movement that decreases the angle between a segment and its proximal segment. Extension is the opposite of flexion, describing a straightening movement that increases the angle between body parts [42]. Figure 3.2 shows how flexion and extension occurs schematically.

Input signals were designed as step functions. Six different step functions were used in this study. These step functions consisted of three different magnitudes in two different directions. Table 3.2 shows the information of the input signals. The negative direction indicates flexion and positive direction indicates extension.

Table 3.2: Properties of step functions (input signals)

Input No.	Magnitude (degrees)	Direction	Motion
1	6	-	Flexion
2	4	-	Flexion
3	2	-	Flexion
4	2	+	Extension
5	4	+	Extension
6	5	+	Extension

Signals were designed in using MATLAB. A sampling rate of 20 ms was assigned to the input signals. The duration of each step function ranged of 2.5 to 3 seconds. This gave subjects enough time for their postion to settle after moving to the new location. The hold time was made variable so that participants would not be able to anticipate when the next change in postion would occur. After each step Function, the target position was returned to the resting (or zero) postions before

beginning the next step function. The duration of the resting time was varried between 2 to 3 seconds. Figure 3.3 shows a step function and the returning to the initial postion.

Each subject performed twenty different trials and each trial included twelve step functions. There were two of each step function assigned in each trial. The twenty different trials differed from each other with respect to arrangment and duration of step functions. This was done so that participants would not be able to predict the time, magnitude, or direction of the next step fucntion. Also, Figure 3.4 shows two designed trials. Design of input signals was done at Western Carolina University.

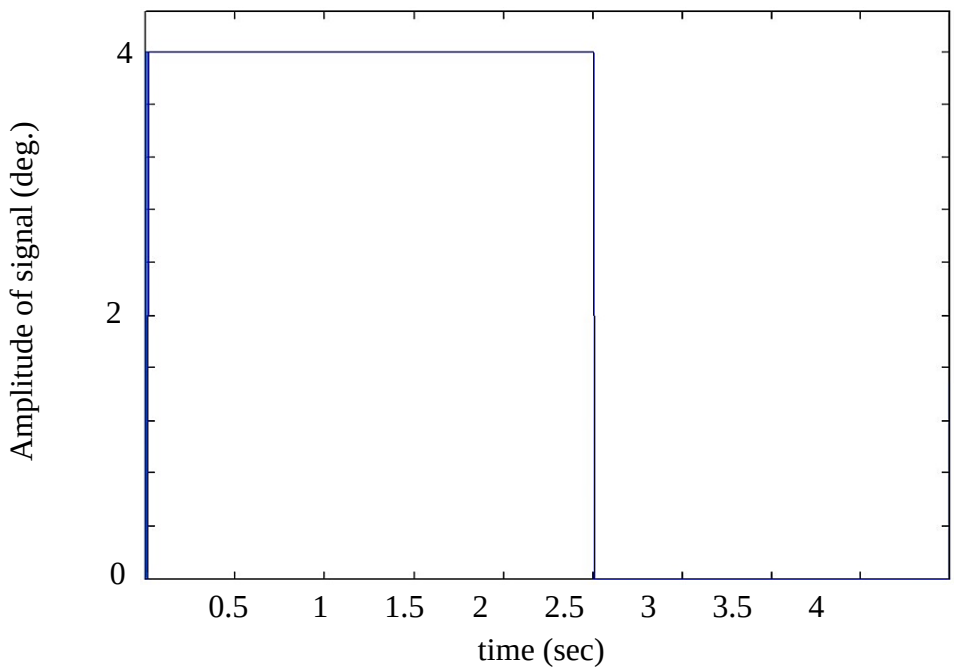

Figure 3.3 step function and the returning after that

After the data were collected at MSU they were sent to WCU for modeling, simulation and analysis. In total there were 200 data sets representing 10 subjects each performing 20 trials. With each trial consisting of 12 step functions, the total number of step functions was 720. Figure 3.5 shows of input signals and corresponding output results for one subject and two different datasets.

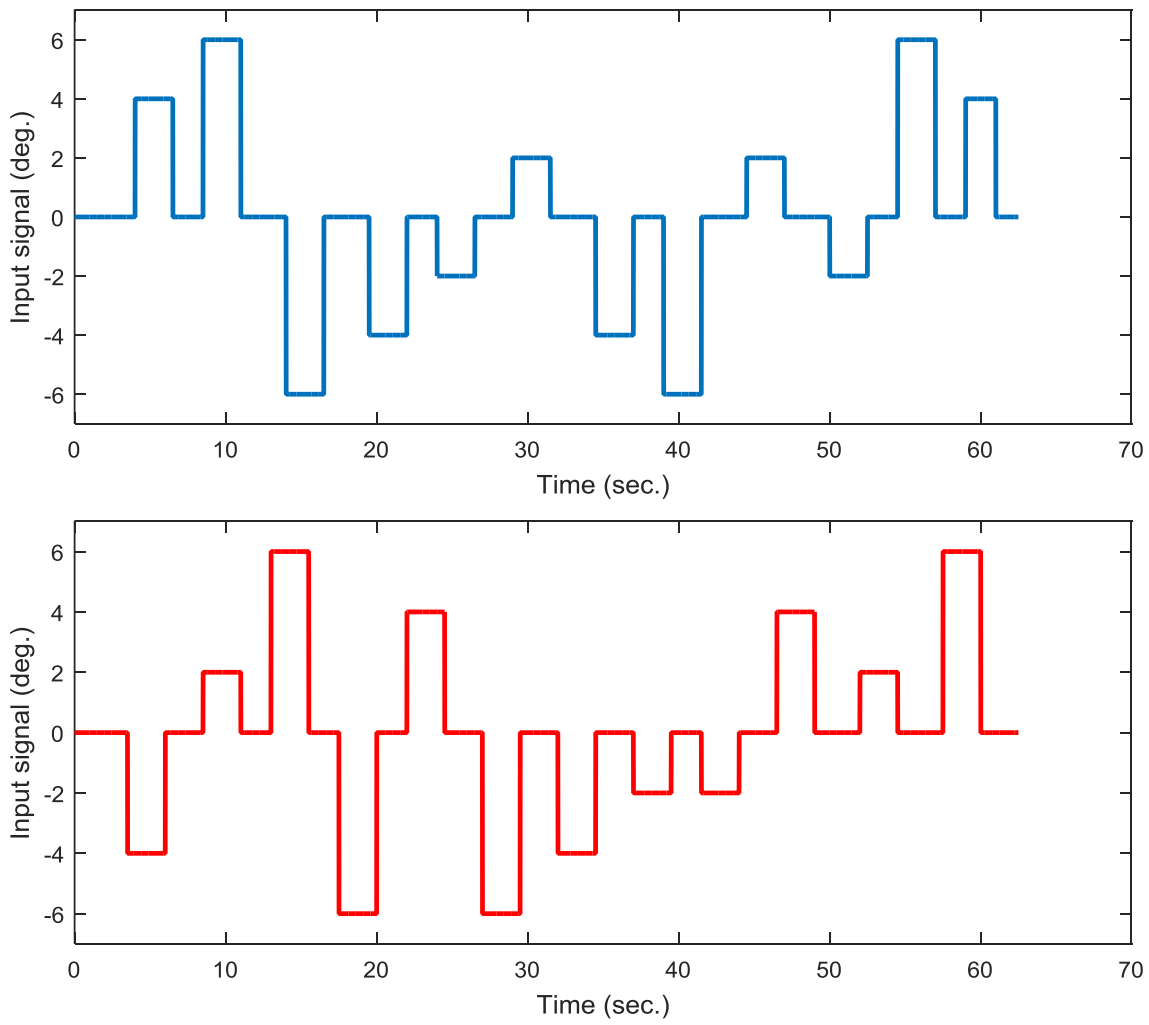

Figure 3.4 two designed input signals for experiment

In some cases, the output response did not achieve a steady state value after the input signal changed. This was because the subject did not have enough time to settle when responding to the input signal. It occurred mostly at the initial input signals of each trial. Because the goal of this study was to analyze the normal response of a person to a step function input, the responses that were teribbly different than others were omitted from the dataset before mathematical modeling and simulation was performed.

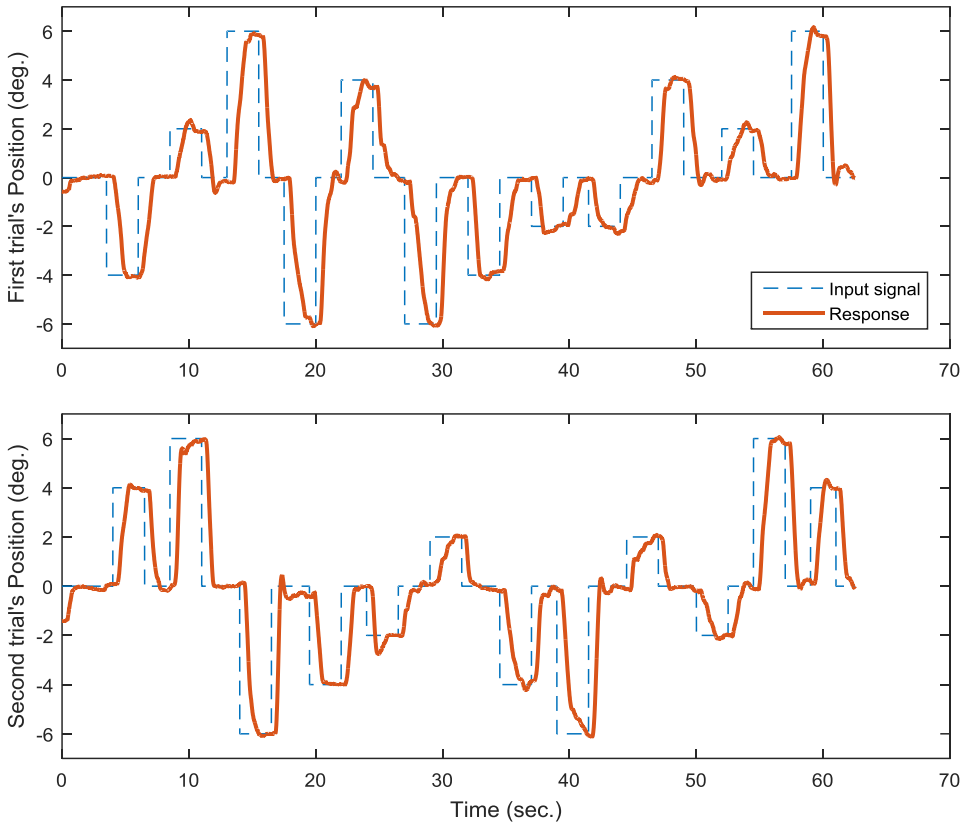

Figure 3.5 different responses and corresponded input signals for one subject

It can be observed in Figure 3.5 that subjects began to response to a change in input signal after a short time delay. After moving to the new postion, their movement settled after a few oscillations. This time delay is caused by the individual's cognitive time delay which is the time necessary for the brain to process that the input signal has changed. A shorter time delay at the start of each motion is desirable. Moreover, subjects are encouraged to track the position and achieve it in the shortest possible time. Hence, it is also desirable to reach the steady state and maintain the target postion in a shorter time and with minimum oscillation.

3.2 Mathematical Modeling

A mathematical model was required to describe the behavior of the dynamical system. The model consists of a mathematical equation that desrcibes the motion. In general, a force or position

input is provided to the model and the response is the movement behavior (i.e. the output). The model of the system should also include the effect of feedback controller.

An inverted pendulum with a proportional controller was used to model the system. The properties of the pendulum and the controller must be considered in the system design. A second order differential equation was used to describe the dynamics of the system. A general mathematical model for a rotational dynamic system was used,

$$I\ddot{\theta}_{(t)} + b\dot{\theta}_{(t)} + k\theta_{(t)} = u_{(t)} \tag{3.1}$$

This model is the Newton's second law for rotation. The angular motion variables change with time. Hence, the position, velocity and acceleration of the system are functions of time and are represented as $\ddot{\theta}_{(t)}$, $\dot{\theta}_{(t)}$ and $\theta_{(t)}$ in the time domain. The parameter *I* represents the moment of inertia of the upper body. Torso stiffness due to the spinal ligaments, and passive muscle tone of the abdominal and back muscles were assigned a stifness value of *k*. Viscous damping of the torso during movment was assigned a value of *b*. In this model, *u(t)* consists of two components. The first is torque generated by active contractions of the abdominal and back muscles. This torque is controlled by the human motor controller in the brain. The second component is the effect of gravity on the system. A mathematical representation of these torques is given by

$$u_{(t)} = mgl\, sin(\theta_{(t)}) + G\left(\theta_d - \theta_{(t)}\right). \tag{3.2}$$

where *G* is the gain of the controller. The paremeters *m*, *g* and *l* are the mass of upper body, acceleration due to gravity and the length of the segment to the center of mass, respectively. θ_d is the desired angular position. Using Euler's approximation for small angles, the mathematical representation of the system is

$$I\ddot{\theta} + b\dot{\theta} + \theta(k - mgl) = G(\theta_d - \theta) \tag{3.3}$$

The above system models human toros dynamics and control, but does not account for controller time delay. This can be significant in human on the order of 200 ms. The cognitive time delay is the time it takes each subject to start to respond after receiving the command. Assume that a subject receives the command at $t = 0$ and starts to move toward the target at $t = \tau$. In this case the cognitive time delay would be τ. Time delay maybe taken into account in the mathematical model of the system by converting it into the following piecewise function

$$\begin{cases} \theta_{(t)} = 0 & 0 \leq t < \tau \\ I\ddot{\theta}_{(t)} + b\dot{\theta}_{(t)} + k\theta_{(t)} = u_{(t)} & \tau \leq t \end{cases} \tag{3.4}$$

where $u_{(t)}$ was given by equation 2.

Finding an analytical solution for equation 3.4 consumes a lot of time. Because it is a piecewise function and is consisted of two different functions of time. Hence, it becomes complex to find an analytical solution that satifies both parts of equation 3.4. Therefore, numerical methods were applied to analyze the behavior of this system.

Simulink (MathWorks, Inc. Natick, Massachusetts) was used to import the mathematical model into the computational environment and simulate the system response. This program is a graphical environment for modeling and simulation of engineering systems. Simulink is designed to model dynamics system and automatic controls. It has many built in features/blocks to model these type of systems. Therefore, the block diagrams are used in this programming environment

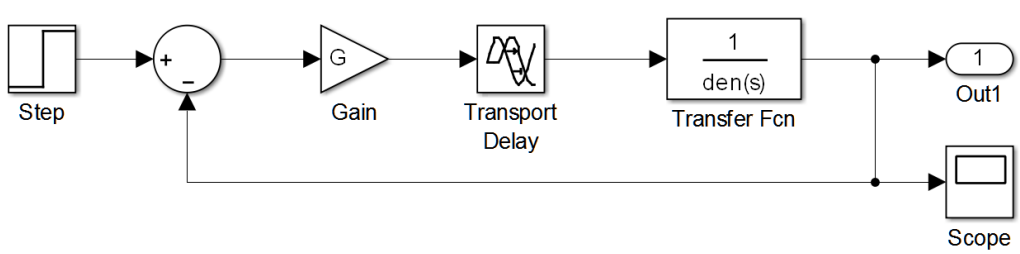

Figure 3.6 proposed block diagram in simulink

as tools to describe the system schematically. The block diagram of our system was created within Simulink. Figure 3-6 shows the block diagram of this system in Simulink.

Each block represents a specific parameter or part of the mathematical model of the system. Description of each block is as follows:

Step input: Input commands are in the form of step functions. The commanding point on the screen moves suddenly from $\theta = 0$ to the $\theta = \theta_d$ and stays in the new position. This block sends the specified command to the plant with respect to a defined conditions in the study.

Sum: A closed-loop feedback control system is used in this study. The error between current position and desired position is calculated by this block. In fact, the controller sends the command to the plant based on the calculation performed in this block. The feedback controller in this system will be described in detail later.

Gain: This block represents the proportional gain of the controller. The calculated error in the previous block is multiplied by this value to provide a scaled feedback control. A larger proportional gain results in a larger change in output for a given error in angular position. [43]

Time delay: The cognitive time delay is assigned in this block. The block *"Transport Delay"* in the block diagram was used to represent this delay in the system.

Plant: General transfer function for the plant is assigned in this block. That transfer function is a fractional function in frequency (i.e. Laplace) domain which determines the ratio between the input and output of the

system. The nominator and denominator of this function describes the general behavior of plant. In our system, the nominator was assigned a value of 1 and denominator will be described in detial later in this section.

Output: Output is the response of our system to the input signal. In other words, it is the position of subject at each moment in time. Thus, it is a matrix consisted of two columns. One column is for time points and another one is the position at each point of time. All of the output data are stored in this block. The sampling rate for data recording was assigned to 0.01 seconds based on the sampling rate in the data collection of experiments. Thus, the time column is an arithmetic sequence with a step of 0.01. The position column includes the position of the modeled system at each time point.

Scope: This block provides a visual representation of output. It outputs a plot of the modeled postion over time.

Let's assume that the applied torque by the controller is the input to the plant. Then, equation (3.3) could be rewritten as

$$I\ddot{\theta} + b\dot{\theta} + \theta(k - mgl) = u(t) \tag{3.5}$$

Where $u(t) = G(\theta_d - \theta)$. Since a proportional feedback controller was assumed for the human's neuromuscular system, a feeback loop was assigned to the system that connects the output to the input. This connectur is shown in the figure 3.6. It provides the capability for the system to calculate the angular difference (instant error) between the input (desired position) and the output (current position) at each point. Based on this comparison, the controller sends the proper command to the plant. The interaction between controller and the plant results in a decrease in the

distance between input and output at each point of time. In other word, the plant moves toward input and decreases its distance to the desired position. As soon as the current position falls within a defined range of angular positional error the plant stops moving. For instance, assume that the absolute value of tolerance is 0.1 degree and the human subject is tracking the input command of 2 degrees. Once his/her position falls within 1.9 to 2.1 degrees, the modeled system stops moving and maintains the position within this range of angular position.

Our controller was a simple proportional controller with closed-loop feedback. Other controllers such a PID controller or even a more complex controller with multiple components were considered. These more complex controller are able to drive the plant to achieve a error value near zero. However, these controller add additional complexity and the additional model paramaters make optimization less reliable. Therefore a simple feedback controller was selected.

To find the transfer function, which is the ratio between the input and output of the system, equation (3.5) was transformed to Laplace domain.

$$\Theta_{(s)}(Is^2 + bs + k - mgl) = U_{(s)} \tag{3.6}$$

Hence

$$tf_{\ (s)} = \frac{\Theta_{(s)}}{U_{(s)}} = \frac{1}{Is^2 + bs + k - mgl} \tag{3.7}$$

Equation (3.7) is the transfer function of our system in Laplace domain. It was used in the transfer function block of the block diagram for the system deacribed above.

3.3 Simulation and parameter estimation

The mathematical model was imported into Simulink in order to have a better understanding of the system, and also to perform the simulation. Before conduction the simulation, parameters of the model must be determined. Having the model with known parameters, we can simulate a

response to various input signals. Thus, the purpose of this section is to determine the parameters that make the mathematical model fit the experimental data.

3.3.1 Mathematical procedure

A cost function was defined that represents the error between the mathematical model and the experimental data. Parameters of the model were determined such that the cost function was minimized. Hence, this stage of the study was to solve an optimization problem. Generally, in optimization problems, the goal is to minimize the defined cost function to find the best fit or model.

Since the focus of this study was not on the development of optimization methods, a standard optimization method was selected, the "Nonlinear Least Squares". This method is suitable for parameter estimation problems. Curve fitting is one of the most useful features of this method. The following paragraphs describe the theory of optimization using the Nonlinear Least Squares method.

Assume we have an experimental time domain data set that consists of m data points. A representation of this data set is

$$Dataset = \{(y_1, t_1), (y_2, t_2), (y_3, t_3), \dots, (y_m, t_m)\} \tag{3.8}$$

Recall the mathematical model for these data are a function of time. That means the point in time is the input to the system and the output of this function is the position of the subject at that specific time point. Let's say it has n parameters that $n < m$ and each parameter is shown as P_j, where j is an integer between 1 to n. To simplify the mathematical representation of the model, consider the set of parameters as a vector of P, such that

$$P = [P_1\ P_2\ P_3 \dots P_n]^T \tag{3.9}$$

Hence, the mathematical representation of the function of model is

$$y = f(P, t) \tag{3.10}$$

In parameter estimation, the goal is to find the vector *P* such that the model minimizes the cost function. In the nonlinear least square method the cost function is defined as [44],

$$C.F. = \sum_{i=1}^{m} (f(P, t_i) - y_i)^2 \tag{3.11}$$

This represents the sum of the squares of errors between model and experimental value at each point of time. The minimum of a function *f(x)* occurrs when

$$\frac{d}{dx} f(x) = 0 \tag{3.12}$$

That is the derivative of the function, with respect to its variable equal to zero. Accordingly, the minimum of the equation 3.11 occurs when partial derivative of *C.F.* with respect to each parameter equals zero. That is

$$\frac{\partial}{\partial P_j} C.F. = 2 \sum_{i=1}^{m} (f(P, t_i) - y_i) \frac{\partial}{\partial P_j} (f(P, t_i) - y_i) = 0 \tag{3.13}$$

Thus, we need to find the best values for the members of vector *P* which are the parameters of the model. These values must satisfy equation 3.13. In order to find the best values for the arrays of vector *P*, a search algorithm was used. The computational method utilizes an itterative process based on the search algorithm to find the best parameters values. The Trust-Region-Reflective was selected as the search algorithm for this system. An understandable definition of this search method in Nonlinear Least Squares optimization is presented below.

Assume a function *f(x)* that has one variable, *x*. To minimize this function computationally, we need to find the value of *x* such that it satisfies the convergence criteria. An initial value of x_o for parameter *x* needs to be determined to start the process of parameter estimation. A subset S_o of points is selected around x_o by determining a radius of *r* and resolution of *d*. A geographical

representation of subset S_o is shown in Figure 3-7. Radius and resolution determine how many points are in the subset S. Subset S_o is called the trust region [8]. Let's say that there are k points in the trust region. The computational search algorithm evaluates all the values of x in the trust region and calculates all the $f(x)$ values. Then x_1 is identified as the value for x at which $f(x)$ is minimized over the interval $[x_o - r , x_o + r]$. After completing the first level of the search process, the trust region is moved to a new interval where the center is x_1. The radius and resolution of the trust region remains constant for each step of search algorithm. Thus, there is a new trust region interval, called S_1, that includes new k points. The search process repeats in the new level, and the search algorithm compares the values of $f(x)$ of the new trust region to find the minimum value for $f(x)$. Hence, x_2 is identified as the new value for x, at which $f(x)$ is minimized over the interval $[x_1 - r , x_1 + r]$, the trust region. This process continues until the convergence criteria is met. Different criteria for convergence could be defined. The goal is to find the x value that causes the cost

function, *f(x)*, to equal zero. However, in most cases this is an ideal criteria that cannot be met. Hence, the most common convergence criteria is the following [8]:

$$\left|\frac{f(x_{k+1}) - f(x_k)}{f(x_k)}\right| < \delta \tag{3.14}$$

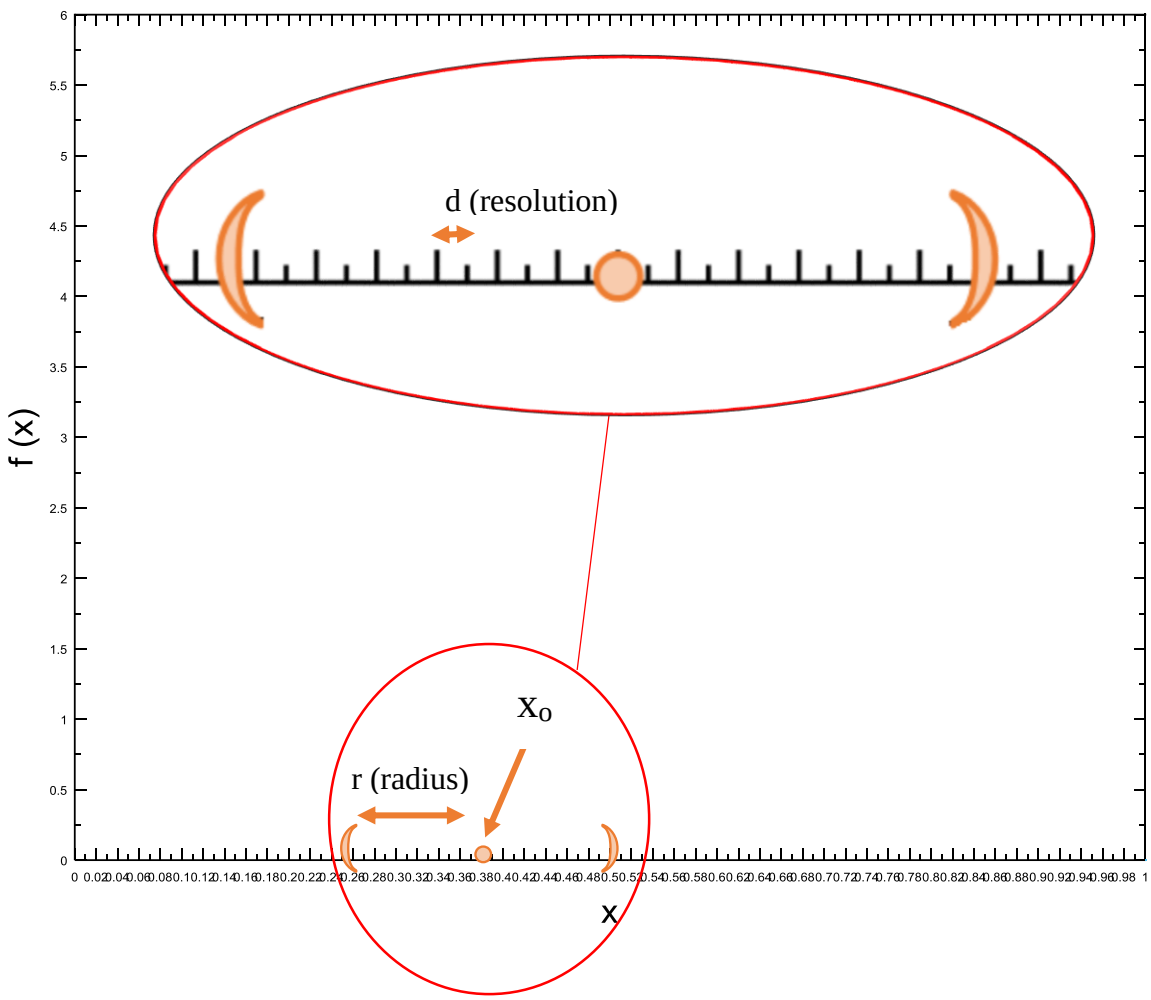

Figure 3.7 Trust-Region-Reflective algorithm procedure

where δ is the tolerance value for the cost function. A smaller value of δ increases the accuracy of the model. However, it increases the duration of optimization and the memory required for the computational search.

The process described above was performed to find optimal paramaters for our system. The only difference is that our model had seven different parameters. An optimization and search algorithm was executed for all of the parameters symultaneously [45]. We will determine a logical initial value for each parameter. Then, according to the accuracy and tolerance that we expect from the model, and also taking into acccount the computational power of the computer, the radius and resolution of the search method will be defined. In the end, the best fitting vector of P, which was the set of model parameters, will be calculated.

Due to the high amount of experimental data and the tedious process of parameter estimation, the process was executed entirely in the MATLAB environment. The output of the defined mathematical model in Simulink and the experimental data from MSU were used in the parameter estimation process. The vector of parameters in our system was

$$P = [I\ b\ k\ \tau\ m\ L\ G]^T \tag{3.15}$$

and each of them has been described in the mathematical modeling section. Importing (3.14) into (3.12) yields the optimization cost function for our system,

$$\frac{\partial}{\partial P_j} C.F. = 2\sum_{i=1}^{m}\left(\theta(P,t_i) - \theta_{m,i}\right)\frac{\partial}{\partial P_j}\left(\theta(P,t_i) - \theta_{m,i}\right) = 0 \tag{3.16}$$

where $\theta(P,t_i)$ is the modeled position, or $\theta_{(t)}$ from (3.4) at $t = t_i$, and $\theta_{m,i}$ is the measured position from the experiment.

For each parameter, a numerical solution for (3.15) was found by the parameter estimation process previously defined. After each optimization, a vector of P_f was determined. It consisted of 7 different parameters that were the optimized for this model. That means the output value of the function, $\theta(P_f, t)$, had the best fit for the experimental data set.

For each subject there were 40 responses to the same step input. These responses were extracted from the experimental data and prepared for the optimization process. For instance, subject “a” had 40 responses to each input signal +6, +4, +2, -2, -4, and -6. Figure 3-8 shows a single response to input signal of -2 degree and the group of all 40 responses for the subject “a”. The graph on the bottom shows the 40 responses in light blue lines, and the average of all of the responses in a solid black line. Also, a band of containing maximum and minimum values of responses at each point of time is shown and boardered by striped blue lines.

The parameter estimation process was performed for each step function separately and optimal parameter values were obtained. This process was repeated 40 times for each individual response to a input signal of the prescribed magnitude. This entire process was repeated for each each input signal magnitude (+6, +4, +2, -2, -4, and -6). Then this process was repeated for each subject (240 optimizations). Thus, with ten subjects, a total of 2400 sets of optimized parameters were calcalated for this study.

3.3.2 Programming in MATLAB

A MATLAB program was created to run the simulations. The code was designed to analyse the resposne to each step function. It used the nonlinear least squares optimization function which was used to find the optimal model parameters using the Simulink outputs. Once the optomized paraemter were determined for the speicific step function being evaluated, the program stored these data for later use. No template from previous research projects were used for modeling and simulation of the system. All the MATLAB code was fully generated and developed by the researchers. Codes is attached to the Appendix G of this thesis.

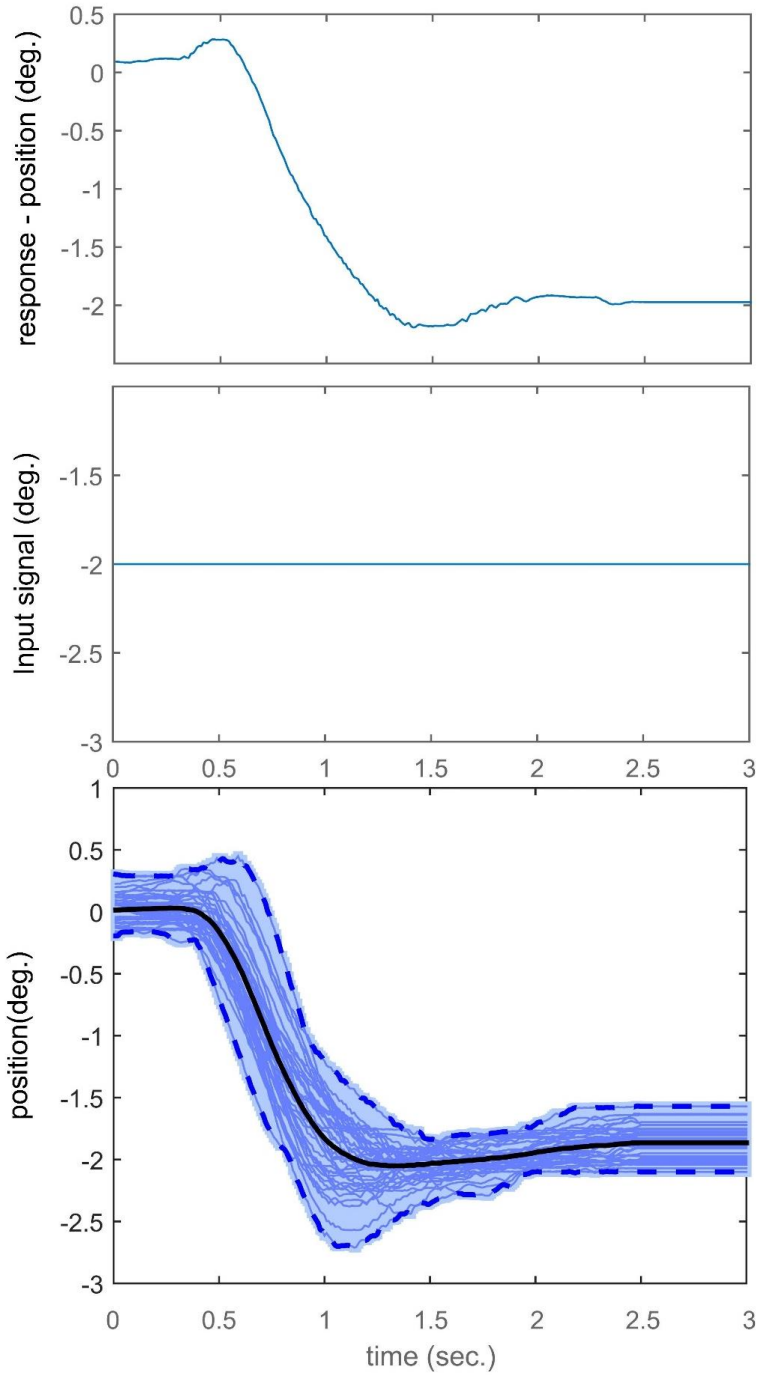

Figure 3.8 group of 40 responses to the input signal of -2 for the subject 1

The function *"lsqcurvefit"* in MATLAB was used for the parameter estimation and curve fitting task. This function calls the following seven inputs to start the execution of the estimation [46], [47].

Function: The function which run the Simulink simulation of the system (see figure 4.18)

Initial values: Initial values of the parameters that will be estimated must be input.

Xdata: It is a vector that includes the assigned values to the horizontal axis of the function. In this problem, the horizontal axis represents time. Since the sampling rate of the experiment was 0.01 sec., this vector is a descretized arithmetic sequence with the common difference of 0.01.

Ydata: This is the vector of the measured angular positions from the position tracking experiment. In other words, Ydata includes the data which the parameter estimation is performed on.

Upper band: A vector of scalars must be input to defing the maximum allowed values for each parameter in the optimization process.

Lower band: Similarly, a vector of scalars must be input to defing the minimum allowed values for each parameter in the optimization process. In other words, lb and ub are the numerical constraints of each parameter.

Options: This is a very important input to *"lsqcurvefit".* All of the properties of optimization and search algorithms are defined in this input. Options is a vector of logical variables that are defined in programming language of MATLAB. The properties that were defined in the options section for optimization process are explained.

Algorithm: The Trust-Region-Reflective was selected as the search algorithm for this project.

Convergence Criteria:	The parameter estimation and Trust Region Reflective algorithm continues until the convergence criteria is met. Equation (3.13) represents the mathematical equation for convergence criteria. The value of δ is defined in this property. Smaller values for δ increase the accuracy of estimation and the duration and power usage of the process. For this project, 10^{-4} was assigned to δ.
Max Iteration:	In some cases, due to selecting unsuitable initial values or flaws in measured data, the optimization process starts to diverge. This process never ends unless another termination criteria is defined. The maximum number of iteration is the termination criteria to prevent this from happening. MaxIt was set at 1000 in this project.

After assigning all of the required properties of *"lsqcurvefit"* and running the code, the output of the optimization function was the vector of estimated parameters, P_f. Due to the large number data sets programming was done using loops. Each optimization task took about 2-3 minutes. Therefore, it took approximately 100 hours for the processing computer at WCU to run the parameter estimation process on 2400 data sets.

3.4 Analysis and Validation

Prior to performing the complete parameter estimation for all trails, a few test rund were conducted to ensure that the code was running properly. In addition, after the execution of the optimization stage, the results were validated by doing a comparison between each model and its corresponding experimental data. The process of analysis and validation is explained in this section.

3.4.1 Pre-processing analysis

The experimental data received from MSU contained 20 continuous trials for each subject. Since the response to each input signal was supposed to be modeled separately, the measured data of the response to each input signal had to be separated from one another. These individual step responses were then called into the program for parameter estimation. Code was generated to classify each step responses based on its magnitude and direction of the input signal and the subject on which the test was performed. Each subject was saved as a data object in the form of *"iddata"* and the name format of "*s_m_d_i*", where each character represents a specific feature of the data object (Table 3.3).

Table 3.3: Identification code for classification of individual step responses

Character	Feature	Values
s	Human subject	a, b, c, … , j
m	Magnitude of input signal	2 , 4 , 6
d	Direction of motion or input signal	n (negative) , p (positive)
i	number of data set	1 , 2 , … , 40

For instance, the twenty seventh response datasets of Subject "d" to the input signal +4 was stored as "*d_4_p_27*".

The format of stored data was "*iddata"*, which is one of the data objects that MATLAB has presented specifically for storing time domain data sets. This data object is consisted of three major components which are input data, output data and sampling rate. All of these components have already been assigned and measured in our project.

The number of cells in each data set was increased in order to have the same length of time in each data set before running the complete parameter estimation process. Data sets were extended

by repeating the steady state value. This was done because in some cases the simulation generated an illogical model (Figure 3.9). Extending the steady state values in the time domiam corrected this problem (Figure 3.10).

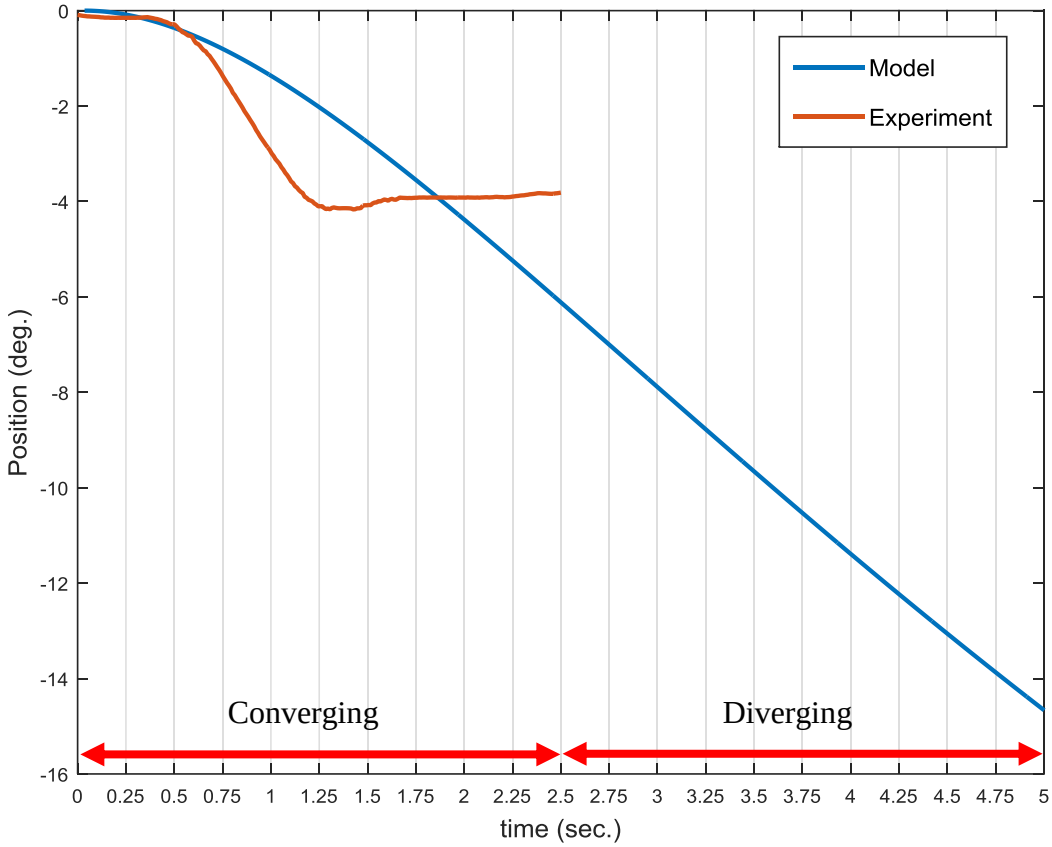

Figure 3.9 problem in convergence for short period trials

The model was properly fit to the experimental data in the time interval of 0 to 3 seconds. However, the model showed a terrible oscillation and divergence after 3 seconds. Figure 3.9 shows this issue before doing the corrections.

To avoid this issue, we increased the number of cells in each data object from 250 to 1000 cells. Then, we did the optimization process over 20 data sets with 1000 cells and all of the models showed a fairly good settling at $t \approx 5$ and it remained at the steady state. Note that the increase in the number of cells in data objects did not make any difference in the actual measured data, because

almost all of the subjects were settled at $t \approx 3$. We just extended the data sets by adding data points to the steady state portion of each response. To execute this, we added cells with the same values as the last measured data point. Then, a white Gaussian noise was added to the extended part of the output data in order to simulate the actual steady state of each response. Figure 3.10 shows the model of same response of Figure 3.9 after correction.

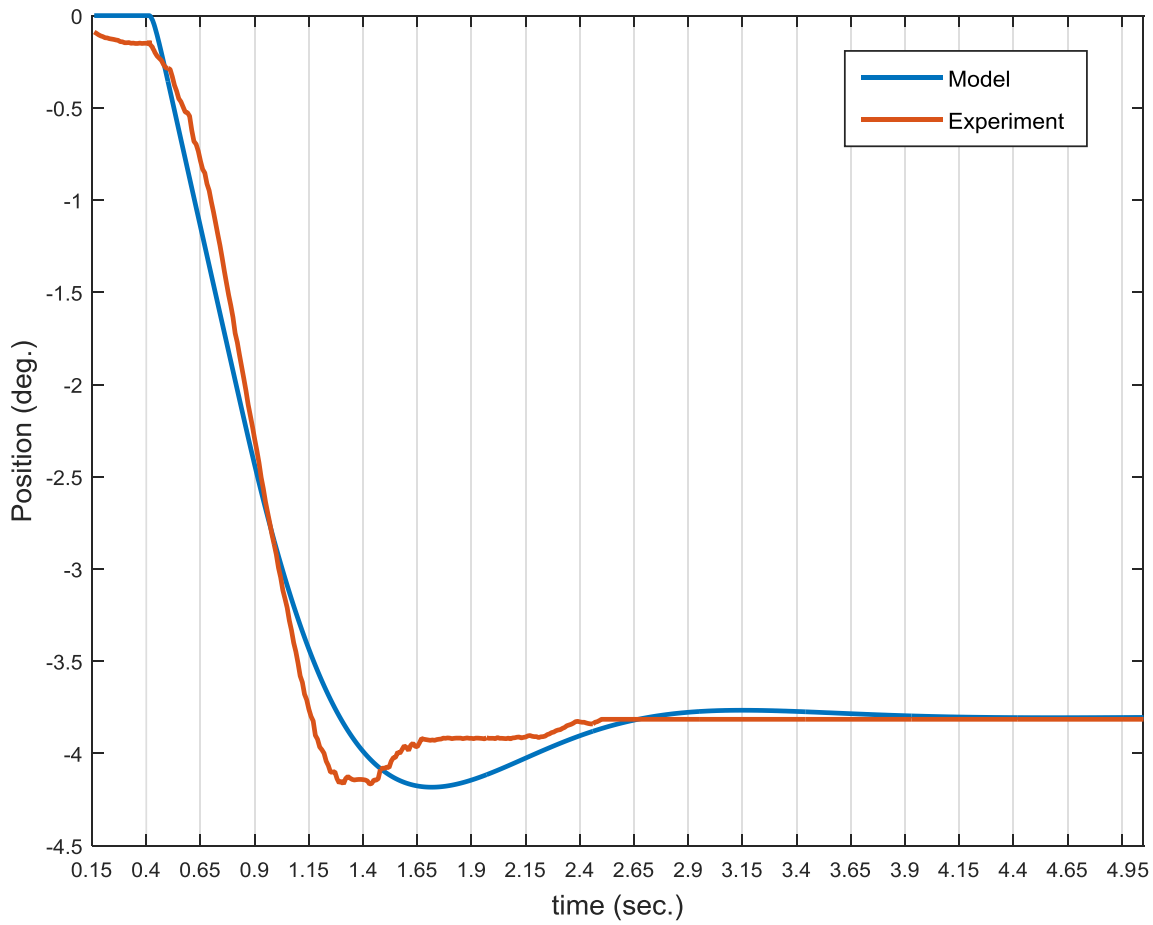

Figure 3.10 model and observed data after convergence

There was another concerns about initial values of each parameter. In order to start the parameter estimation, an initial value for each parameter was required. Different initial values could have different results. Therefore, we had to ensure the correct initial values were put into the

system and the corresponded result was the best fit to the experimental data. For this concern, we created 5 vectors for the initial values, and each vector was different.

The assigned values for each parameter in the vectors of the initial values were selected based upon physical properties of human anatomy. That means, the initial value of each parameter was chosen with respect to the type of parameter and its minimum or maximum value. For instance, none of the initial values of the parameter *"m"* were less than 5kg, or more than 100kg, because the mass of the human's upper body could not be out of these bound. Twenty step responses were selected randomly. For each of the these step responses, parameter optimization was performed using 5 different initial values vectors to see if there would be any significant difference among the results. In the end, it was observed that all of the results (optimized parameters) using different initial conditions were the same. It proved that different initial values for the parameters would not result in different optimization results for the mathematical models. Hence, the average of the 5 vectors of the initial conditions were presented as the vector of initial condition for the complete parameter estimation process.

The last task in the preparation was to assign proper bounds for each parameter. In other words, the constraints of the optimization task needed to be determined, in order to avoid an illogical optimization value for each parameter. Although the values of the optimized parameters could satisfy the mathematical model and optimization equations, they would be beyond physiological limits.

Assigning proper constraint bounds to the parameters b, k and G was done randomly, because parameter no data was available for this type of experiment. The only definite fact was that they were all positive values. Hence, the bound of $(0 , +Inf)$ was assigned to them as constraints. The parameters m, L and I were respectively the mass of the upper body, the distance between the

center of mass and the center of motion, and the moment of inertia of the upper body around the hip joint, respectively. Based on the physical information of the subjects and the studied references, Table 3.4 was proposed for the bounds of the mentioned parameters [48] , [49].

Table 3.4: Constraints for *m* , *L* and *I*

Parameter	Lower bound	Upper bound
$I\ (kg.m^2)$	0.01	5
$m\ (kg)$	1	90
$L\ (m)$	0.1	1

For cognitive time delay parameter, τ, the bound was assigned after observation of the 20 different experimental data sets. Generally, this parameter was not more than 0.5 seconds; therefore, the assigned constraint bound for this parameter was *[0.3, 1]*.

3.4.2 Post-processing validation

Although most of the issues in the simulation process were resolved in the preparation stage, the validation had to be performed after the simlation and parameter estimation. This included some general visual observations and computational comparisons between the simulated output and the experimental data.

The simplest way to validate the models was to compare the output of a model with the output of the position tracking experiment. For this task, we generated code at the end of the optimization loop to create a plot of these outputs. A visual observation of the plots was performed and those plots with significant errors were either removed or the simulation to find model parameters performed again. The majority of the outcomes were fairly close to the experimental data.

Another validation technique that was used was the *"fit percentage"* in the MATLAB code. The function *"compare"* in MATLAB returns a plot of the model and experimental (validation) data with a fit percentage. The generated code in this project returned two more outputs alongside the fit percentage. The output, *"State"*, was defined to show the quality of fitness. It varied from *"poor"* to *"very good"* based on the percentage of fitness. The last output of this function determined if the parameter estimation process needed to be repeated for the current model. Table 3.5 shows the corresponded information. Figure 3.11 represents the general format of output of this function.

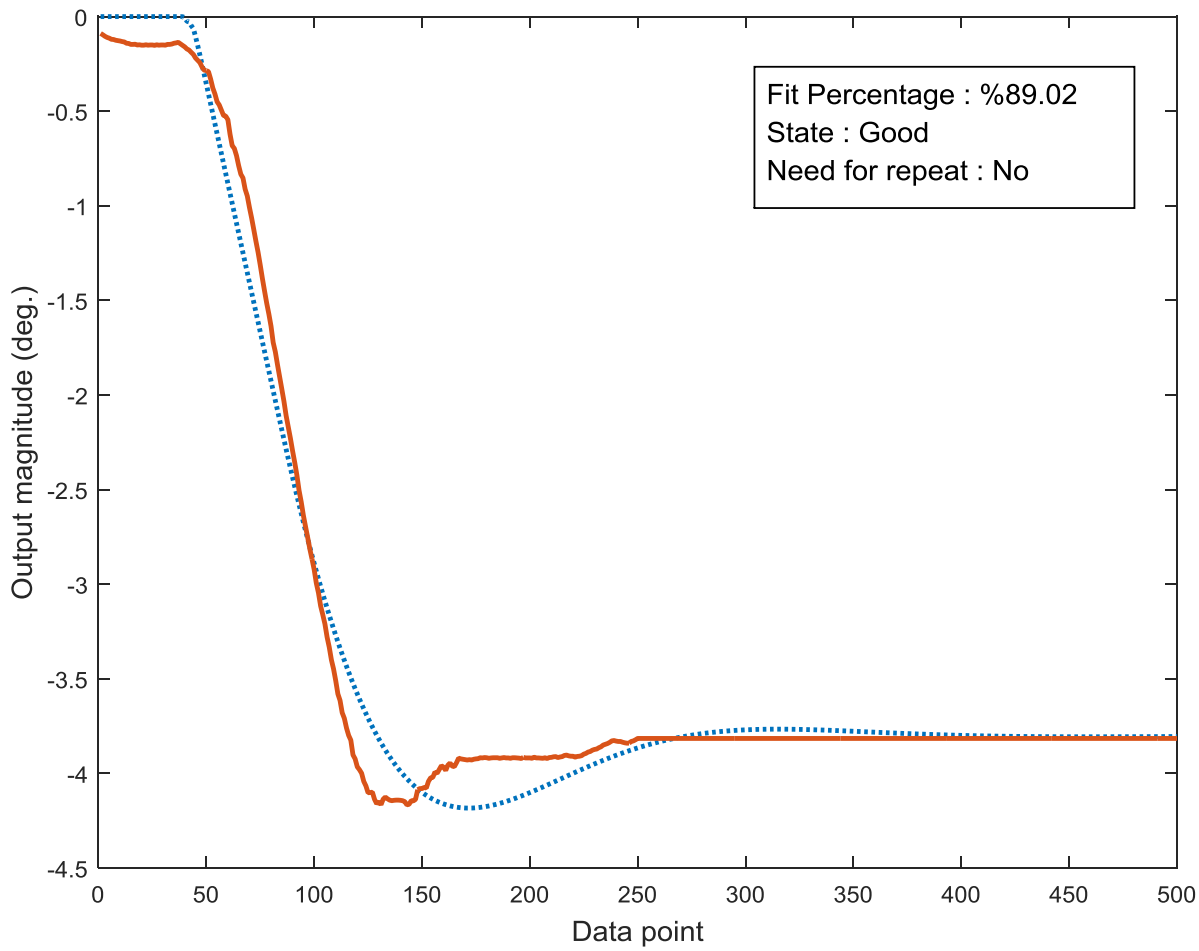

Figure 3.11 model and obsevred data with %fit

Table 3.5 : Detail of *"fit percentage"* outputs

% Fit	State	Need for repeat
90-100	Very good	No
85-90	Good	No
80-85	Fair	No
75-80	Poor	Yes (conditionally)
< 75	Very Poor	Yes

3.5 Bandwidth and other characteristics of the system

All of the previous steps were done to provide the data required for these calculations. Optimized mathematical models for different input signals were analyzed and the bandwidth was determined based on their outcome. Along with the bandwdith, other characteristics of the models such as percentage of overshoot, time delay, settling time, rise time and steady-state, were determined.

3.5.1 Bandwidth calculation technique

Using the definition of bandwidth from the previous sections, we needed to deterine the frequency at which the magnitude of frequency response dropped by 3 dB. There are several methods to calculate bandwidth frequency. A direct technique from classical control theory was used to determine the bandwidth of each model.

The experimental data and outputs from models were in the time domain. The first step was to convert data from time domain to frequency domain. The Fourier transform was used to convert the data to the frequency domain. Since the experimental and modeled data sets were discrete time-domain data, the discrete fourier transfrom had to be used. Another trick is to convert the mathematical model from the time-domain to Laplace-domain and then to Frequency-domain, by

substituting s with $j\omega$. Hence, we recall the Laplace-domain representation of the transfer function of the model in the equation (3.4), and substitute s with $j\omega$ [50]. Remember that the controller was a feed-back system and it had to be considered in the proposed transfer function. It was shown in the figure 3-6.

$$tf_{(s)} = \frac{\Theta_{(s)}}{U_{(s)}} = \frac{Ge^{-\tau s}}{Is^2 + bs + k - mgl + Ge^{-\tau s}} \tag{3.17}$$

Substituting $j\omega$ for s and simplifying,

$$tf_{(j\omega)} = \frac{\Theta_{(j\omega)}}{U_{(j\omega)}} = \frac{Ge^{-j\tau\omega}}{-I\omega^2 + jb\omega + k - mgl + Ge^{-j\tau\omega}} \tag{3.18}$$

Converting the complex term $Ge^{-j\tau\omega}$ from exponential form to trigonometric form we have

$$tf_{(j\omega)} = \frac{\Theta_{(j\omega)}}{U_{(j\omega)}} = \frac{G(cos\,(-\tau\omega) + j\,sin\,(-\tau\omega))}{-I\omega^2 + jb\omega + k - mgl + G(cos\,(-\tau\omega) + j\,sin\,(-\tau\omega))} \tag{3.19}$$

The variables of the equation may be reducing by defining A and B as

$$\begin{aligned} A &= -I\omega^2 + k - mgl + G\,cos(\tau\omega) \\ B &= b\omega - G\,sin(\tau\omega) \end{aligned} \tag{3.20}$$

By importing (3.20) into (3.19), simplifying the outcome, and the multiplying denominator by its conjugate, yeilds

$$tf_{(j\omega)} = \frac{[GAcos(\tau\omega) - GBsin(\tau\omega)] + j[-GAsin(\tau\omega) - GBcos(\tau\omega)]}{A^2 + B^2} \tag{3.21}$$

Obviously $tf_{(j\omega)}$ is a complex function and it can be represented as

$$tf_{(j\omega)} = Re_{tf} + j\,Im_{tf} \tag{3.22}$$

where

$$Re_{tf} = \frac{GAcos(\tau\omega) - GBsin(\tau\omega)}{A^2 + B^2} \tag{3.23}$$

and

$$Im_{\ tf} = \frac{-GAsin(\tau\omega) - GBcos(\tau\omega)}{A^2 + B^2} \tag{3.24}$$

A complex number can be represented as a position vector in a two-dimensional Cartesian coordinate system, called the Complex Plane [51]. The horizontal axis shows the real component and the vertical axis shows the imaginary component of the complex number [52]. This vector can also be represented by its magnitude and direction relative to the origin (phase space). The magnitude and direction of the complex vector is determined by equations below.

$$|tf| = \sqrt{Re_{\ tf}^{\ 2} + Im_{\ tf}^{\ 2}} \ \ , \ \ \angle tf = tg^{-1}\frac{Im_{\ tf}}{Re_{\ tf}} \tag{3.25}$$

The variable in equations (3.18) to (3.25) is the frequency, ω. Using the parameters found in the parameter estimation process, a specific magnitude and direction can be assigned for any value of ω.

The power of the modeled signal needed to be determined, in order to calculate the bandwidth. Therefore, the magnitude equation in (3.25) was converted to the logarithmic scale. The reason is that power is often represented with the unit of Decibel in signal processing. Decibel is a logarithmic unit which represents the ratio of two quantities. There is a relationship between the logarithmic representation of magnitude and power. It is

$$10\ log\frac{P_{current}}{P_{source}} = \ 10\ log\left(\frac{|tf|_{current}}{|tf|_{source}}\right)^2 = \ 20\ log\ \left(\frac{|tf|_{current}}{|tf|_{source}}\right) \tag{3.26}$$

where

$$|tf|_{source} = \lim_{\omega \to 0} \ |tf| = 1 \tag{3.27}$$

Setting the equation (3.26) equal to -3 dB results in a set of frequencies, at which the magnitude of the frequency response is $\frac{1}{\sqrt{2}}$ of its maximum. In other words, the power is $\frac{1}{2}$ of its maximum.

The last value of this set, which is obviously the largest one, is the bandwidth frequency. The set of frequencies less than the bandwidth frequency is the bandwidth of the system.

Bode Plot could be an advantageous visual tool to gain a better understanding of the equation (3.26) and the bandwidth of the system. Bode plot of the transfer function was created by generating plots for the magnitude and phase of the transfer function. The function *"bode"* in MATLAB returns a bode plot of data in the frequency domain. This function was used to validate the bandwidth calculated using the equation (3.26). Figure 3.12 shows a bode plot with the bandwidth frequency and the bandwidth. Bode plots of models are attached in the result section.

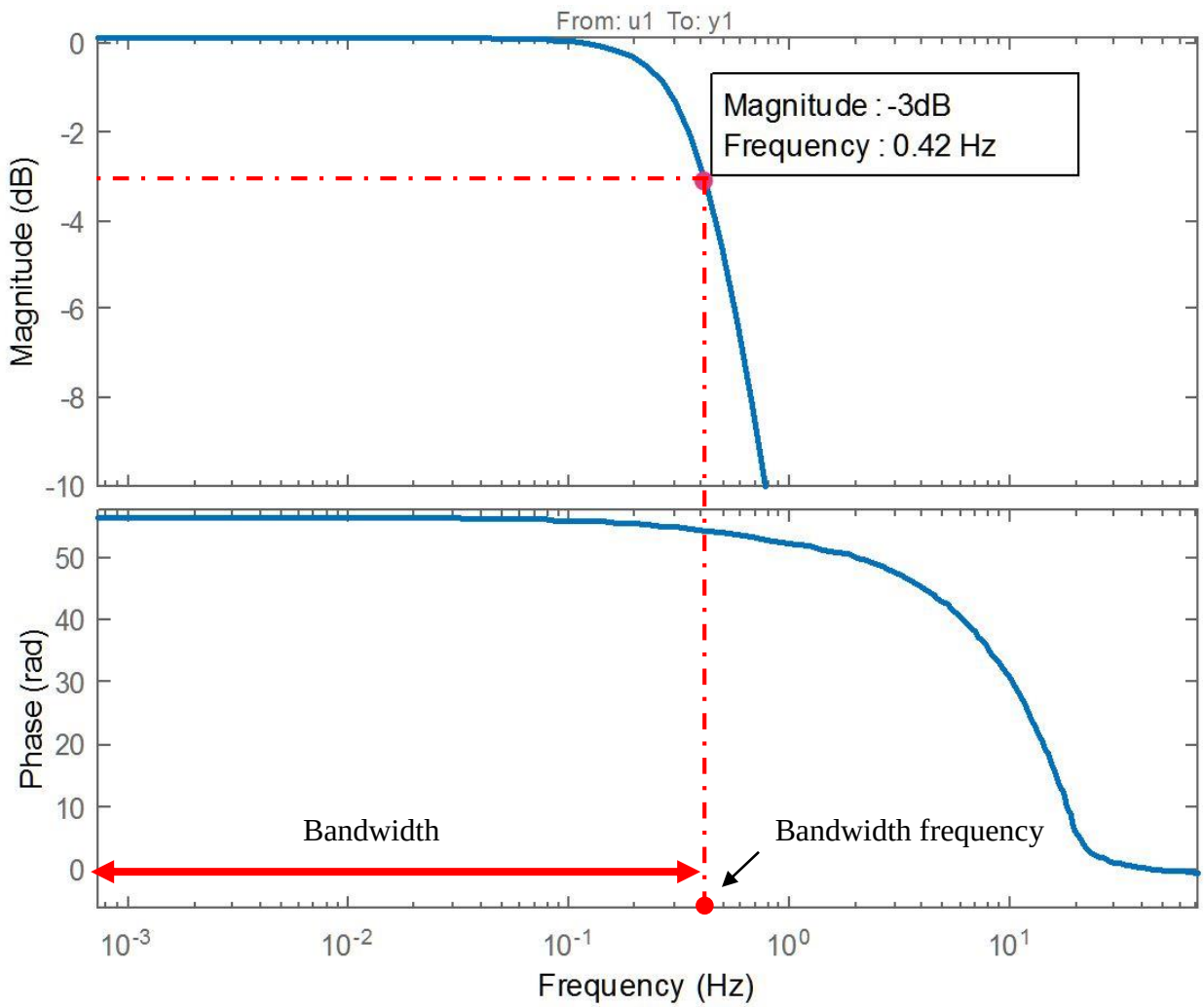

Figure 3.12 bode plot and determination of bandwidth

3.5.2 Other characterstics of models

Along with the bandwidth frequency, other characteristics of the model were determined. Unlike bandwidth, these characteristics were determined in the time domain by assessing the output models. Rise time is the time needed for the subject reaches 90% of the input signal [43]. Rise time is calculated by solving the equation (3.28) for *t*,

$$\theta_{(t)} = 0.9\theta_d \tag{3.28}$$

where $\theta_{(t)}$ and θ_d were defined as the current angular position and the desired angular position (step input signal). Solution of equation (3.28) for each model was coded in a loop in the program. The answer was stored after each the program was executed for each input signal. The values are attached in result section.

The percentage of overshoot is a quantity that represents how much the subject exceeds his/her target in the position tracking experiment. It is calculated by the equation

$$\%PO = 100 \times \frac{\theta_{peak} - \theta_{steady\ state}}{\theta_{steady\ state}} \tag{3.29}$$

,where θ_{peak} is the the first maximum absolute value of the position after the subject starts to respond. This quantity is a useful indicator in assessing the quality of task performance. Lower overshoot is desirable. However, it alone could not determine if the quality of the response is high. That means, other characteristics must be determined to make sure that the task has been done with high quality.

Settling time and error band are other characteristics of system. These two characteristics are related. Settling time is the time needed for the step response to falls within the error band and not leave it. Hence, error band is a symmetrical neighborhood around the target into which the response falls after the settling time. Another qualitative definition for the settling time is the time required for the response curve to reach and maintain a certain tolerance range around of the final

value. It is usually expressed as a percentage (usually 5% or 2%) [53]. These concepts are illustrated in Figure 3.13.

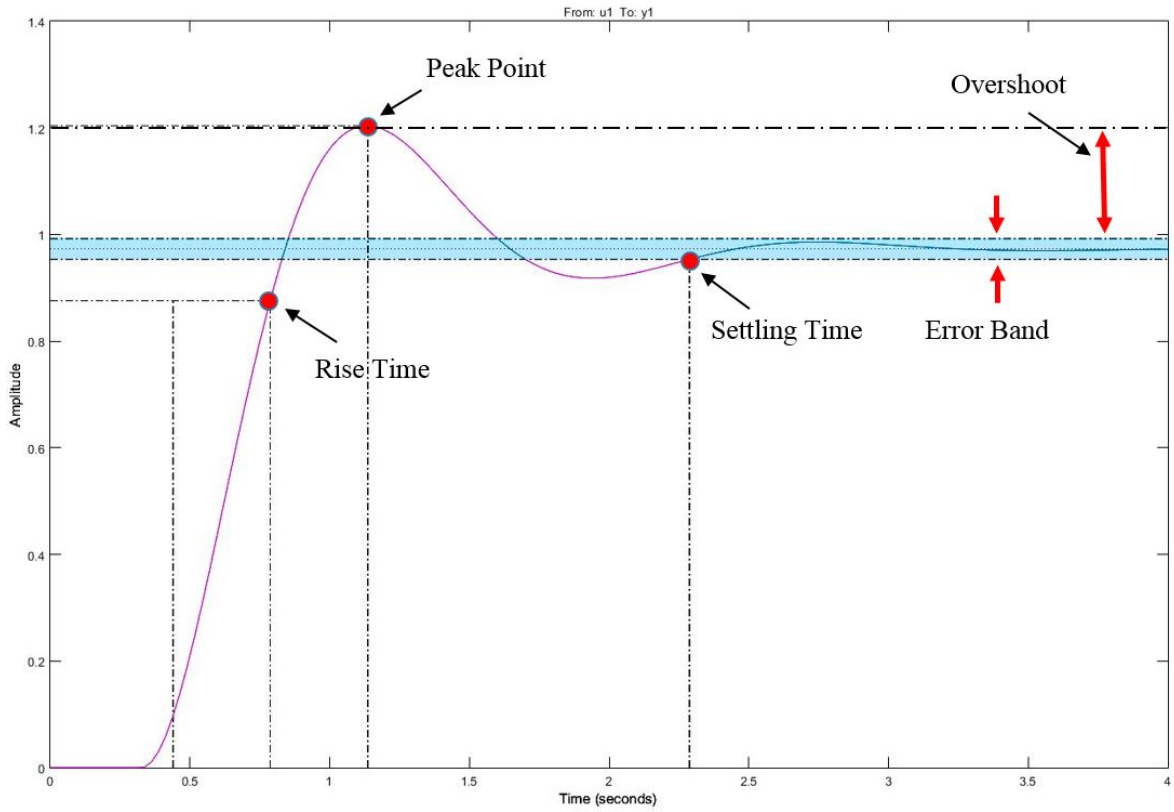

Figure 3.13 step response and characteristics of system

CHAPTER 4 : RESULTS AND DISCUSSION

4.1 Experimental results

The 200 trials were performed at Michigan State University and the measured responses of human subjects in position tracking tasks were sent to Western Carolina University. As mentioned in the last chapter, although the results showed each subject had been passed the settling time, the number of data points of each trial was not enough for simulation. Hence, the steady state of each data set was extended.

Figure 4.1 shows the outcome of the experiments and also the extension of data on subject “a”. Subject “a” may be considered as a typical subject. Recall that for each subject, there were 40 responses for each input signal. Each individual response for Subject “a” is shown on the figure 4.1 by a light blue line. The mean value of the responses was calculated by averaging the value of the position at each point of time for all 40 step responses. The black solid line represents the average value of measured step responses. The minimum and maximum values of the data points for the 40 responses at each point of time are represented by striped blue lines. Moreover, the blue area bounded by minimum and maximum lines represent the finite region in which all of the responses fell. It is obvious in the figures that each response acheived at the steady state before $t = 3$ seconds. Data extensions were performed for data points after $t = 3$ seconds and it did not cause any problem in the reliability of the results.

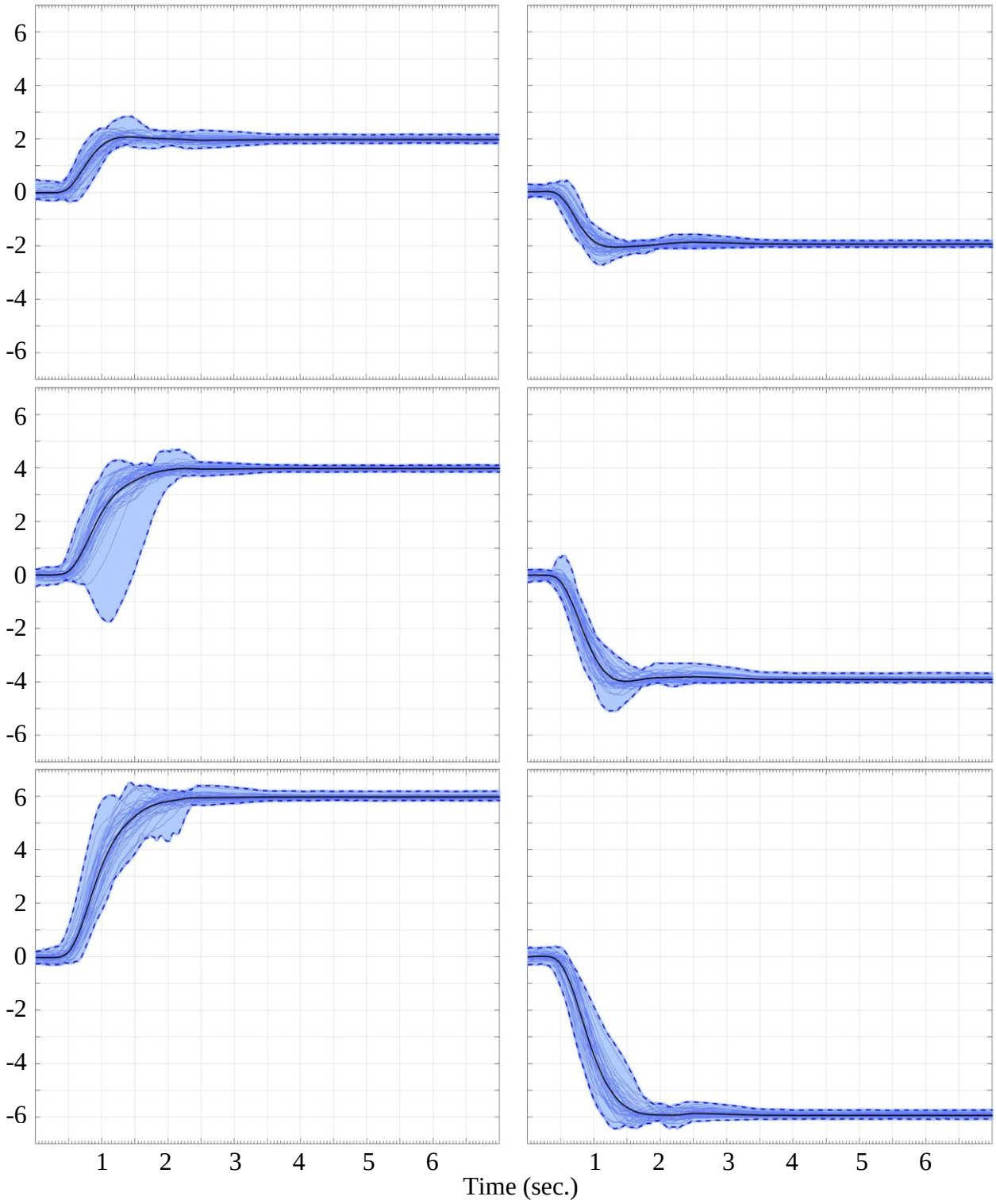

Figure 4.1 each individual response of subject 1 to different targets

The upper left plot in Figure 4.1 shows the results for a smallest extension (+2), while the upper right plot shows the results for a smallest flexion (-2). Middle and lower plots show the results for the other motion types. This plot was generated using all the data from subject “a”. It was useful for visualizing the general treands of the data sets. Figure 4.2 represents all the responses of Subject “a”.

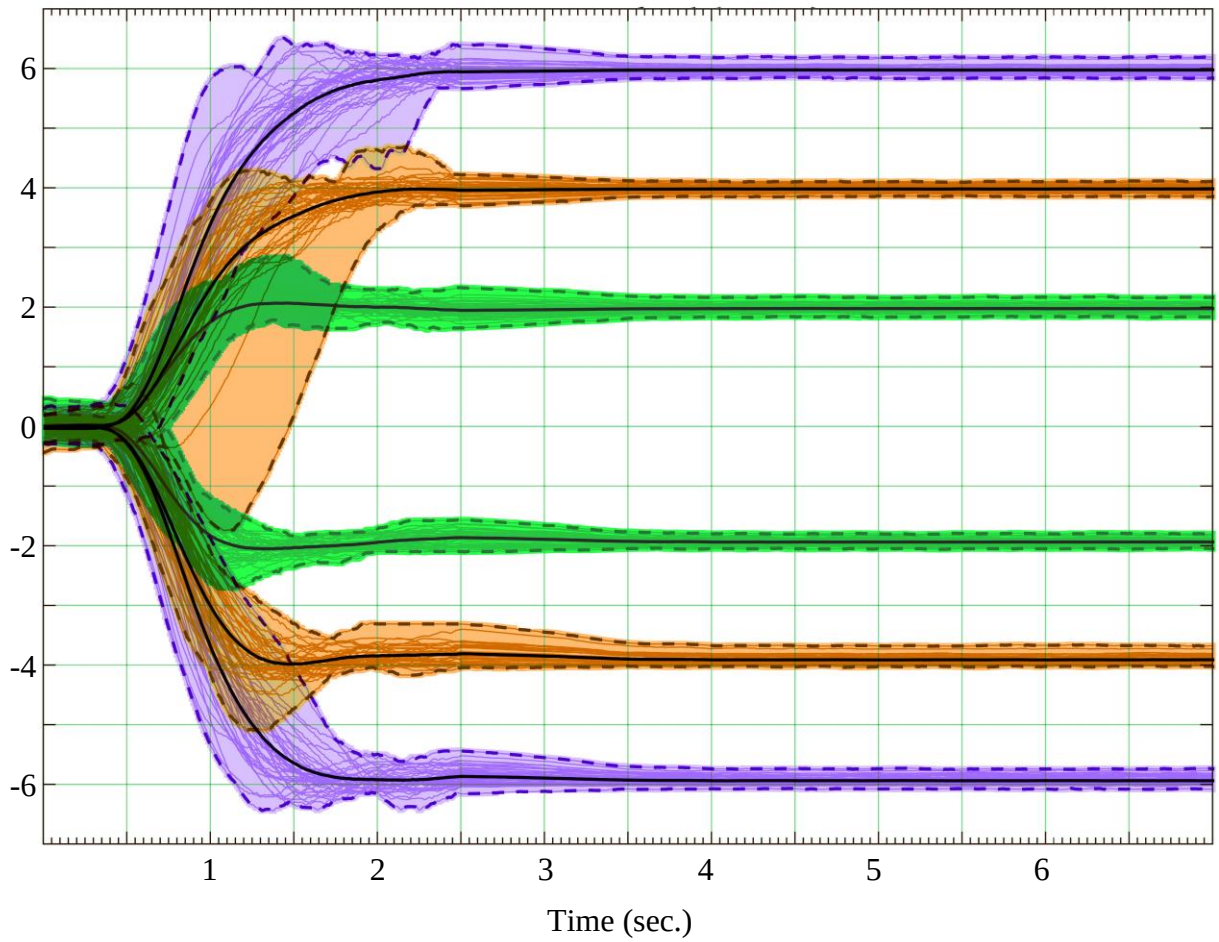

Figure 4.2 all of the responses of subject 1 to different targets

In Figure 4.2, the results shown in purple are responses of Subject “a” to the largest input signals. The orange plot represents the responses to the middle size input signals, and the green ones show the responses to the smallest input signal. The bottom group of curves show the responses to flexion input signals and top curves are the responses to extension input signals. The

same plots were generated for each of the other subjects in order to validate the results of experiments. All the plots are found in the appendix. Except in a few cases, results were remarkably consistent with each other. Those groups of data which were significantly different than the general tendency of the results, were eliminated from data before mathematical modeling and computational simulation.

4.2 Parameter estimation results

Two types of plots were generated for each group of results. One was for assessing the estimated parameters within the groups of each subject's responses. Another one was to evaluate the outcomes within the groups of responses of all sujects to a specific target. A comprehensive table consisting of estimated numerical values for each parameter is presented along with the plots. In this section, with the exception of some cases, only the plots of two subjects and two targets are shown for each single parameter. The plots for other subjects and other targets are attached in the appendix.

4.2.1 Moment of inertia

Figure 4.3 shows the results for the estimation of parameter *"I"* for subjects 1 and 2. The vertical axis represents the values of the moment of inertia. The horizontal axis shows the magnitude and direction of the input signals. These plots were used to determine if the moment of inertia changed with the magnitude and direction of the input signals. The plots include the mean, maximum and minimum values, and also the standard deviation values of the moment of inertia. Observing Figure 4.3, results were fairly consistent for estimated values of *"I"* within the data sets over the different input signals. The same plots were created for all of the subjects and parameters. These can be found in the appendix. Figure 4.4 shows the numerically estimated values of the parameter *"I"* for different subjects with the same input signals, +2 degree and -2 degree. This

figure provides a visual tool to compare subjects to one another. The plots showing the estimated values of this parameter for other input signals are included in the appendix. Table 4.1 displays the estimated numerical values for this parameter in kg·m^2.

Table 4.1: Mean of estimated values for parameter *I* (standard deviations in the parenthesis)

	Target (input signal)					
Subject No.	-6°	-4°	-2°	2°	4°	6°
1	0.58 (0.23)	0.55 (0.27)	0.51 (0.22)	0.38 (0.19)	0.50 (0.22)	0.55 (0.22)
2	0.48 (0.18)	0.53 (0.20)	0.67 (0.25)	0.41 (0.15)	0.51 (0.23)	0.46 (0.20)
3	0.38 (0.17)	0.35 (0.13)	0.45 (0.27)	0.61 (0.27)	0.53 (0.22)	0.45 (0.18)
4	0.30 (0.07)	0.43 (0.15)	0.33 (0.14)	0.36 (0.17)	0.34 (0.09)	0.38 (0.16)
5	0.28 (0.10)	0.37 (0.12)	0.39 (0.14)	0.33 (0.14)	0.47 (0.19)	0.39 (0.17)
6	0.42 (0.28)	0.55 (0.33)	0.53 (0.19)	0.39 (0.12)	0.53 (0.28)	0.56 (0.22)
7	0.45 (0.17)	0.45 (0.10)	0.39 (0.26)	0.46 (0.12)	0.38 (0.16)	0.53 (0.17)
8	0.42 (0.15)	0.52 (0.14)	0.45 (0.18)	0.41 (0.08)	0.47 (0.17)	0.40 (0.12)
9	0.46 (0.20)	0.42 (0.12)	0.51 (0.19)	0.40 (0.17)	0.36 (0.11)	0.53 (0.18)
10	0.28 (0.11)	0.41 (0.26)	0.27 (0.12)	0.45 (0.21)	0.38 (0.19)	0.34 (0.09)

As seen in Table 4.1 and Figures 4.3 and 4.4, the mean values for *"I"* are ranging between 0.25 to 0.60 kg·m^2. The results were compared to available references and they were fairly consistent with those data [54]. Looking at the plots and table, there are no obvious trends among the results. This may be due to the small amplitude of motion and minimal momentum generated durign the experiment.

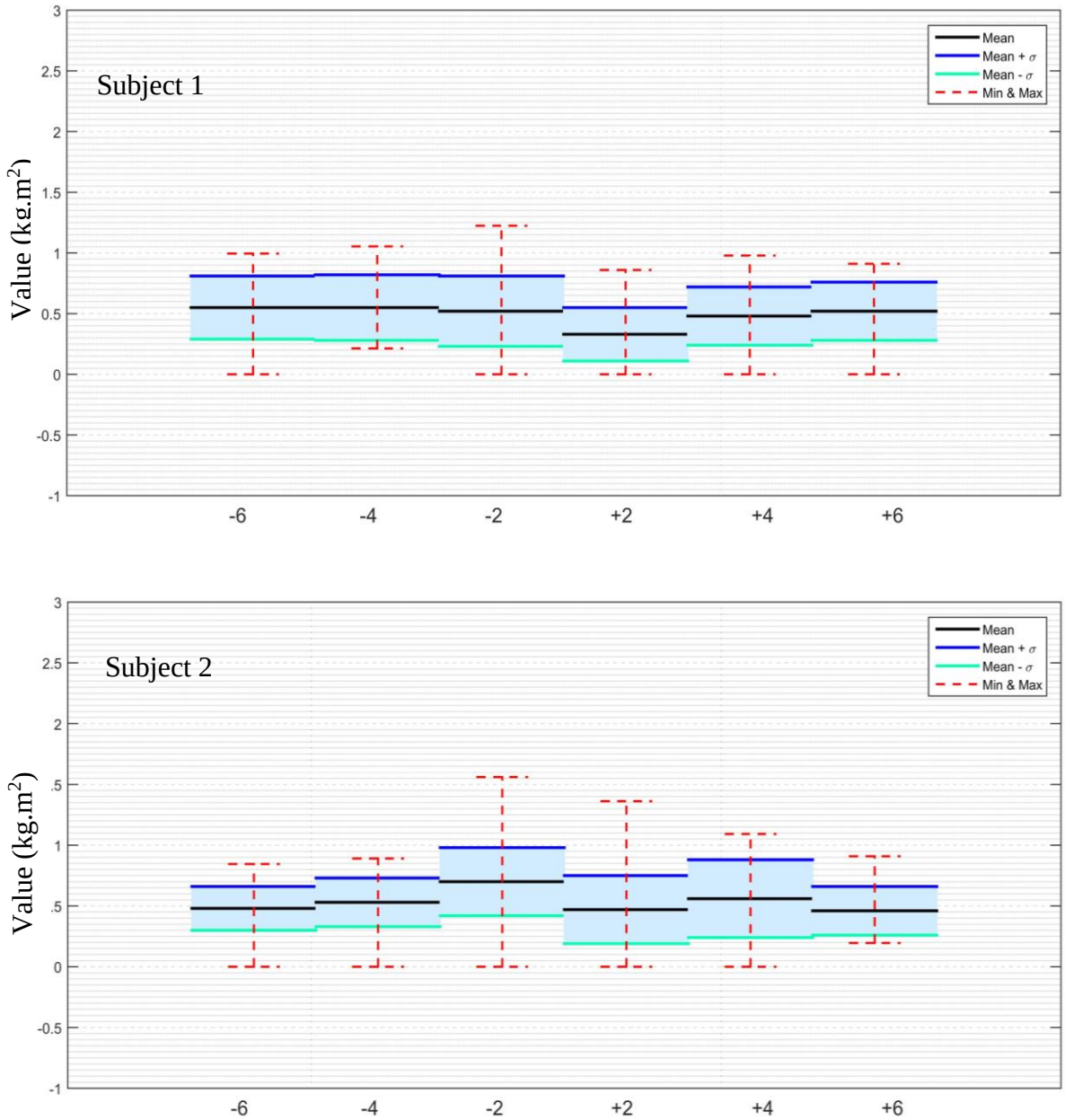

Figure 4.3 estimation of parameter "*I*" for subjects 1 and 2

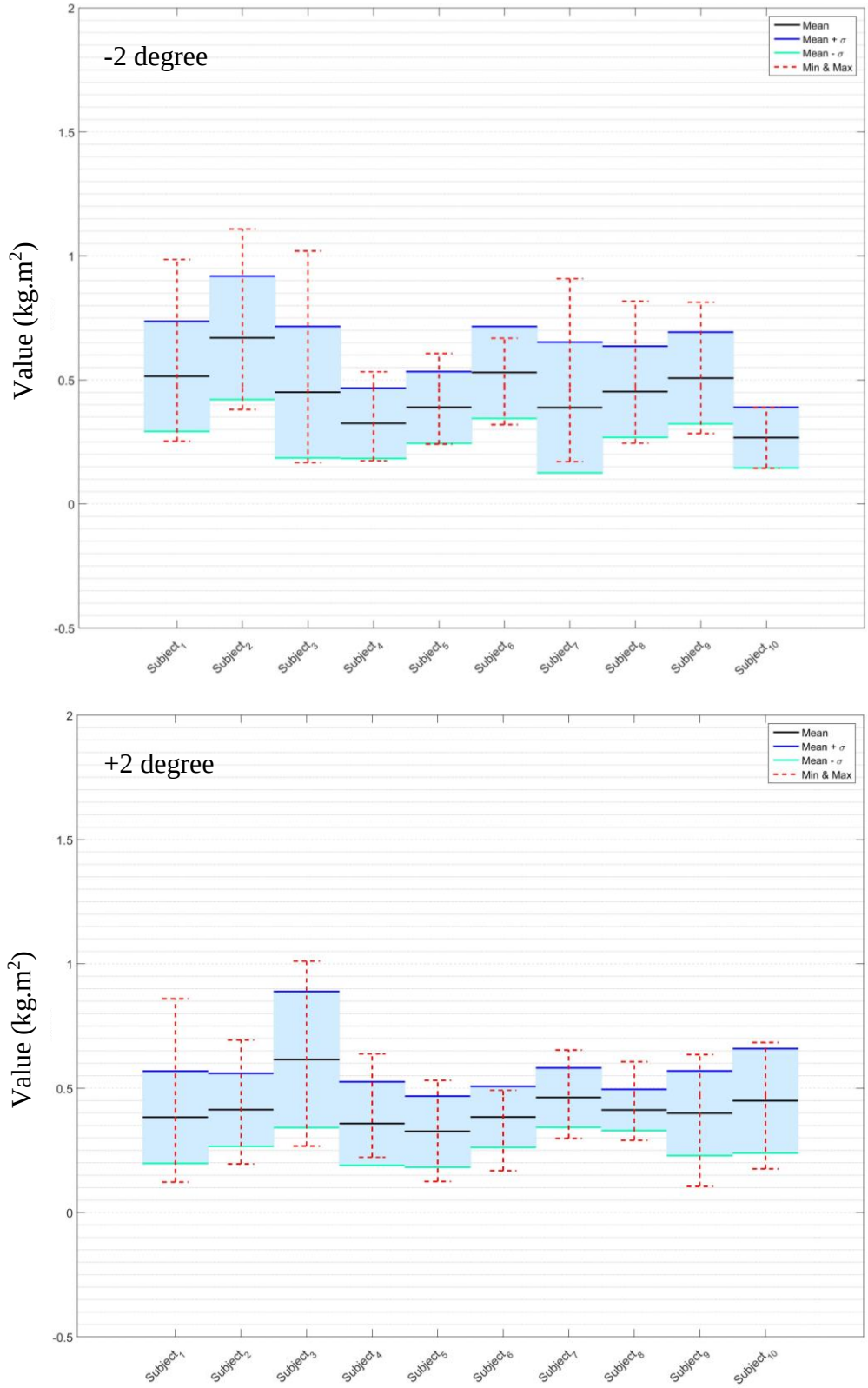

Figure 4.4 estimated values of parameter "I" for different subjects responses to ±2 deg

4.2.2 Effective mass

Comparing with the moment of inertia, the estimated numerical values of effective mass had more consistency. Figure 4.5 shows the results for subjects 1 and 2. The results for target -4 degree and +4 degree are shown in the Figure 4.6. It is observable that most of the results are close to 8.4 kg with a small standard deviation. However, the estimated values for mass in responses to the target of +2 degree had larger standard deviation values. Figure 4.7 shows the estimated values for mass in the tracking tasks of ±2 degree. Observation of the results for the paramter *"m"* raises two opinions.

One of the opinions states that the proposed model for this dynamic system takes the same value of mass into account for all human subjects. That means the parameter *"m"* is an independent parameter in the mathematical model and is not a specification of individual subject. This parameter is approximately 8.4 *kg* for this specific type of motion of human body. It does not change if the model would be used for different human subjects.

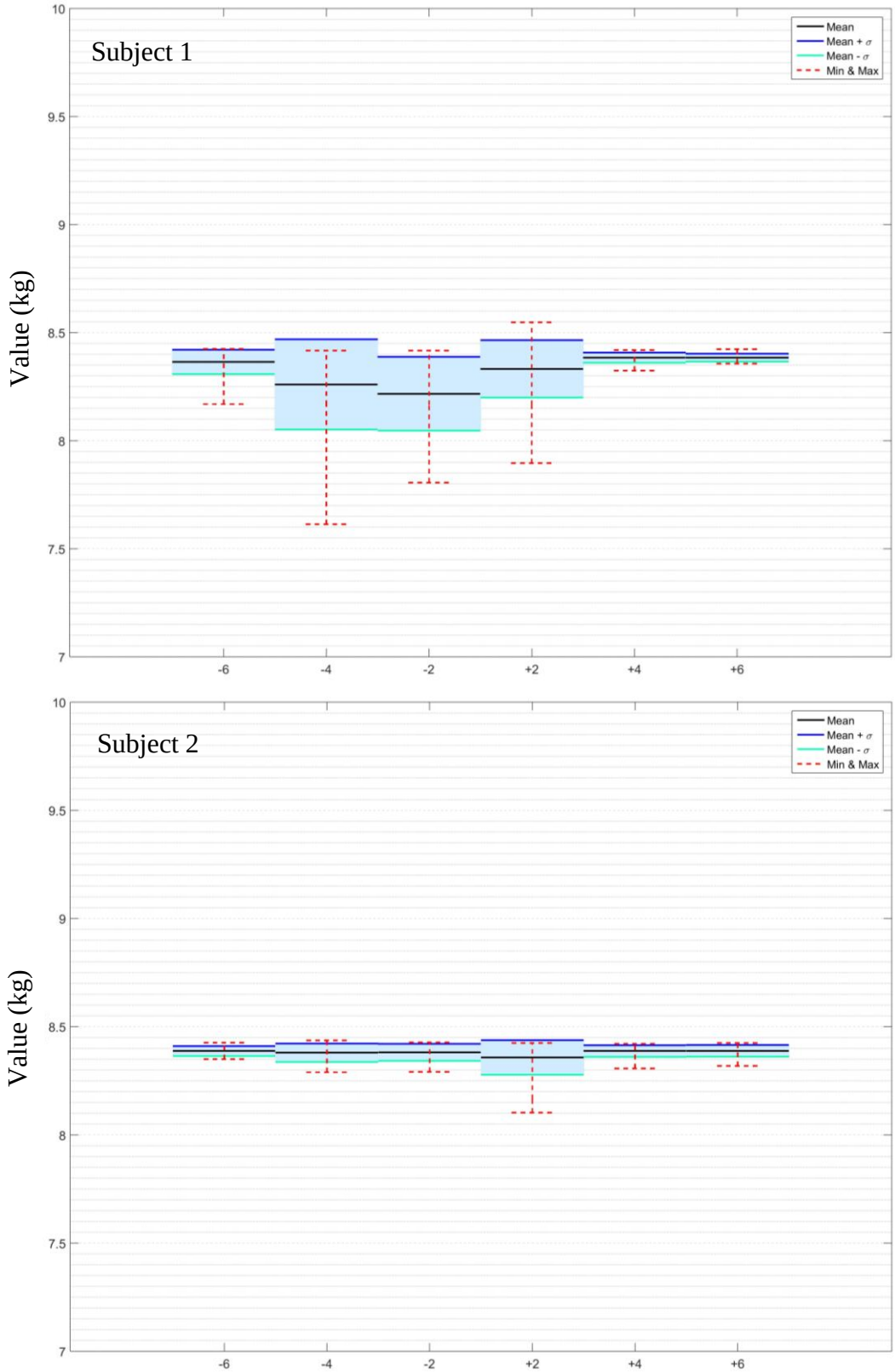

Figure 4.5 estimation of parameter "*m*" for subjects 1 and 2

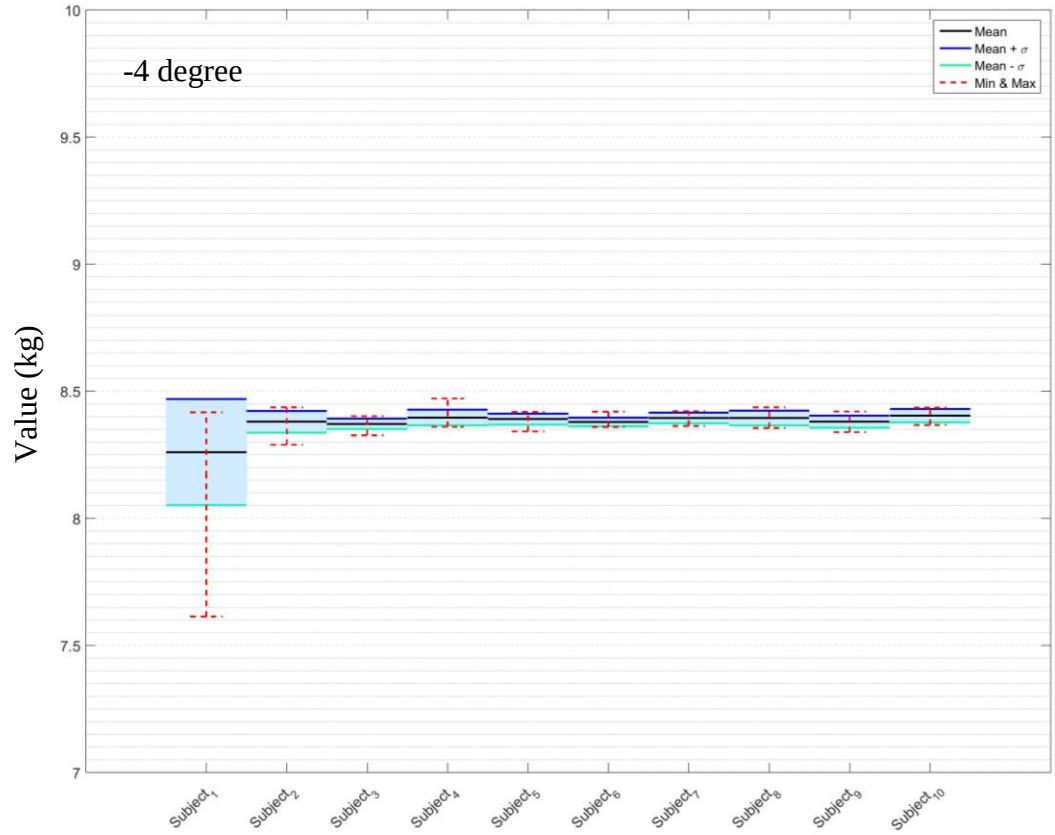

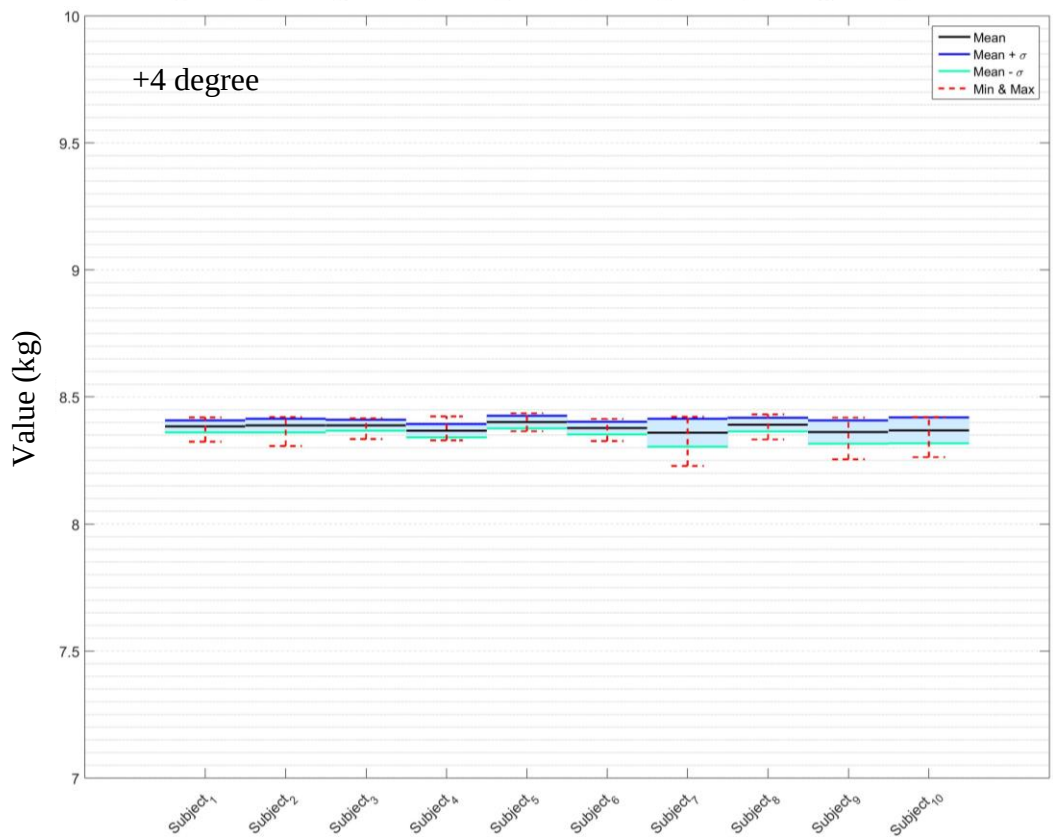

Figure 4.6 estimated values of parameter "*m*" for different subjects responses to ±4 deg

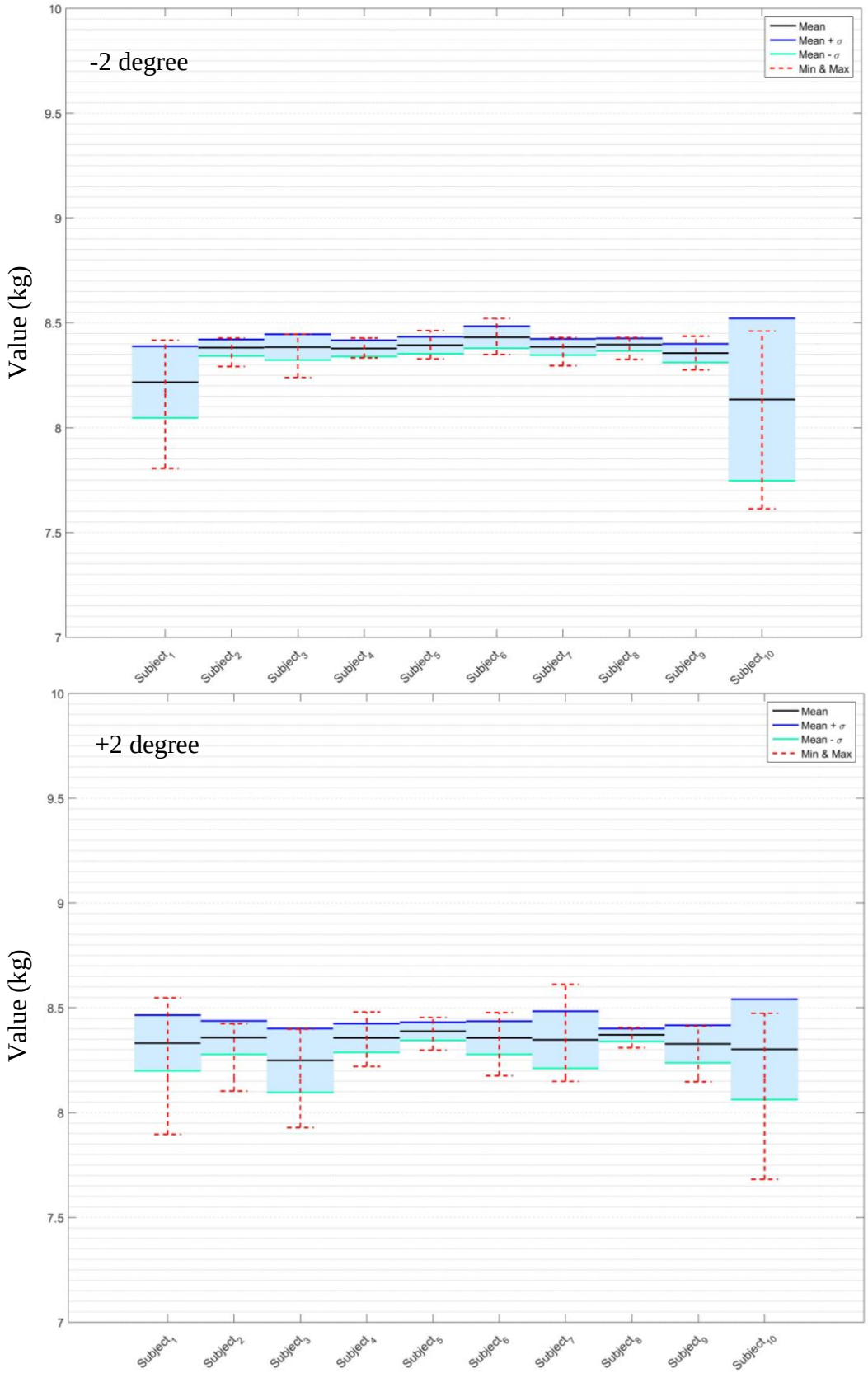

Figure 4.7 estimated values of parameter "*m*" for different subjects responses to ±2 deg

Another opinion expresses that the sensitivity of this parameter with respect to change of human subject is very low. Different human subjects have different anatomies. The difference in anatomy does not make a considerable difference in the parameter *"m"* in the defined mathematical model of this system's dynamics. Table 4.2 is a comprehensive representation of the results for the effective mass in kg.

Table 4.2: Mean of estimated values for parameter *m* (standard deviations in the parenthesis)

	Target (input signal)					
Subject No.	-6°	-4°	-2°	2°	4°	6°
1	8.37 (0.06)	8.26 (0.21)	8.22 (0.17)	8.33 (0.13)	8.38 (0.02)	8.38 (0.02)
2	8.39 (0.02)	8.38 (0.04)	8.38 (0.04)	8.36 (0.08)	8.39 (0.03)	8.39 (0.03)
3	8.39 (0.02)	8.37 (0.02)	8.38 (0.06)	8.25 (0.15)	8.39 (0.02)	8.39 (0.03)
4	8.39 (0.02)	8.40 (0.03)	8.38 (0.04)	8.36 (0.07)	8.37 (0.03)	8.38 (0.03)
5	8.41 (0.02)	8.39 (0.02)	8.39 (0.04)	8.39 (0.04)	8.40 (0.03)	8.40 (0.02)
6	8.39 (0.02)	8.38 (0.02)	8.43 (0.05)	8.36 (0.08)	8.38 (0.03)	8.38 (0.03)
7	8.39 (0.02)	8.39 (0.02)	8.38 (0.04)	8.35 (0.14)	8.36 (0.06)	8.38 (0.04)
8	8.40 (0.02)	8.39 (0.03)	8.40 (0.03)	8.37 (0.03)	8.39 (0.03)	8.40 (0.02)
9	8.38 (0.03)	8.38 (0.02)	8.36 (0.04)	8.33 (0.09)	8.36 (0.05)	8.39 (0.04)
10	8.31 (0.23)	8.40 (0.03)	8.13 (0.39)	8.30 (0.24)	8.37 (0.05)	8.34 (0.07)

4.2.3 Effective length

Parameter *"L"* of the model represents the effective length of rotation defined as the distance of the effective mass from the center of rotation (pelvis). Figure 4.8 shows the estimated effective length for subjects 1 and 2 for all values of the input signals. Also, Figure 4.9 displays the same result for all the subjects to input signals of ±6 degree.

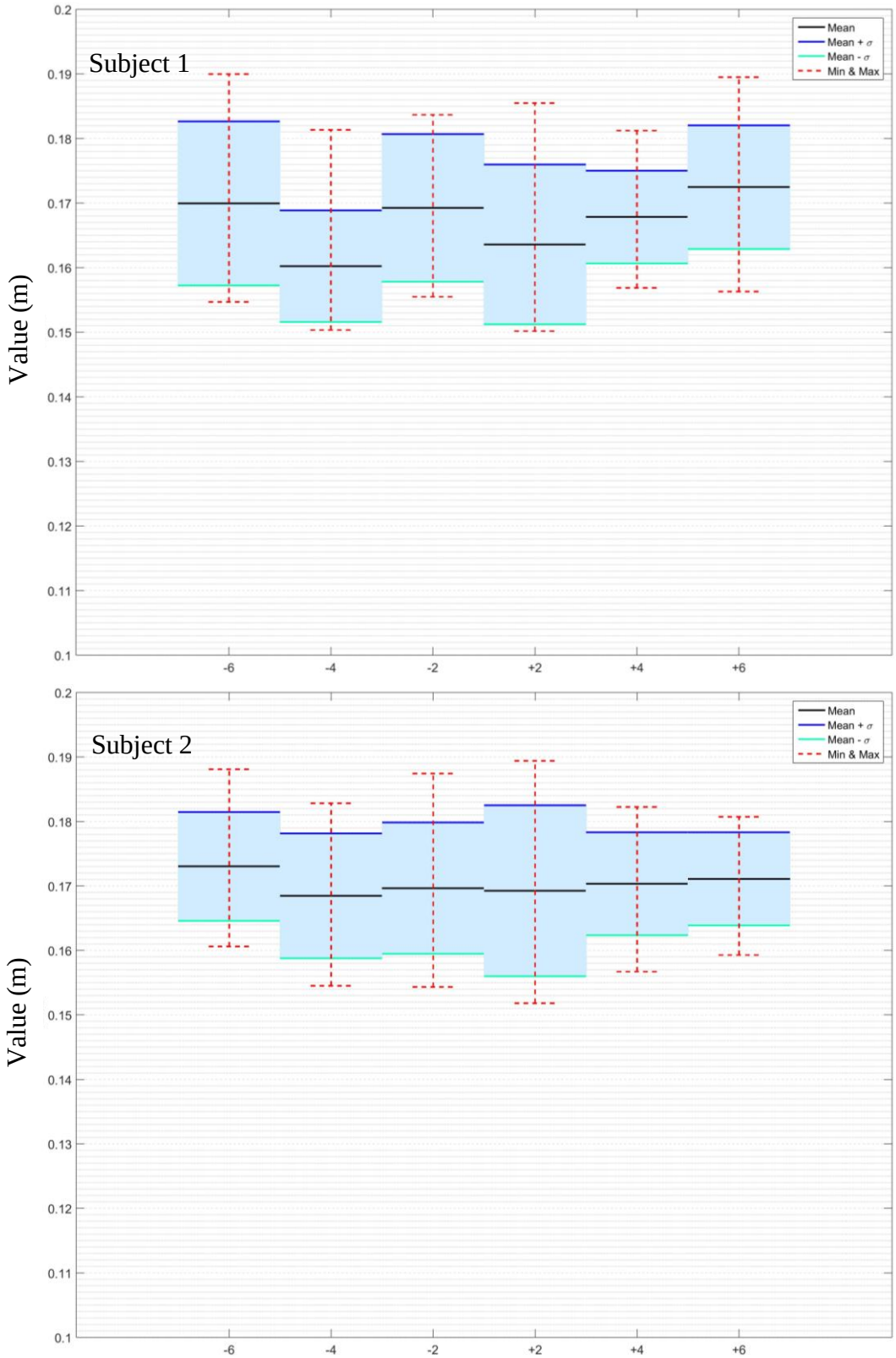

Figure 4.8 estimation of parameter "*l*" for subjects 1 and 2

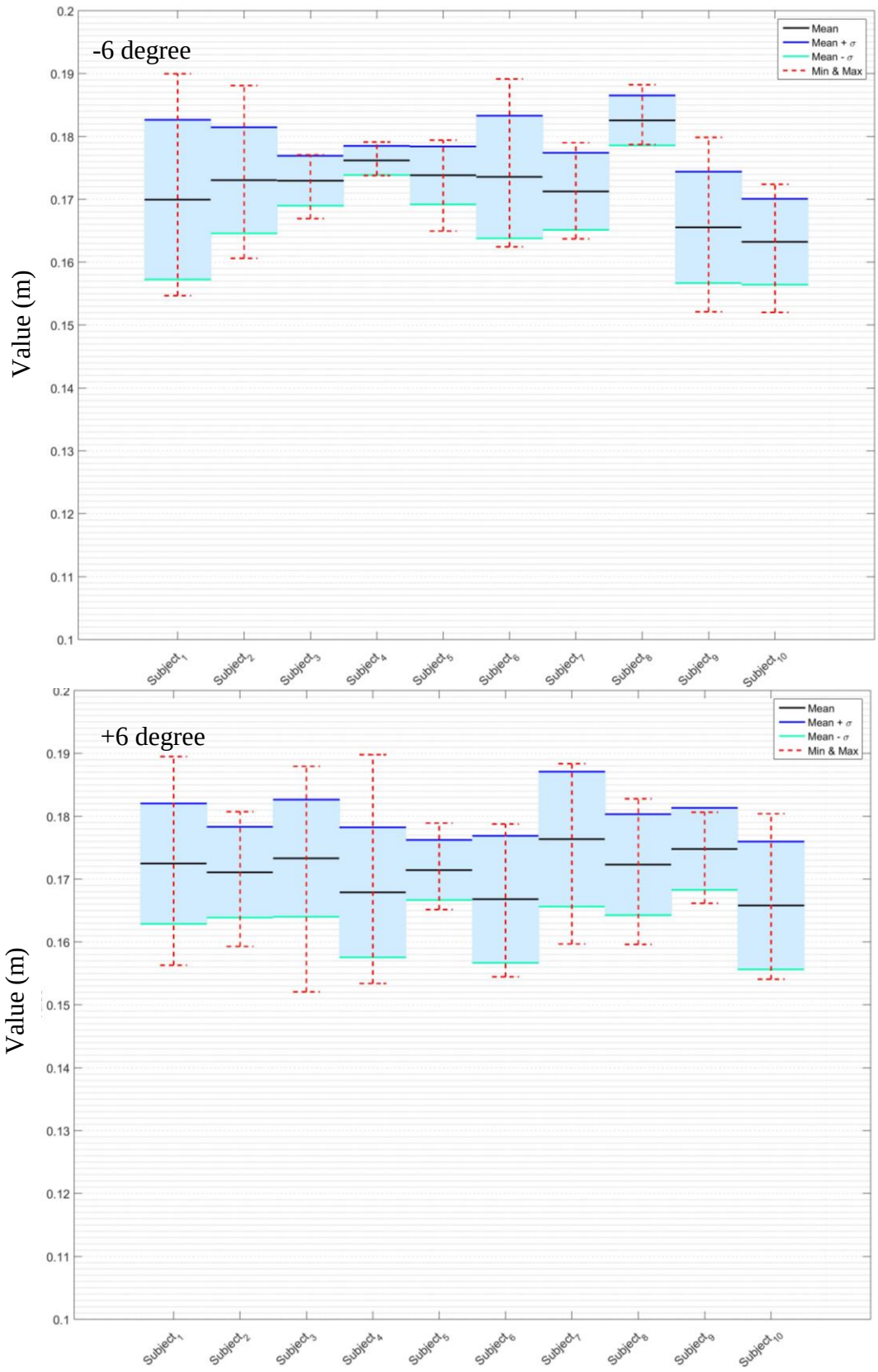

Figure 4.9 estimated values of parameter "*l*" for different subjects responses to ±6 deg

It may be observable from the figures that the estimated values for the parameter *"L"* are mostly ranging between 0.16 to 0.18 meters. By comparing the results with the references, they were fairly close to the expected values based on subject height [55]. Table 4.3 represents the average of estimated numerical values for the parameter *"L"*.

Table 4.3: Mean of estimated values for parameter *L* (standard deviations in the parenthesis)

	Target (input signal)					
Subject No.	-6	-4	-2	2	4	6
1	0.17 (0.01)	0.16 (0.01)	0.17 (0.01)	0.16 (0.01)	0.17 (0.01)	0.17 (0.01)
2	0.17 (0.01)	0.17 (0.01)	0.17 (0.01)	0.17 (0.01)	0.17 (0.01)	0.17 (0.01)
3	0.17 (0.00)	0.17 (0.01)	0.17 (0.01)	0.17 (0.01)	0.17 (0.01)	0.17 (0.01)
4	0.18 (0.00)	0.17 (0.01)	0.17 (0.01)	0.17 (0.02)	0.17 (0.01)	0.17 (0.01)
5	0.17 (0.01)	0.17 (0.00)	0.17 (0.00)	0.17 (0.01)	0.17 (0.01)	0.17 (0.01)
6	0.17 (0.01)	0.17 (0.01)	0.17 (0.01)	0.16 (0.01)	0.17 (0.01)	0.17 (0.01)
7	0.17 (0.01)	0.17 (0.01)	0.17 (0.01)	0.17 (0.01)	0.16 (0.01)	0.18 (0.01)
8	0.18 (0.00)	0.18 (0.01)	0.17 (0.01)	0.17 (0.01)	0.17 (0.01)	0.17 (0.01)
9	0.17 (0.01)	0.17 (0.01)	0.17 (0.01)	0.16 (0.01)	0.17 (0.01)	0.17 (0.01)
10	0.16 (0.01)	0.18 (0.01)	0.17 (0.01)	0.17 (0.01)	0.17 (0.01)	0.17 (0.01)

All of the values in the table above range from 0.16 to 0.18 meters with the standard deviation of 0.01 meter. It brings up the same theories that were mentioned for the parameter *"m"*. Hence, it can be stated that the parameter *"L"* in the model of this specific system and specific motion is independent of the subject who is performing the tracking experiment. Or, based on the other theory, the sensivity of parameeter *"L"* to the change of subject is very low and can be neglected.

4.2.4 Delay

It was mentioned in the method section that all the subjects had a time delay before responding to a change in the input signal. The term *"$e^{-\tau s}$"* of the mathematical model in Laplace domain was associated with the time delay showed by *"τ"*. Since the time delay was observed to change with both the magnitude/direction of the input signal and for each human subjects, we decided to

estimate is using the optimization cost function. Figure 4.10 shows the estimated values of *"τ"* for subjects 1 and 2. Also, Figure 4.11 is shows the estimated values of *"τ"* for all subjects at an input signal of ±2 degree. A trend was noticed in this figure. By looking at the Figure 4.11, it turns out that there is a decrease in time delay moving from subject 1 toward subject 5. And again, in both plots it is observable that the estimated time delay increases moving from subject 5 toward subject 8. Figure 4.12 shows the same trend for the responses of all of the subjects to the input signals of ±4 degree. The mentioned trend is shown by the striped orange line on the Figure 4.12. This trend was also seen in the plots of responses to the targets ±6 degree which is found in the appendix. Table 4.4 represents the mean values of time delay for different subjects and different targets. The unit for time delay is the second. The discussed observation is also noticeable on Table 4.4. Hence, we can state that the subjects 3 and 4 have the lowest time delay in the response to the target among all the subjects. It could be influencing the bandwidth and bandwidth frequency of the corresponded subjects considerably. Because one of the determinative parameters in calculation of bandwidth frequency is the time delay before starting to track the target position.

It is important to note that the subject numbering is arbitrary. Thus pattern observed in the time delay results only show that there are similarities in resonse time for subjects at different aplitudes of the input signal. This is logical because the time dealy is attributed to the cognitive processign time and should not be affected by the aplitude of the input signal.

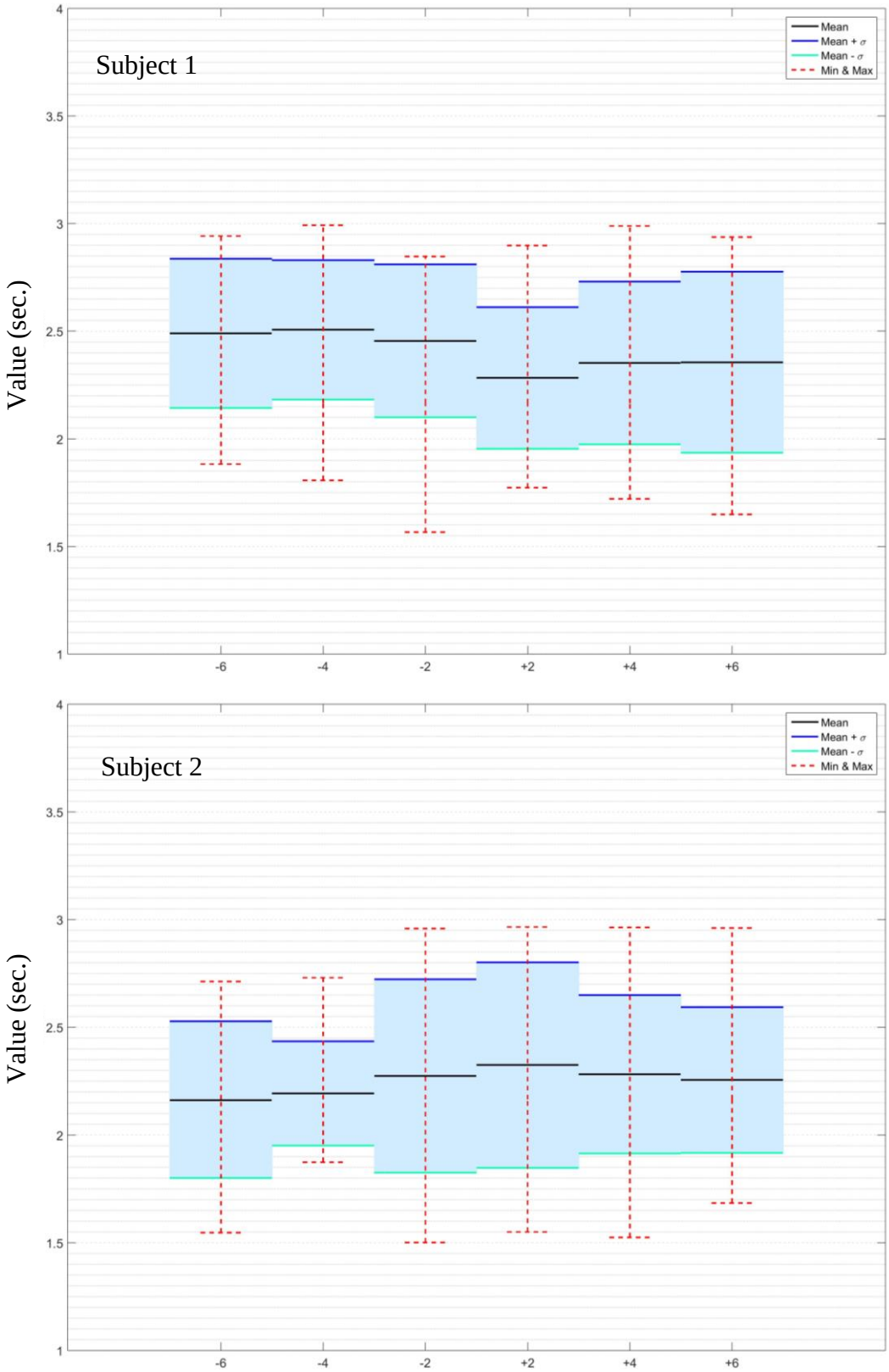

Figure 4.10 estimation of time delay for subjects 1 and 2

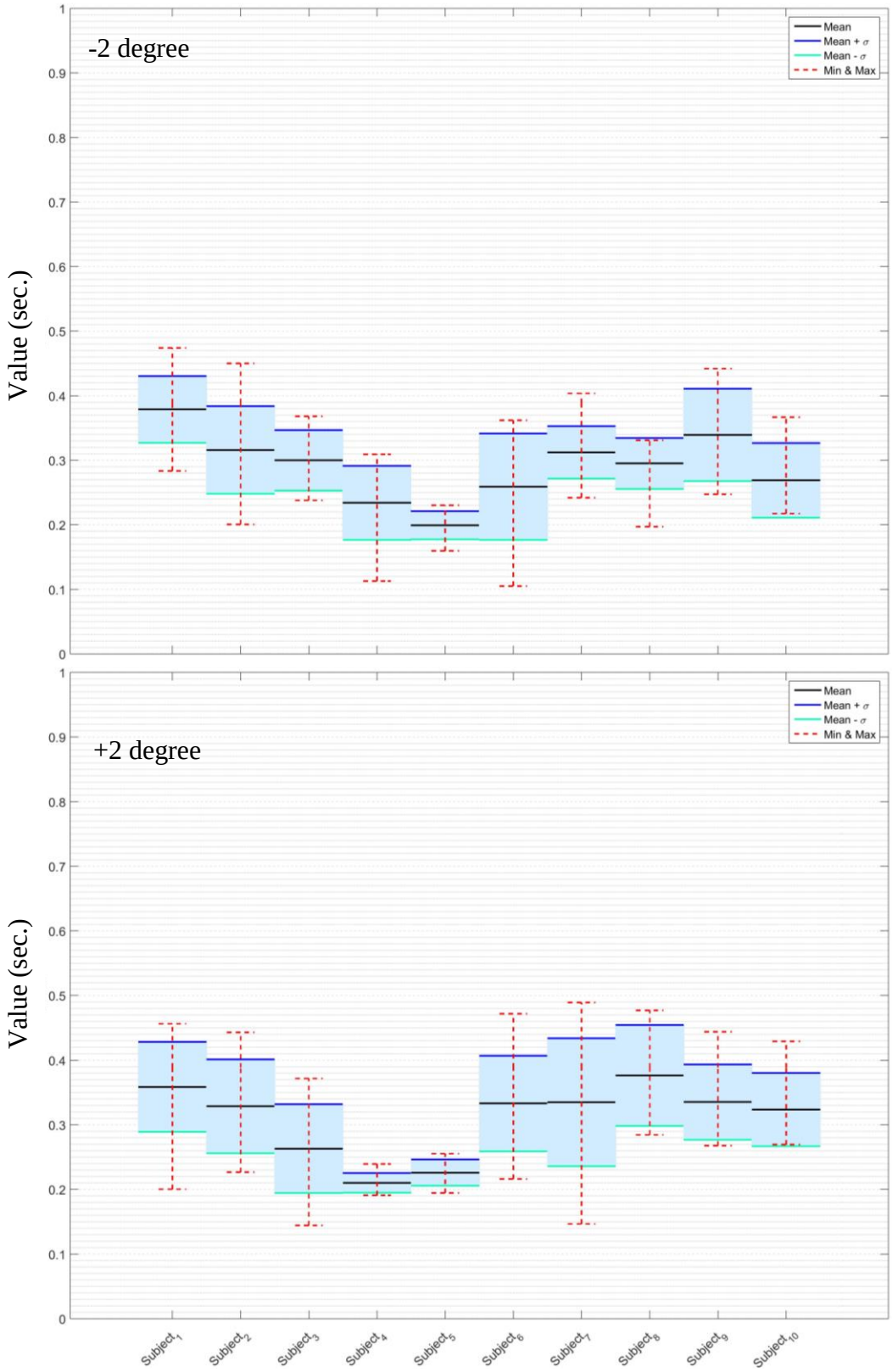

Figure 4.11 estimated values of time delay for different subjects responses to ±2 deg

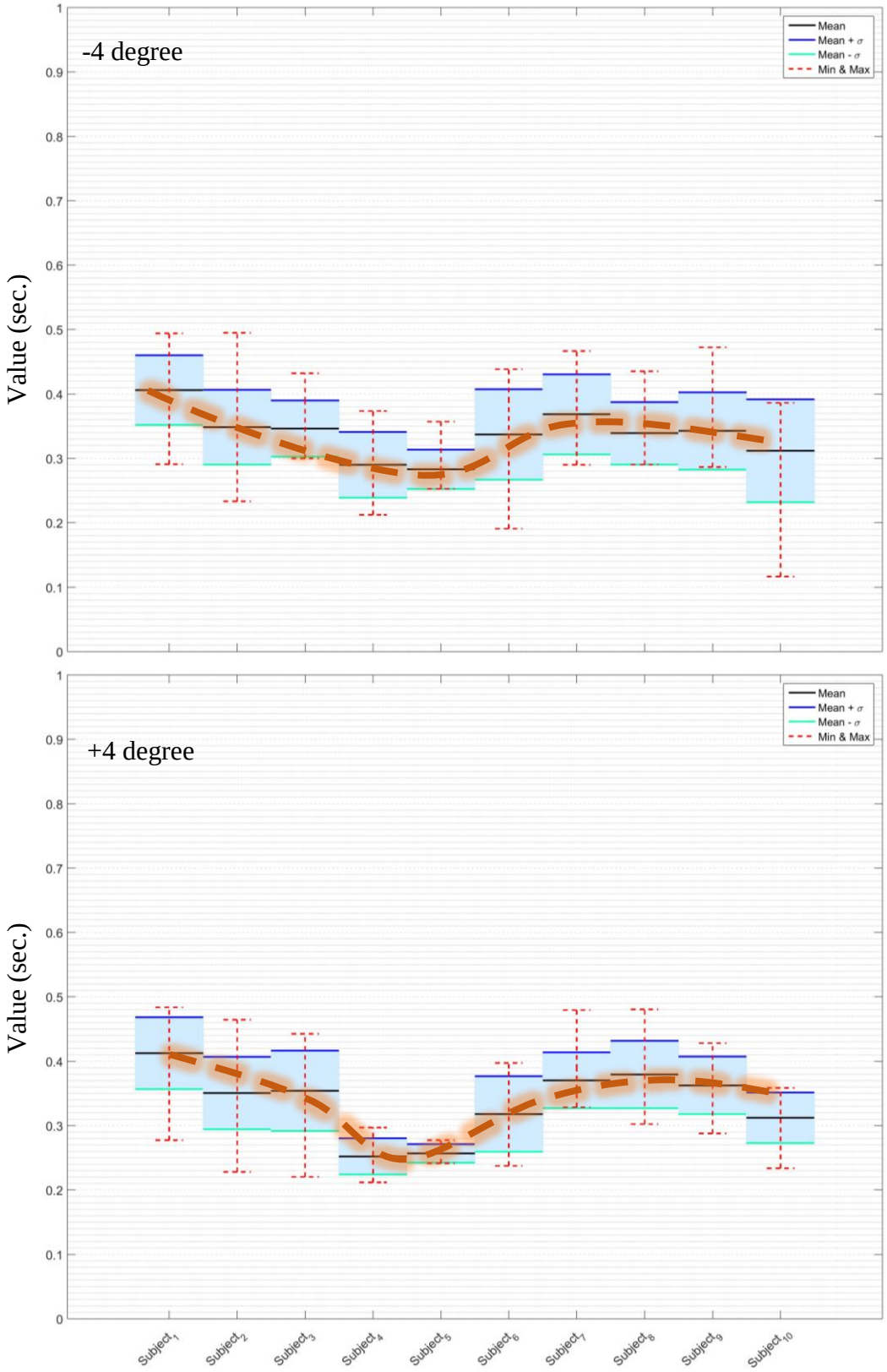

Figure 4.12 estimated values of time delay for different subjects responses to ±4 deg

Table 4.4: Mean of estimated values for parameter τ (standard deviations in the parenthesis)

	Target (input signal)					
Subject No.	-6	-4	-2	2	4	6
1	0.41 (0.06)	0.41 (0.05)	0.38 (0.05)	0.36 (0.07)	0.41 (0.06)	0.41 (0.05)
2	0.37 (0.04)	0.35 (0.06)	0.32 (0.07)	0.33 (0.07)	0.35 (0.06)	0.37 (0.05)
3	0.36 (0.03)	0.35 (0.04)	0.30 (0.05)	0.26 (0.07)	0.35 (0.06)	0.38 (0.04)
4	0.26 (0.03)	0.29 (0.05)	0.23 (0.06)	0.21 (0.01)	0.25 (0.03)	0.27 (0.04)
5	0.30 (0.03)	0.28 (0.03)	0.20 (0.02)	0.23 (0.02)	0.26 (0.01)	0.28 (0.05)
6	0.38 (0.06)	0.34 (0.07)	0.26 (0.08)	0.33 (0.07)	0.32 (0.06)	0.35 (0.07)
7	0.39 (0.03)	0.37 (0.06)	0.31 (0.04)	0.34 (0.10)	0.37 (0.04)	0.38 (0.04)
8	0.38 (0.04)	0.34 (0.05)	0.29 (0.04)	0.38 (0.08)	0.38 (0.05)	0.37 (0.04)
9	0.38 (0.05)	0.34 (0.06)	0.34 (0.07)	0.34 (0.06)	0.36 (0.04)	0.38 (0.06)
10	0.34 (0.04)	0.31 (0.08)	0.27 (0.06)	0.32 (0.06)	0.31 (0.04)	0.34 (0.04)

4.2.5 Stiffness coefficient

It was mentioned that the system was assigned a stiffness coefficient of *k*. This represents the stiffness of the torso. Torso stiffness is due to spinal ligaments, and passive muscle tone of the abdominal and back muscles. Figure 4.13 shows the estimated values torso stiffness for subject 1 and 2. Also, Figure 4.14 shows the torso stiffness all subjects resulting from a input signal of ±2 degrees. The plots for other subjects and other input signals are in the appendix. The unit of *"k"* is *"N·m / deg"*. Table 4.5 contains the mean values and standard deviation of estimated siffness coefficients for different subjects' responses to different targets. It may be observed from the figures and also the table that the values are similar to each other. The average results for this parameter range between 15 and 16 *N·m / deg*.

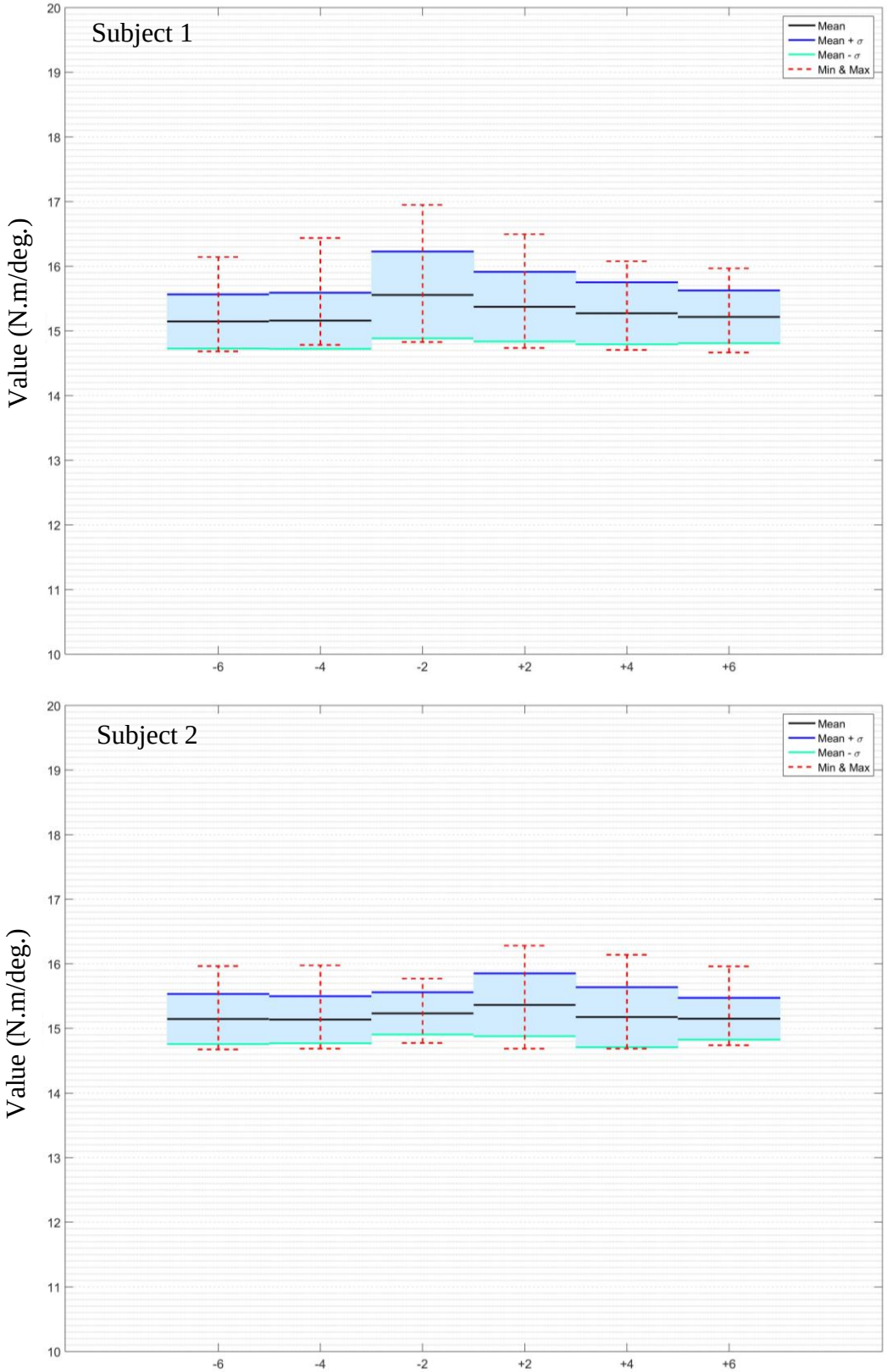

Figure 4.13 estimation of parameter "*k*" for subjects 1 and 2

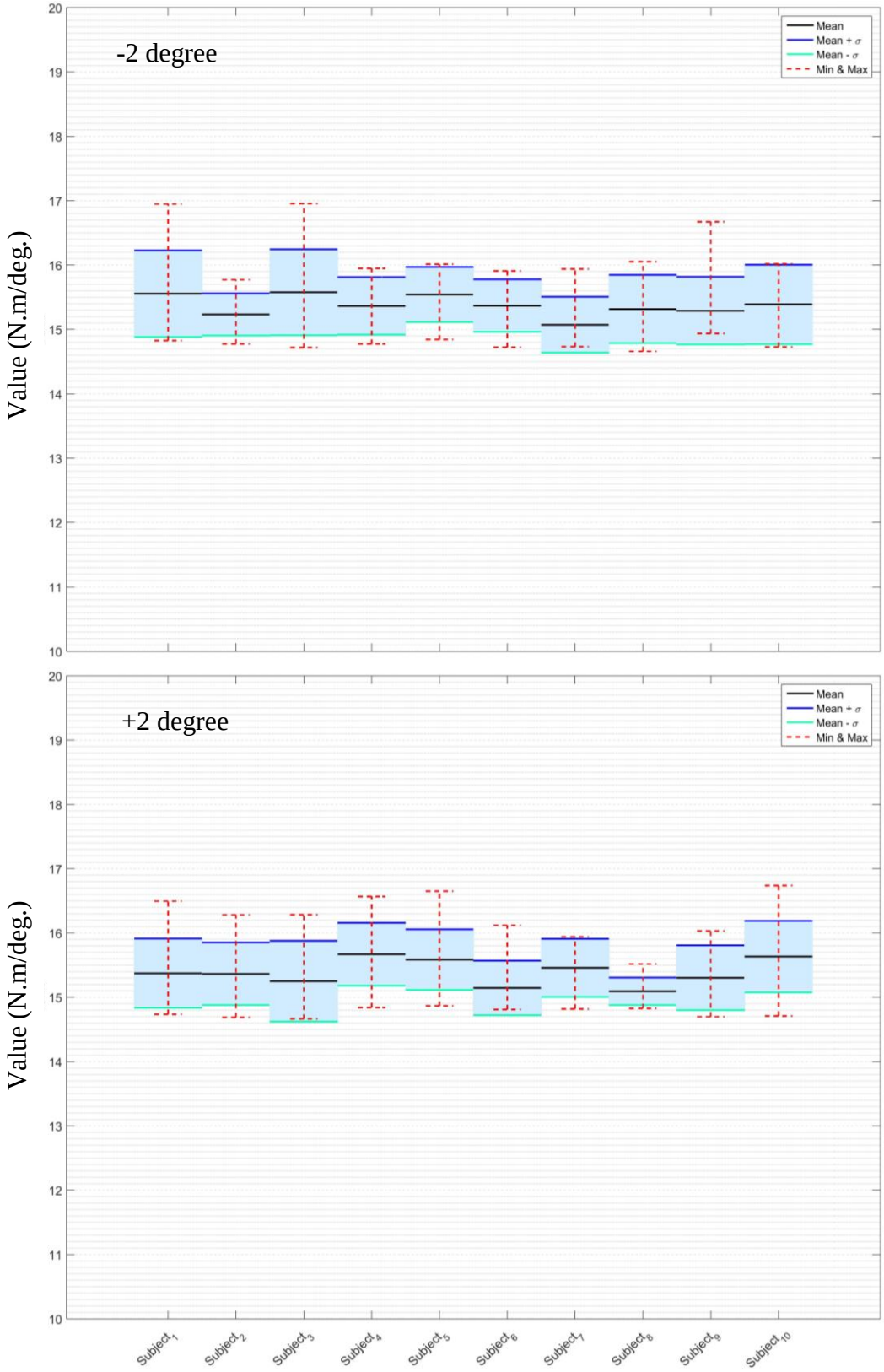

Figure 4.14 estimated values of parameter "*k*" for different subjects responses to ±2 deg

Table 4.5: Mean of estimated values for parameter *k* (standard deviations in the parenthesis)

	Target (input signal)					
#	-6	-4	-2	2	4	6
1	15.15 (0.42)	15.16 (0.43)	15.56 (0.67)	15.37 (0.54)	15.27 (0.48)	15.22 (0.41)
2	15.15 (0.39)	15.14 (0.36)	15.23 (0.33)	15.37 (0.49)	15.18 (0.47)	15.15 (0.32)
3	15.11 (0.31)	15.16 (0.34)	15.58 (0.67)	15.25 (0.63)	15.24 (0.43)	14.99 (0.21)
4	15.45 (0.29)	15.44 (0.35)	15.36 (0.45)	15.67 (0.49)	15.42 (0.42)	15.07 (0.26)
5	14.97 (0.20)	15.32 (0.73)	15.54 (0.43)	15.59 (0.47)	15.30 (0.36)	14.99 (0.33)
6	15.15 (0.47)	15.24 (0.37)	15.37 (0.41)	15.15 (0.42)	15.33 (0.38)	15.27 (0.41)
7	15.01 (0.22)	15.03 (0.21)	15.07 (0.43)	15.46 (0.45)	15.00 (0.36)	15.25 (0.34)
8	15.24 (0.21)	15.27 (0.33)	15.32 (0.53)	15.09 (0.21)	15.02 (0.20)	14.97 (0.15)
9	14.95 (0.18)	15.05 (0.48)	15.29 (0.53)	15.31 (0.50)	15.07 (0.43)	15.21 (0.35)
10	14.91 (0.25)	15.16 (0.28)	15.39 (0.62)	15.63 (0.56)	15.01 (0.28)	15.25 (0.41)

4.2.6 Damping coefficient

Viscous damping of the torso during the movement was assigned a value of *"b"*. Recall that this parameter represents the damping cause by interaction between internal tissues that consume energy in the system. Figure 4.15 shows the average estimated values for viscous damping for subjects 1 and 2. Figure 4.16 plots the mean values of *"b"* for all subjects with an input signal of ±2 degree. The unit of this parameter is *"N·m·s / deg."* Table 4.6 also shows the mean values of *"b"* for different subjects and different input signals. A pattern was observed in the results shown in Figure 4.16. The average of damping coefficient for different subjects and targets range from 25 to 30 *N·m·s / deg.* One may construct a theory that states that the viscous damping coefficient is dependent upon the subject who is performing the motion. It might also influence the bandwidth.

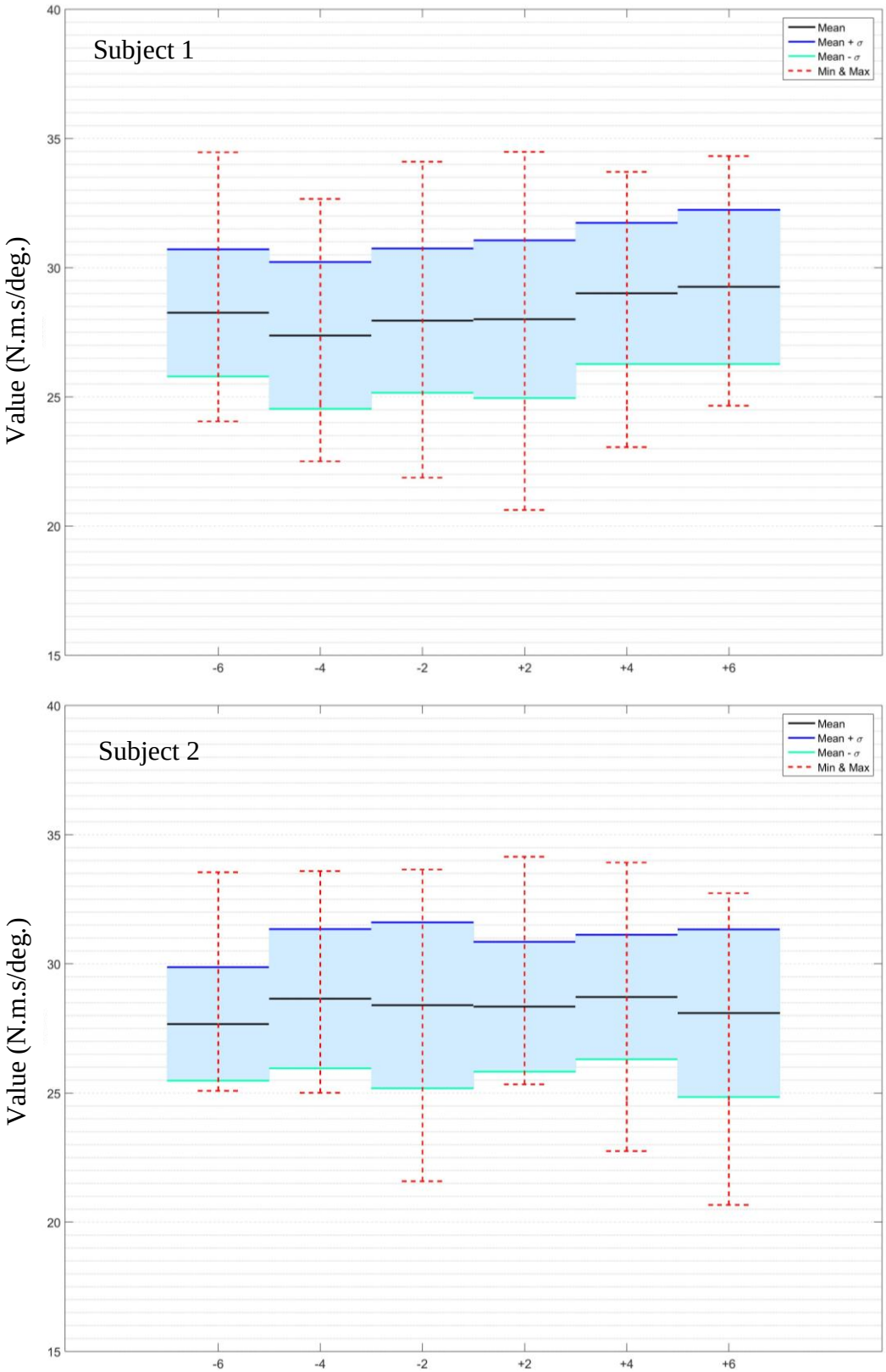

Figure 4.15 estimation of parameter "*b*" for subjects 1 and 2

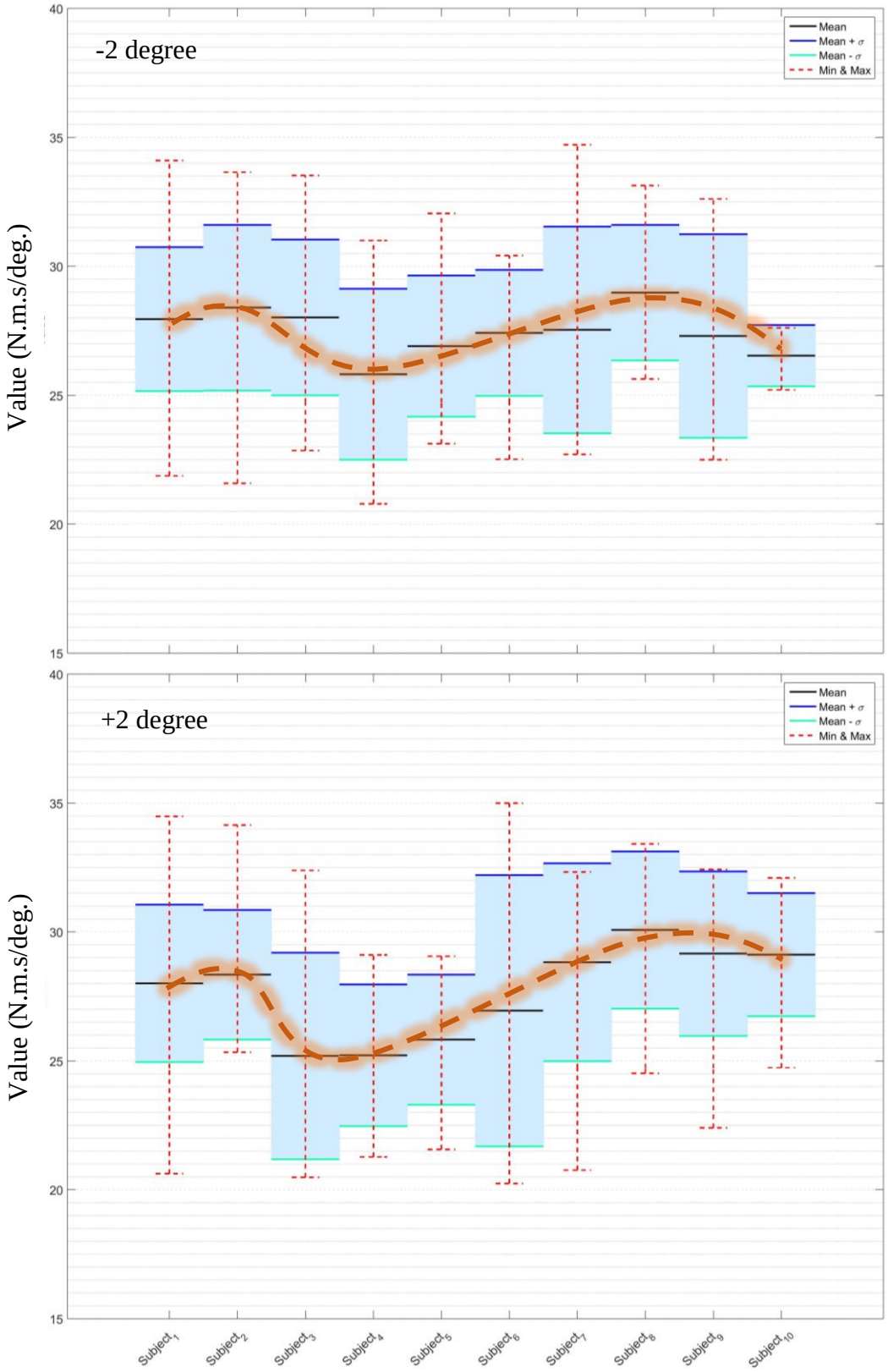

Figure 4.16 estimated values of parameter "*b*" for different subjects responses to ±2 deg

The pattern shown on the Figure 4.16 was observed for the targets -4, -6 and +6 degrees. The results for parameter *"b"* should be assessed to see if is there any correlation between the viscous damping ratio and the bandwidth frequency. Table 4.6 shows the mean values for the parameter *"b"*.

Table 4.6: Mean of estimated values for parameter *b* (standard deviations in the parenthesis)

	Target (input signal)					
#	-6	-4	-2	2	4	6
1	28.25 (2.46)	27.38 (2.84)	27.95 (2.79)	28.01 (3.06)	29.01 (2.73)	29.26 (2.98)
2	27.67 (2.20)	28.65 (2.69)	28.40 (3.21)	28.34 (2.51)	28.72 (2.41)	28.09 (3.24)
3	27.18 (2.80)	28.15 (2.72)	28.02 (3.02)	25.19 (4.01)	28.51 (3.14)	27.40 (2.28)
4	27.75 (3.25)	29.06 (2.94)	25.82 (3.32)	25.22 (2.75)	29.39 (4.75)	27.14 (3.98)
5	27.76 (2.69)	28.99 (2.52)	26.90 (2.74)	25.82 (2.52)	26.36 (1.94)	27.29 (2.88)
6	28.44 (3.45)	29.30 (3.16)	27.42 (2.44)	26.95 (5.26)	28.37 (3.32)	27.86 (3.24)
7	28.06 (2.21)	28.38 (3.38)	27.54 (4.01)	28.82 (3.84)	28.60 (3.44)	29.26 (2.71)
8	27.65 (2.95)	27.82 (2.38)	28.98 (2.63)	30.07 (3.05)	26.17 (2.28)	28.86 (1.10)
9	27.97 (3.50)	27.97 (2.52)	27.30 (3.94)	29.16 (3.19)	26.00 (2.79)	27.69 (3.18)
10	26.76 (2.63)	27.14 (3.33)	26.54 (1.19)	29.12 (2.39)	28.89 (2.02)	25.88 (2.33)

4.2.7 Proportional gain

The proportional controller was described in detail in the method section. The proportional gain of the controller was given the symbol *"G"* and it was optimized in the parameter estimation process. Figures 4.17 and 4.18 show the results for *"G"*. By observing Figures 4.18 and 4.19 a pattern seemed to develop. This pattern is shown by striped orange lines.

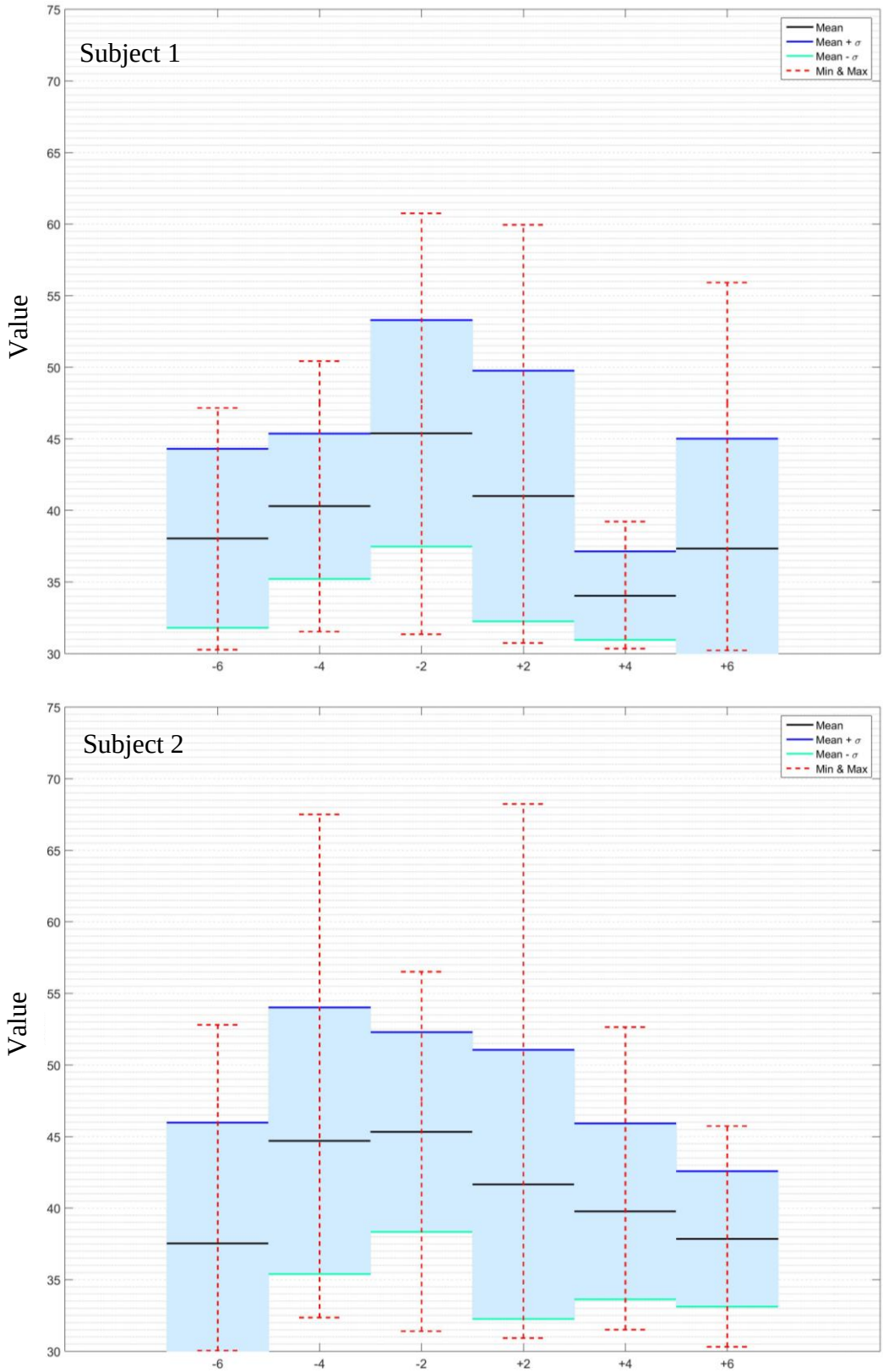

Figure 4.17 estimation of parameter "*G*" for subjects 1 and 2

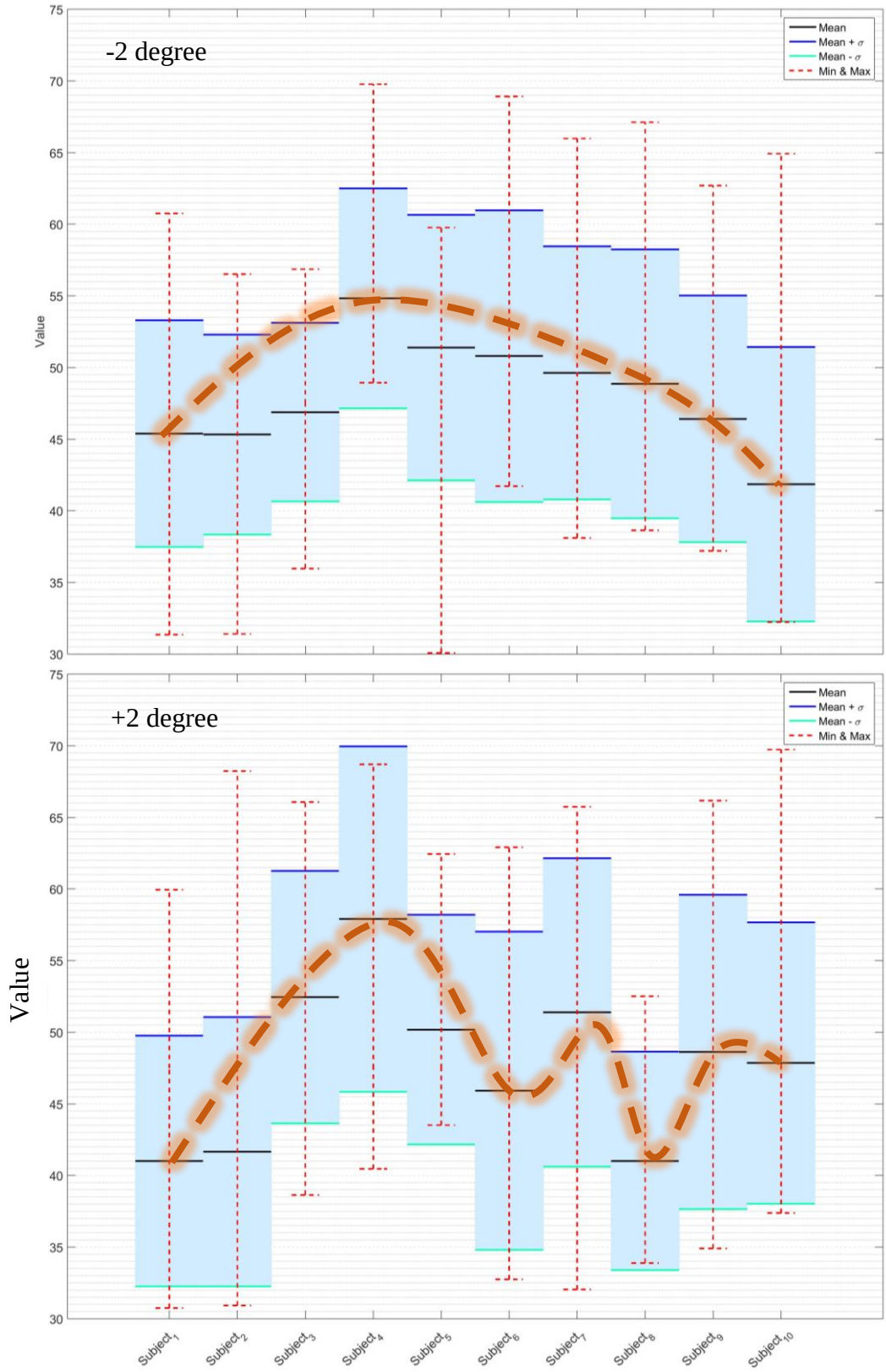

Figure 4.18 estimated values of parameter "*G*" for different subjects responses to ±2 deg

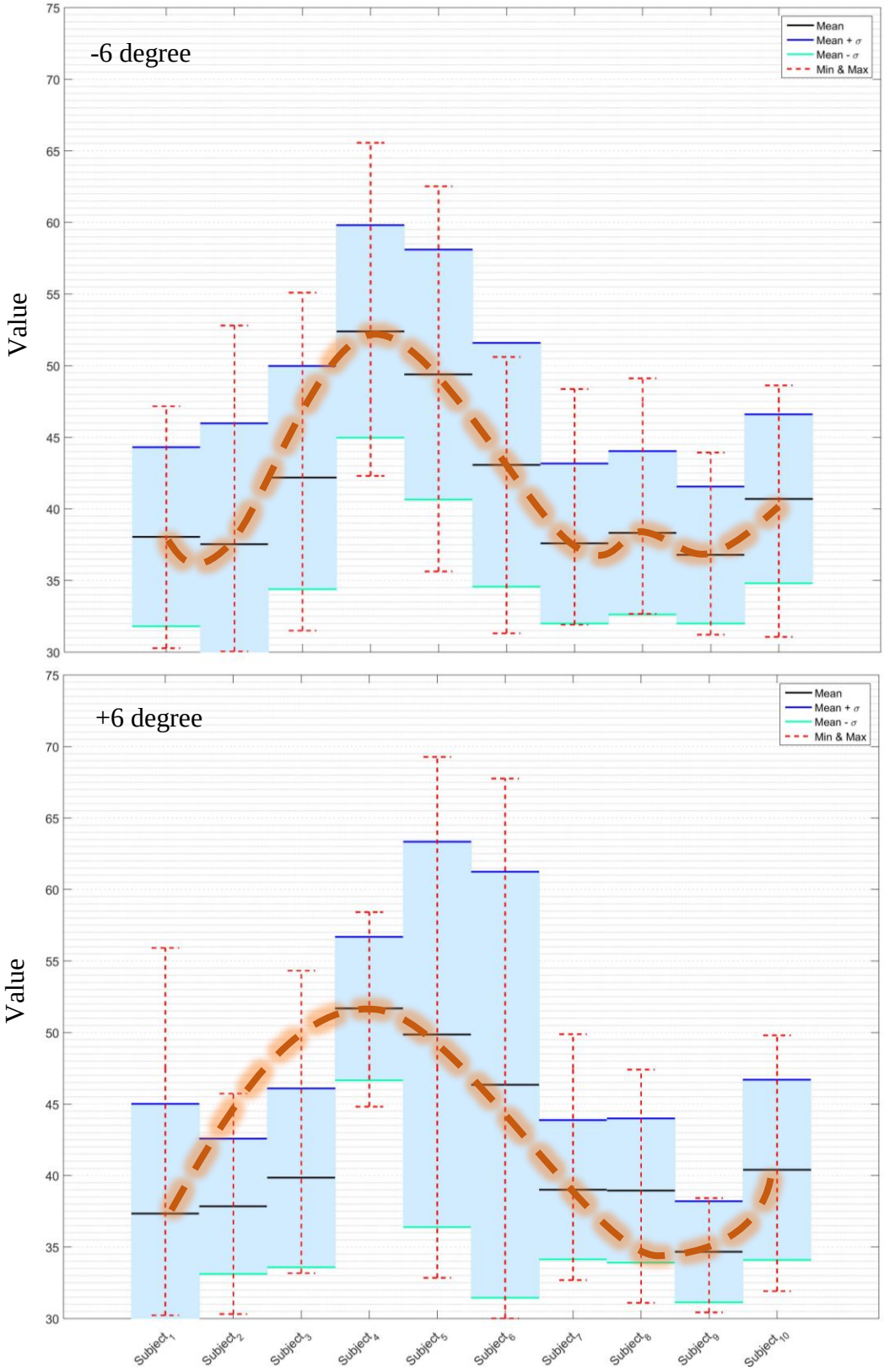

Figure 4.19 estimated values of parameter "*G*" for different subjects responses to ±6 deg

By looking at figures 4.17 through 4.19, it is observed that the estimated values for *"G"* range from 35 to 57. Moreover, it is noticed that the subject 4 has the maximum value of *"G"* among the estimated values for responses of all subjects to different input signals. Subject 4 also had the least estimated values for parameters *"b"* and *"τ"*. The estimated values of *"G"* for all subjects and all targets are shown in Table 4.7.

Table 4.7: Mean of estimated values for parameter *G* (standard deviations in the parenthesis)

	Target (input signal)					
#	-6	-4	-2	2	4	6
1	38.05 (06.25)	40.30 (05.07)	45.39 (07.91)	41.01 (08.75)	34.05 (03.09)	37.34 (07.68)
2	37.54 (08.43)	44.71 (09.31)	45.32 (06.98)	41.66 (09.39)	39.78 (06.14)	37.85 (04.72)
3	42.19 (07.79)	49.29 (12.89)	46.88 (06.23)	52.44 (08.81)	41.80 (07.30)	39.84 (06.25)
4	52.39 (07.42)	51.73 (07.03)	54.82 (07.68)	57.90 (12.06)	55.10 (07.61)	51.68 (05.01)
5	49.38 (08.72)	56.88 (08.60)	51.39 (09.26)	50.18 (08.02)	50.17 (08.45)	49.87 (13.48)
6	43.07 (08.51)	45.67 (06.89)	50.80 (10.17)	45.91 (11.11)	40.32 (07.07)	46.34 (14.90)
7	37.58 (05.59)	40.36 (06.25)	49.63 (08.83)	51.38 (10.76)	42.90 (10.20)	39.00 (04.86)
8	38.33 (05.70)	40.15 (05.26)	48.85 (09.38)	41.02 (07.63)	40.75 (05.78)	38.95 (05.04)
9	36.78 (04.78)	44.47 (05.82)	46.41 (08.60)	48.62 (10.97)	38.45 (04.97)	34.67 (03.53)
10	40.70 (05.90)	43.44 (10.24)	41.85 (09.57)	47.85 (09.82)	48.35 (09.67)	40.40 (06.30)

4.3 Simulation results

The optomized parameters values for each step response were imported into the Simulink model and a simulated response was generated. In total, 2400 simulation were performed representing all subjects, all condtions and all repetitions. Figures 4.20 and 4.21 show the simulated responses of subjects 1, 2, 3 and 4 and also the corresponded measured data for just one trial of each input signal.

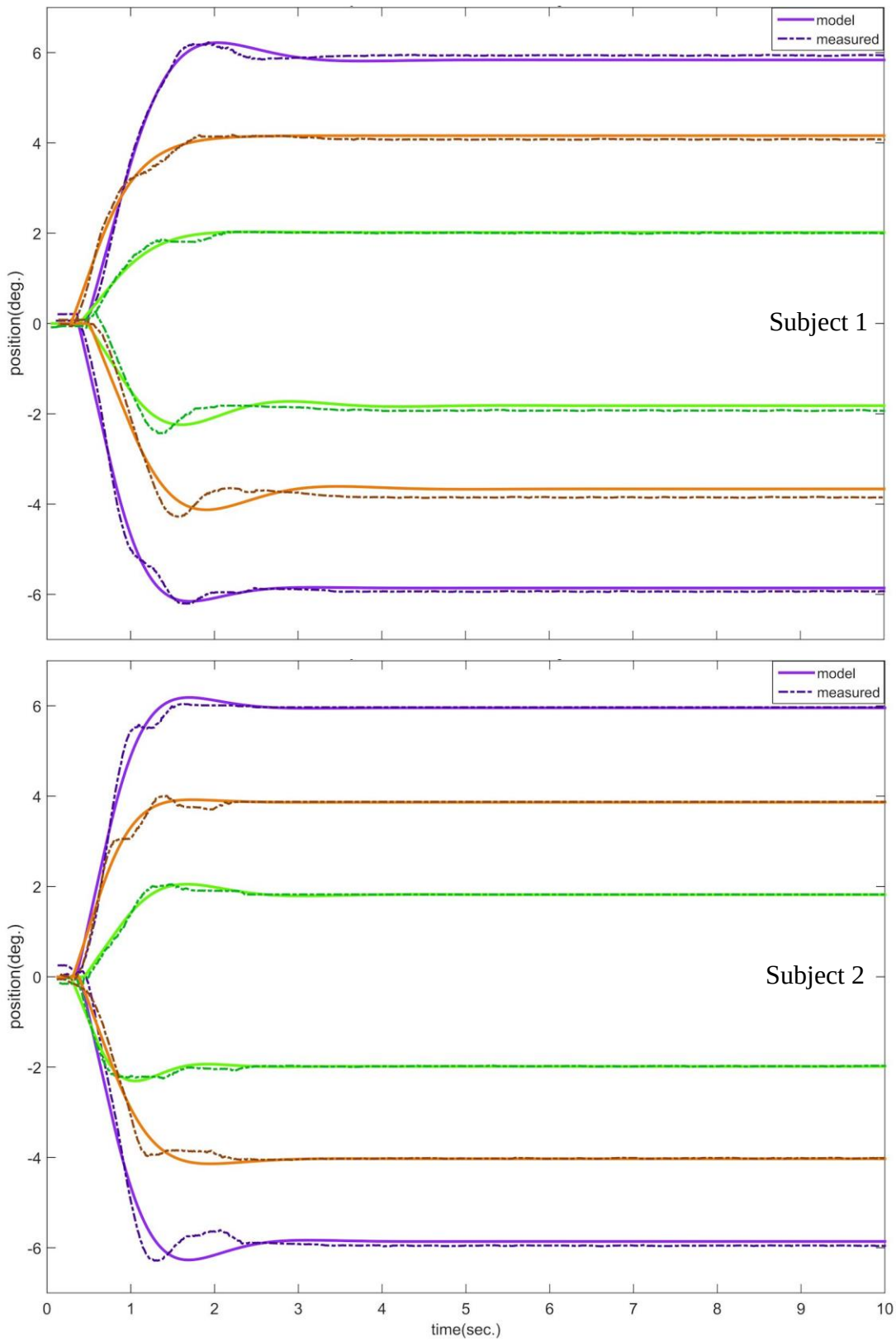

Figure 4.20 simulated and observed responses of subject 1 and 2

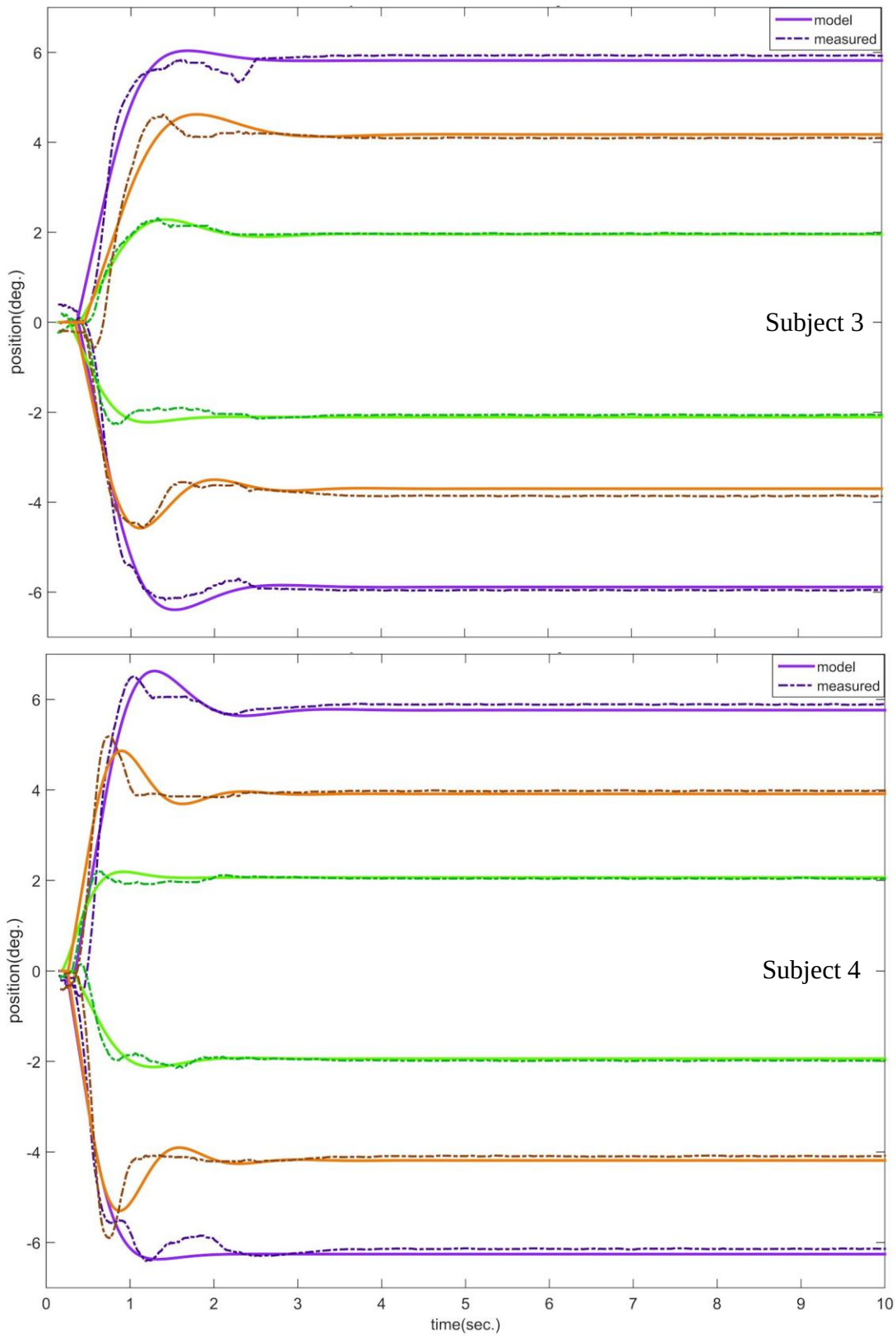

Figure 4.21 simulated and observed responses of subject 3 and 4

As it is seen in the figures, the simulated responses fit fairly well to the experimental data. There were a few cases where the simulated data was considerably different that the corresponded experimental data. These were eliminated and not used for the bandwidth calculation. Other plots of the simulated responses for other subjects are included in the appendix. Figure 4.22 is a comprehensive representation of all simulated reponses of subjects 1 and 2 to different input signals. The simulated responses were observed to be consistent for a given input signal. No irregular oscillation with high percentage of overshoot were seen. It demonstrates that the computational and mathematical methods used in the study have been reliable and able to reproduce the original signals.

It was essential to use simulated data that fit the experimental data well with a high fit percentage. Except in a few cases, the simulated response fit the corresponded experimental data with a fit percentage between 85% and 95%. Overall, the plots shown in the Figure 4.22 were generated by finding a solution for the equation (3.4) with estimated parameters in time interval [0 , 7].

An example of how the model parameters are applied to the dynamical system equation is shown below. Equation (3.4) was rewritten with one set of optimized parameter for subject 1's response to the input signal +2,

$$\begin{cases} \theta_{(t)} = 0 & 0 \leq t < 0.41 \\ 0.58\,\ddot{\theta}_{(t)} + 28.25\,\dot{\theta}_{(t)} + 15.15\,\theta_{(t)} = 38.05\,(2 - \theta_{(t)}) & 0.41 \leq t \end{cases} \tag{4.1}$$

Solving the differential equation (4.1) would result in the function of angular position for that specific subject's response to the selected input signal in the time domain.

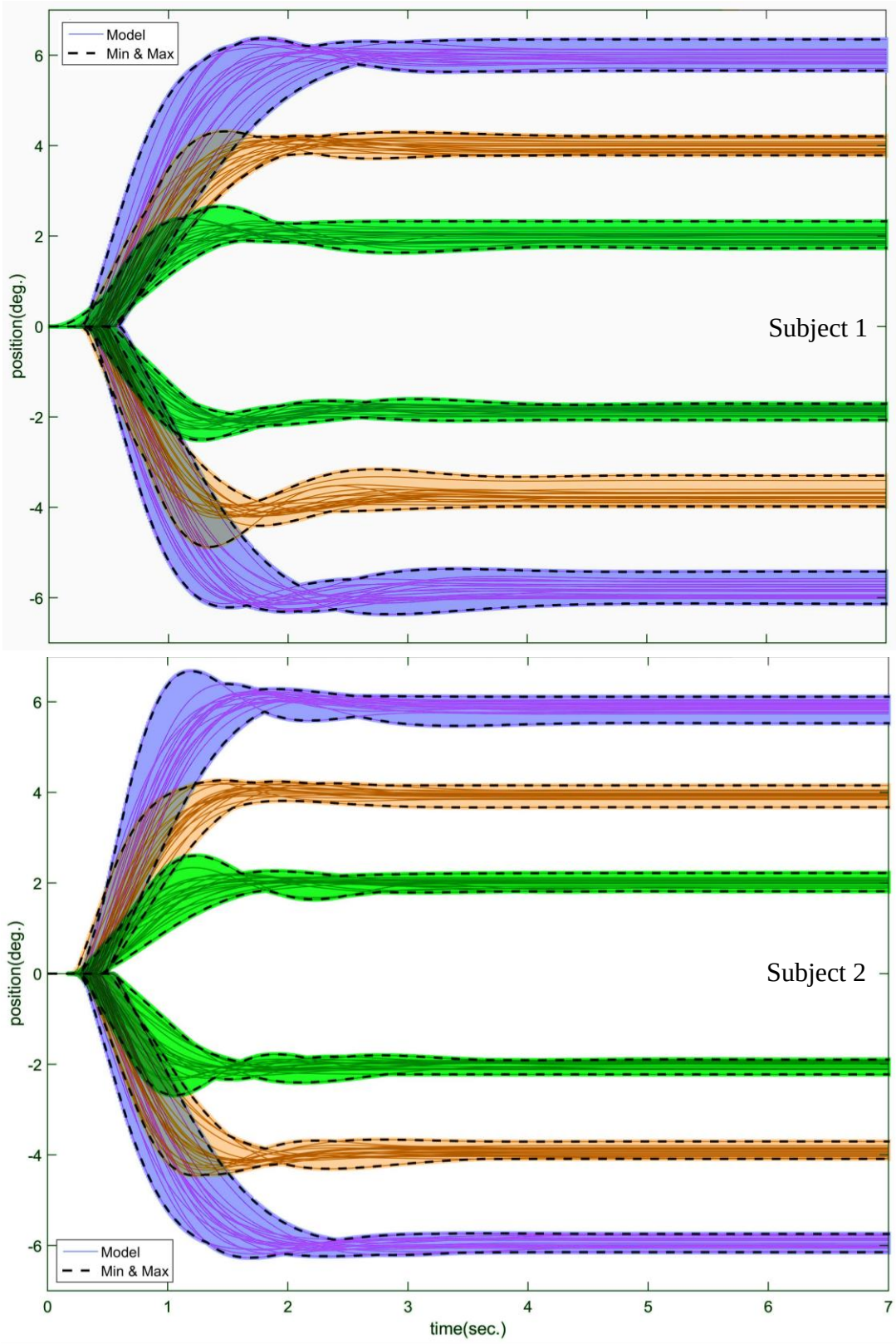

Figure 4.22 simulated responses of subjects 1 and 2

In order to have a better understanding of bandwidth, it is important to recognize its relation with other dynamical system characteristics such as percentage of overshoot and settling time. Figure 4.23 shows the percentage of overshoot for subjects 1 and 2. It was shown in all of the overshoot plots that smaller input signals caused a higher percentage of overshoot. It could be because of the high initial speed of reaction of subjects. As soon as the subject sees the input signal change on the screen, he/she immediately move his/her body toward the target. This may cause a relatively large angular displacement in the beginning of the tracking task.

It causes the subject to pass the small target and to start turning back toward it. However, due to the high angular velocity it requires time to stop the motion and change the direction. Moreover, at the same time that the subject is decreasing speed to change direction, he/she moves further from the target. This may explain the larger percentage of overshoot that is observable in the Figure 4.23 and also the Table 4.8. It is seen in the table and also in the figures that the percentage of overshoot for subjects is not more than 25%.

The other evaluated characteristic of the simulated models was the settling time. Recall that settling time is the time needed for the subject's position falls within a specified tolerance band around the target. A shorter settling time indicates the the system reaches steady state in a shorter time and is a good characteristic for a system. Figures 4.24 and 4.25 show the mean values of settling time for input signals of ±2 and ±4 degrees. It is observable that there is a decrease from subject 1 to subject 5 and then an increase from subject 5 to subject 10. This pattern is shown on the figures by the striped orange line.

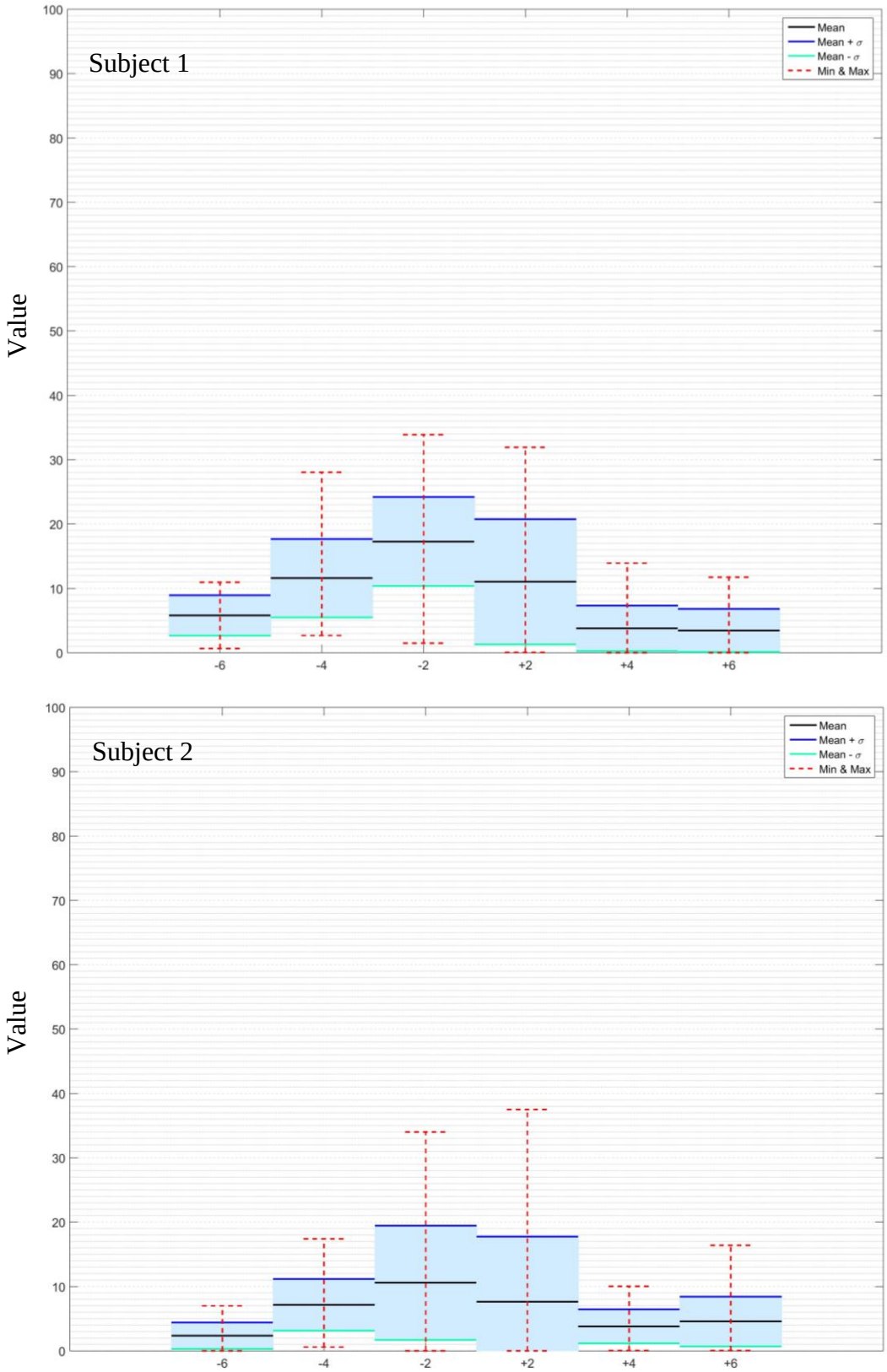

Figure 4.23 percentage of overshoot in responses of subjects 1 and 2

Table 4.8: Mean of percentage of overshoot (standard deviations in the parenthesis)

	Target (input signal)					
#	-6	-4	-2	2	4	6
1	05.80 (03.13)	11.58 (06.10)	17.28 (06.92)	11.04 (09.73)	03.81 (03.54)	03.46 (03.33)
2	02.35 (02.05)	07.14 (04.01)	10.58 (08.87)	07.63 (10.11)	03.81 (02.62)	04.57 (03.85)
3	06.90 (02.48)	10.26 (05.08)	12.33 (12.64)	22.41 (13.40)	07.91 (04.47)	07.18 (03.58)
4	06.90 (05.13)	13.21 (07.90)	17.07 (09.86)	22.81 (17.63)	13.51 (08.22)	08.94 (04.59)
5	07.74 (04.43)	11.89 (09.25)	07.96 (12.70)	11.69 (14.39)	05.20 (03.71)	06.49 (04.17)
6	07.38 (02.90)	09.06 (03.75)	17.29 (13.24)	10.08 (08.00)	04.32 (04.53)	03.46 (04.92)
7	05.23 (03.44)	07.49 (02.34)	11.71 (05.37)	15.96 (10.56)	10.14 (07.75)	06.49 (03.99)
8	04.50 (01.90)	05.18 (03.36)	08.49 (07.60)	13.79 (09.02)	09.40 (03.85)	06.49 (03.83)
9	04.04 (03.45)	05.98 (04.00)	14.70 (12.34)	14.26 (14.36)	08.52 (05.86)	07.25 (06.49)
10	11.57 (12.91)	05.12 (02.93)	24.49 (23.23)	15.96 (13.97)	06.35 (04.55)	10.52 (06.32)

Table 4.9 contains the average and standard deviation of settling time associated with responses of all subjects to different input signals. The same trend that was observed on the figures is also seen in the numerical values shown in Table 4.9. It is important to note that the magnitude of the tolerance band effects the settling time. Both the tolerance band and the setteling time are important characteristics used to describe the state of the system. Assume that an error band is defined to tolerate angular positions within the range of the *"target ± 1 degree"*. Obviously it is not a proper error band for a system that is moving within the magnitudes of 2, 4 and 6 degrees. This large error band results in a very short settling time that represents a good specification of the system. However this concultion is a mistake. The tolerance band should be within a reasonable distance from the input signal, commonly this is within 5% of the target's magnitude.

So far, some perceptible patterns have been observed in the parameters proportional gain, time delay and damping coefficient. In addition, some trends were also seen in the characteristics of overshoot and settling time. After calculating the bandwidth of the simulated responses, the association of these parameters and characteristics with bandwidth will be evaluated.

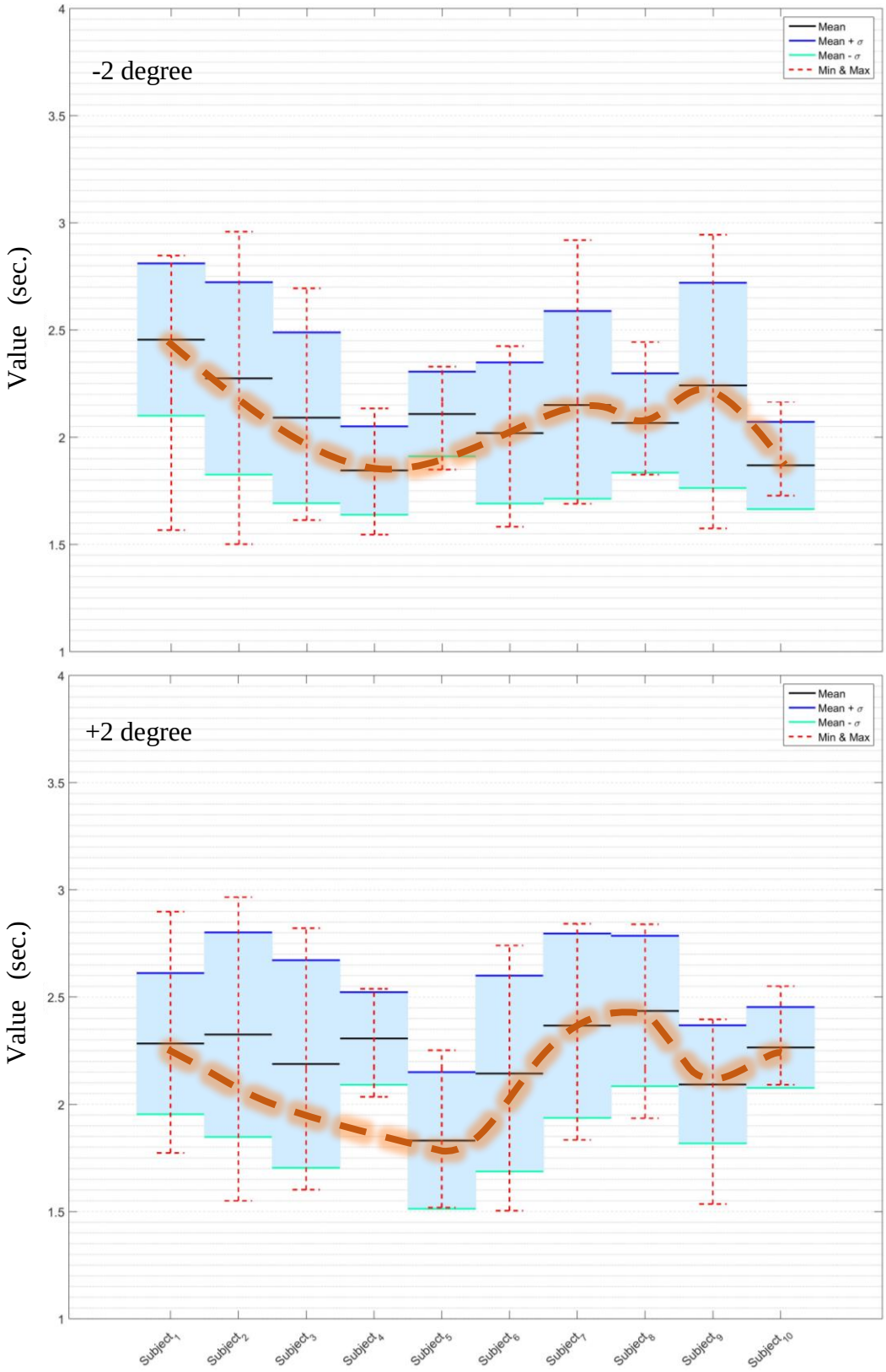

Figure 4.24 settling time in responses of subjects to ±2 deg

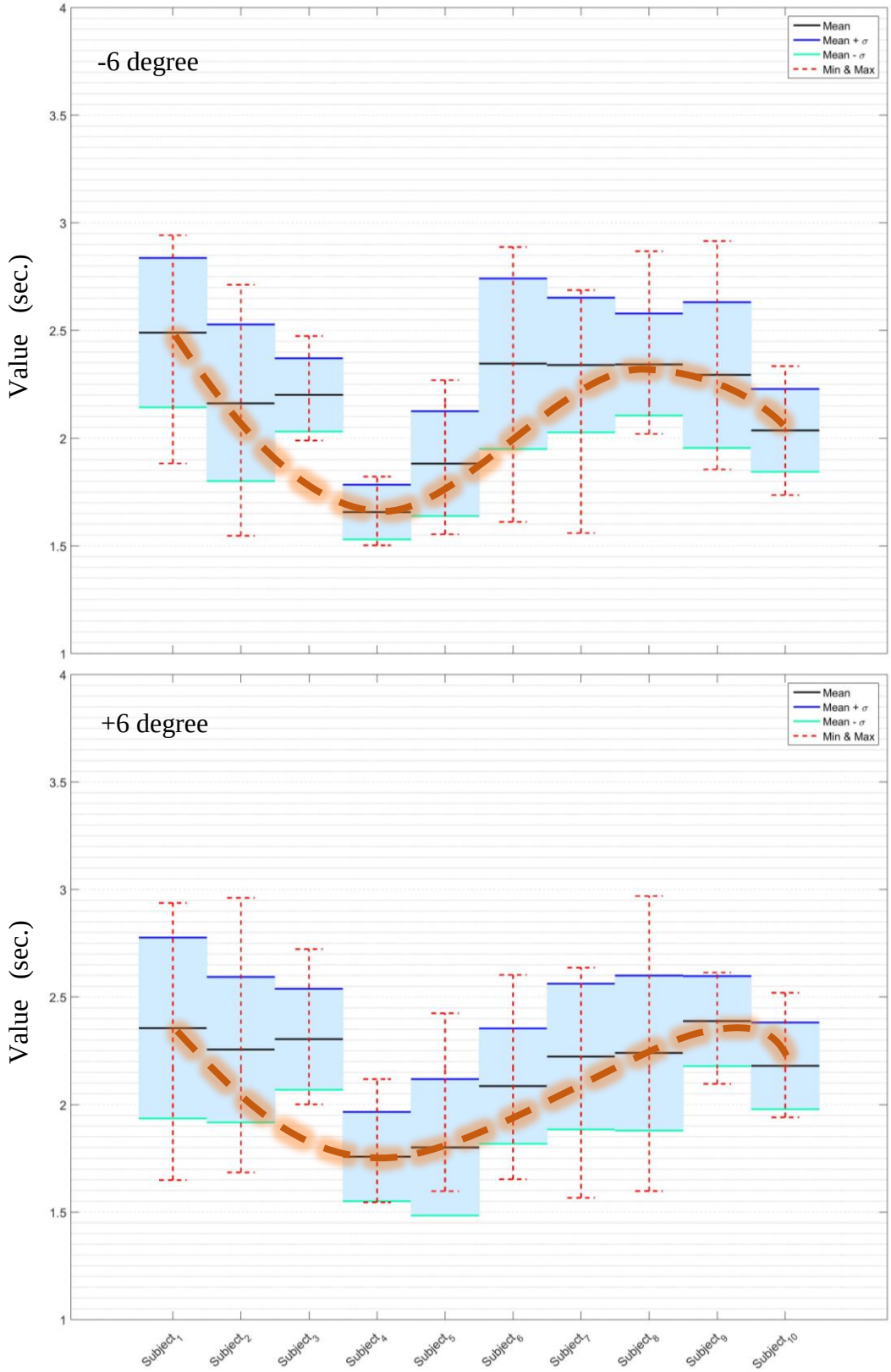

Figure 4.25 settling time in responses of subjects to ±6 deg

Table 4.9: Mean of settling time (standard deviations in the parenthesis)

	Target (input signal)					
#	-6	-4	-2	2	4	6
1	02.49 (0.35)	02.51 (0.32)	02.46 (0.35)	02.28 (0.33)	02.35 (0.38)	02.36 (0.42)
2	02.16 (0.36)	02.19 (0.24)	02.27 (0.45)	02.33 (0.48)	02.28 (0.37)	02.26 (0.34)
3	02.20 (0.17)	02.17 (0.23)	02.09 (0.40)	02.19 (0.48)	02.22 (0.31)	02.30 (0.23)
4	01.66 (0.13)	02.05 (0.25)	01.85 (0.21)	02.31 (0.22)	01.86 (0.19)	01.76 (0.21)
5	01.88 (0.24)	01.71 (0.25)	02.11 (0.20)	01.83 (0.32)	01.65 (0.11)	01.80 (0.32)
6	02.35 (0.40)	02.14 (0.25)	02.02 (0.33)	02.14 (0.46)	02.06 (0.41)	02.09 (0.27)
7	02.34 (0.31)	02.28 (0.30)	02.15 (0.44)	02.37 (0.43)	02.38 (0.36)	02.22 (0.34)
8	02.34 (0.24)	02.16 (0.27)	02.07 (0.23)	02.44 (0.35)	02.36 (0.29)	02.24 (0.36)
9	02.29 (0.34)	02.10 (0.41)	02.24 (0.48)	02.09 (0.28)	02.16 (0.31)	02.39 (0.21)
10	02.04 (0.19)	02.14 (0.14)	01.87 (0.20)	02.27 (0.19)	02.01 (0.32)	02.18 (0.20)

4.4 Bandwidth

The mathematical model was determined for each subject's response to each input signal. Then the parameters of the mathematical model were determined that mininized the error between model and measured data. Using these optomized parameter, the responses were simulated. Finally, the simulated responses were used to calculate the bandwidth frequency and determine the bandwidth of the system. Figures 4.26 through 4.28 contain the average, standard deviation, minimum and maximum values of the calculated bandwidth frequencies for all the subjects and input signals. These values have the unit of Hertz. Almost all of the numerical results for bandwidth fall withing a range from 0.5 to 0.8 Hz. Table 4.10 contains the average values and standard deviations of the calculated bandwidth for all the responses.

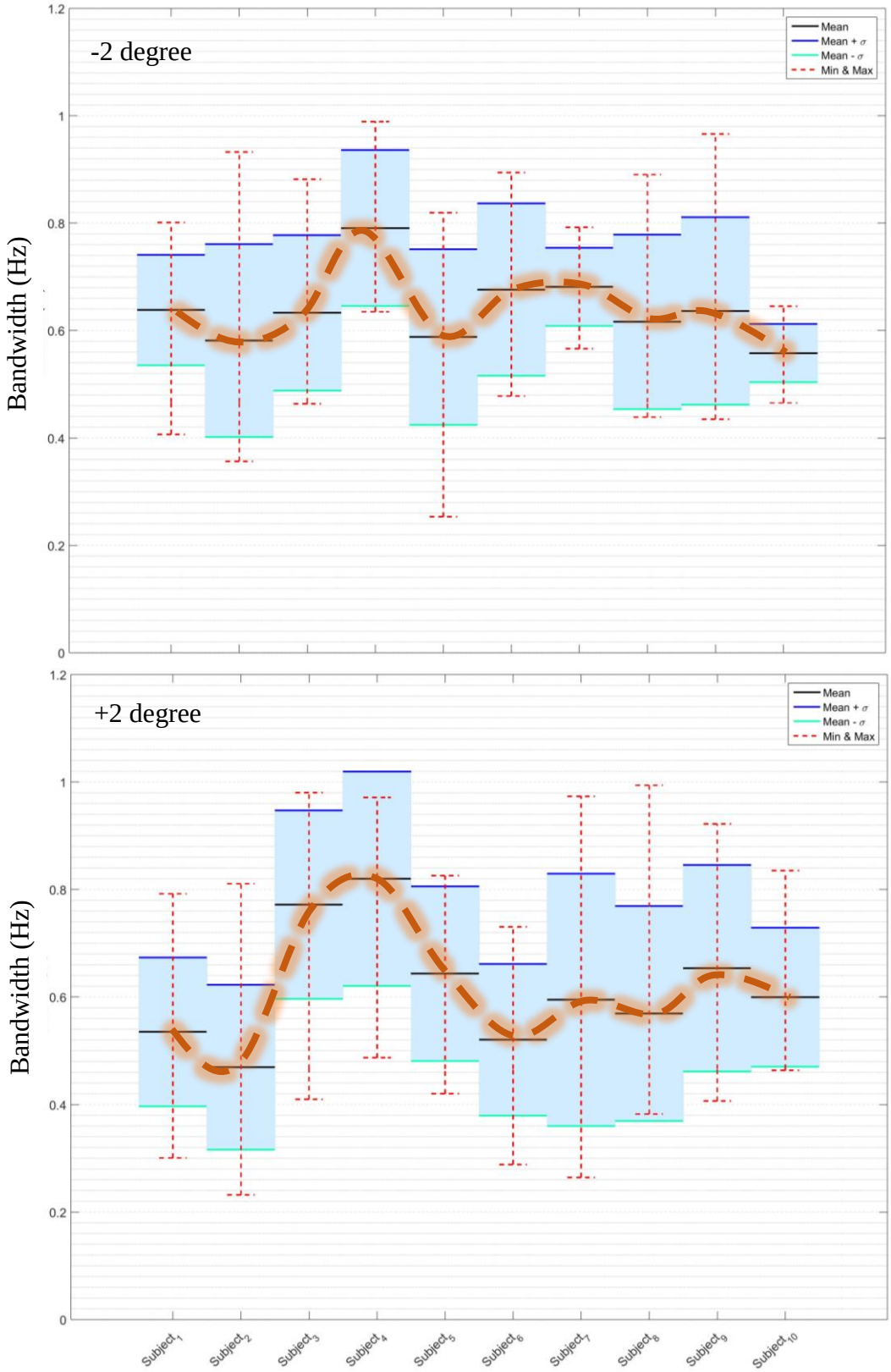

Figure 4.26 bandwidth of responses of subjects to ±2 deg

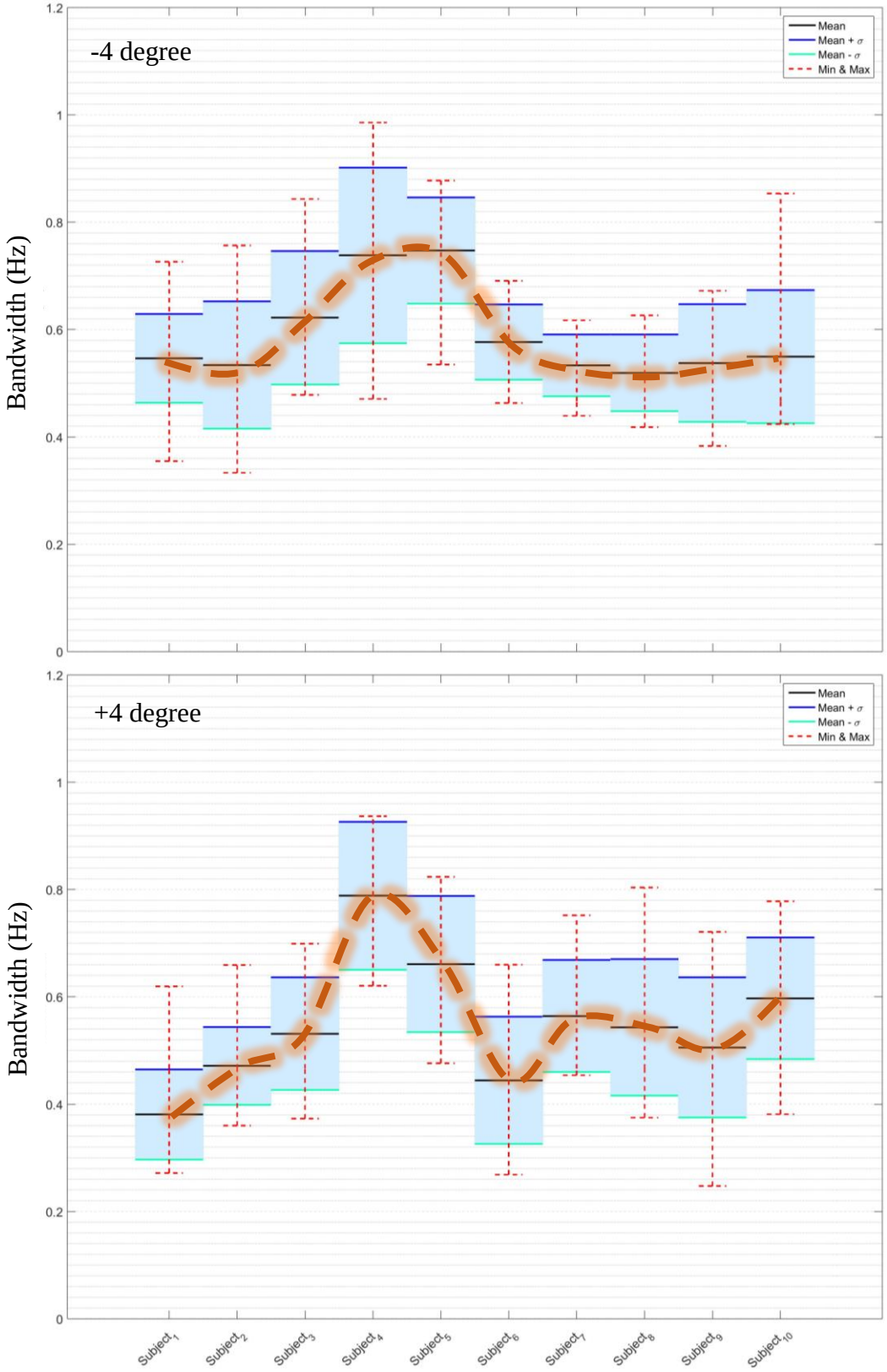

Figure 4.27 bandwidth of responses of subjects to ±4 deg

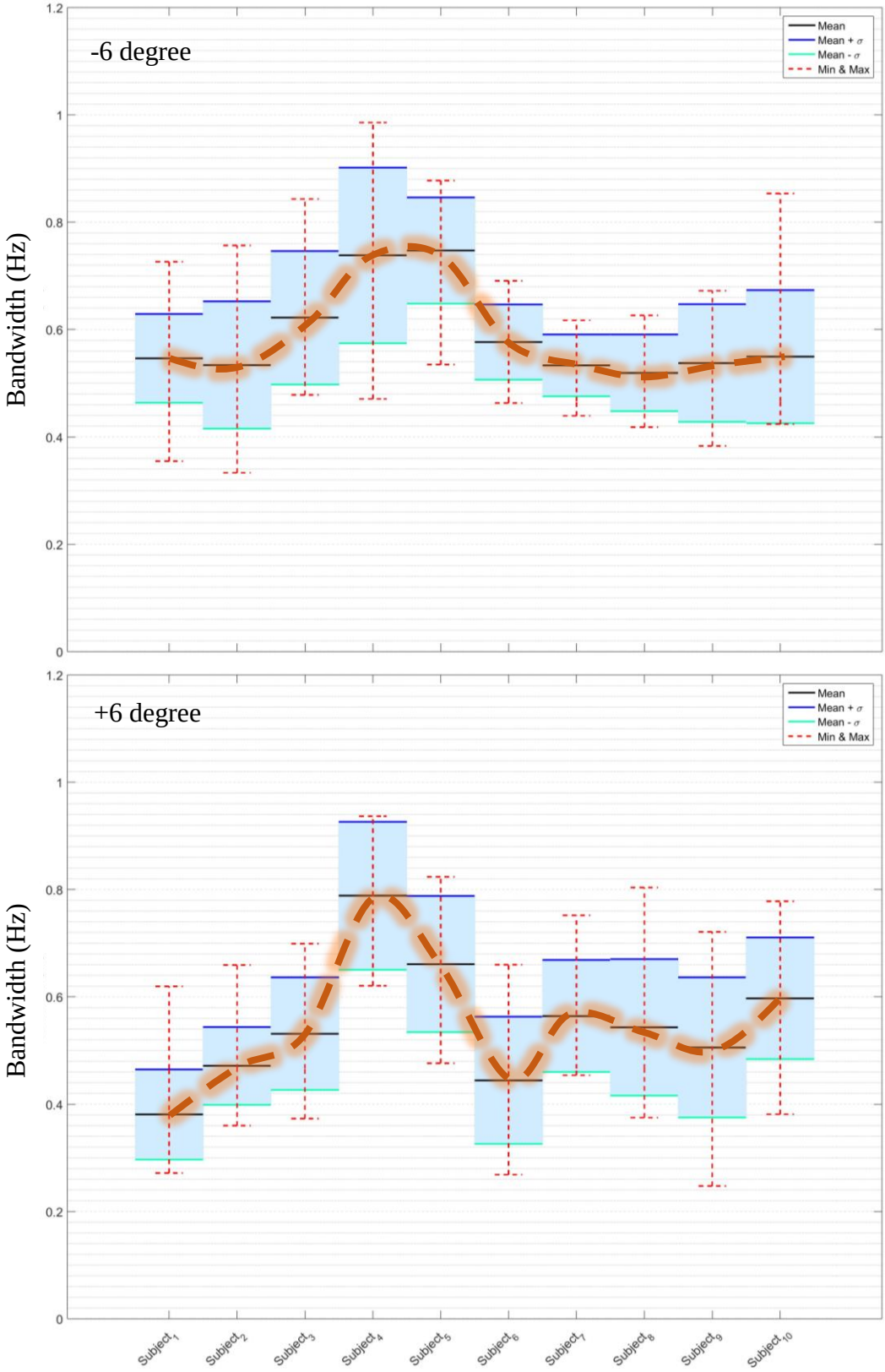

Figure 4.28 bandwidth of responses of subjects to ±6 deg

Table 4.10: Mean value of bandwidth frequency (standard deviations in the parenthesis)

	Target (input signal)					
#	-6	-4	-2	2	4	6
1	0.43 (0.08)	0.55 (0.08)	0.64 (0.10)	0.54 (0.14)	0.38 (0.08)	0.37 (0.09)
2	0.39 (0.07)	0.53 (0.12)	0.58 (0.18)	0.47 (0.15)	0.47 (0.07)	0.47 (0.09)
3	0.54 (0.07)	0.62 (0.12)	0.63 (0.14)	0.77 (0.17)	0.53 (0.11)	0.51 (0.07)
4	0.68 (0.07)	0.74 (0.16)	0.79 (0.14)	0.82 (0.20)	0.79 (0.14)	0.76 (0.10)
5	0.66 (0.11)	0.75 (0.10)	0.59 (0.16)	0.64 (0.16)	0.66 (0.13)	0.67 (0.14)
6	0.49 (0.09)	0.58 (0.07)	0.68 (0.16)	0.52 (0.14)	0.45 (0.12)	0.43 (0.17)
7	0.46 (0.06)	0.53 (0.06)	0.68 (0.07)	0.59 (0.23)	0.56 (0.11)	0.48 (0.10)
8	0.46 (0.06)	0.52 (0.07)	0.62 (0.16)	0.57 (0.20)	0.54 (0.13)	0.50 (0.10)
9	0.44 (0.08)	0.54 (0.11)	0.64 (0.17)	0.65 (0.19)	0.51 (0.13)	0.45 (0.14)
10	0.58 (0.06)	0.55 (0.12)	0.56 (0.05)	0.60 (0.13)	0.60 (0.11)	0.59 (0.12)

A trend was observed in the figures 4.26 through 4.28 that might be associated with the other patterns seen in plots of the parameters and system's characteristics. It is clear from the figures that Subject 4 had the highest bandwidth among all subjects. In most cases, Subjects 3 and 5 also had the high bandwidths. By doing some investigation on the plots of the bandwidth and the plots of the results, a consistency was observed. This consistency is between the patterns observed in the bandwidth plots and those observed in the plots of parameter *"G"*. The rises and falls in both patterns are visually correlated. Through more investigation and comparison of the plots, it is observable that the patterns in the plots of bandwidth were almost the inverse of the patterns in the plots of *"I", "b"*, *"τ"* and the settling time. A theory forms from these examinations, which states that the bandwidth of the human's neuromuscular system might be associated with the proportional gain of its controller, the viscous damping coefficient of the torso, the moment of inertia of the upper body and also the movement settling time.

Figures 4.29 and 4.30 show the calculated bandwidth frequencies of the Subjects 1, 2, 3 and 4. The previously discussed patterns were also observed in the plots for different input signals. The

pattern of the bandwidth plot is consistent with the pattern of plots for the parameter *"G"* and is generally the inverse of the plots of the parameter *"τ"*.

However, it was observe in Figures 4.29 and 4.30 that higher bandwidth frequencies are associated with the lower magnitudes of the input signal. It was previously discussed that the tracking of a smaller input signal is accociated with a higher percentage of overshoot. A higher amount of overshoot is considered to be a poor system characteristic, while higher bandwidth frequency is considered to be a good system characteristic. One theory to explian this appearent contridiction may be that bandwidth is somewhat independent of overshoot. That means overshoot and bandwidth are two separate indicators of system performance. Another theory is that the effect of overshoot on the bandwidth of a system is minimal.

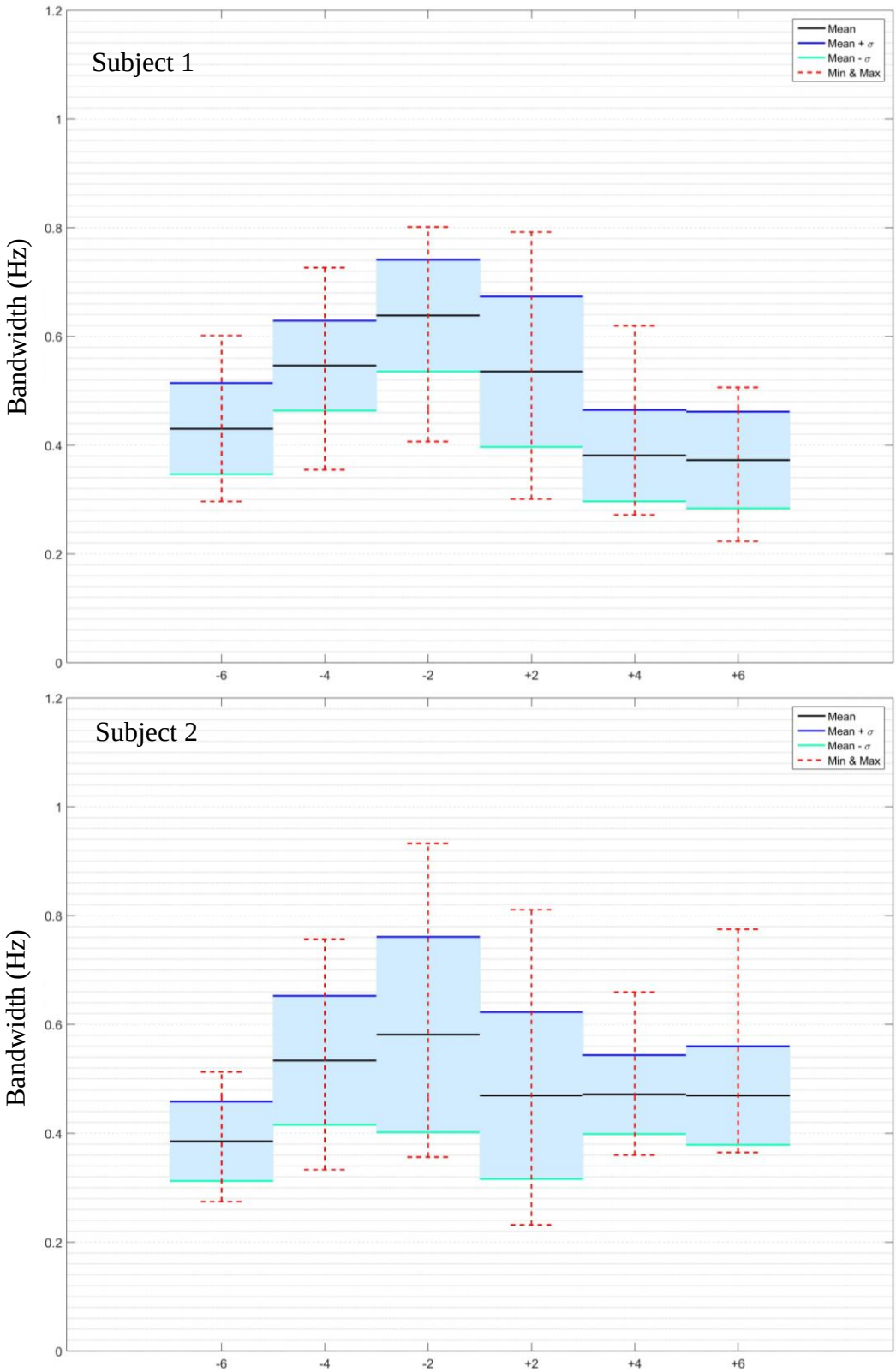

Figure 4.29 bandwidth in responses of subjects 1 and 2

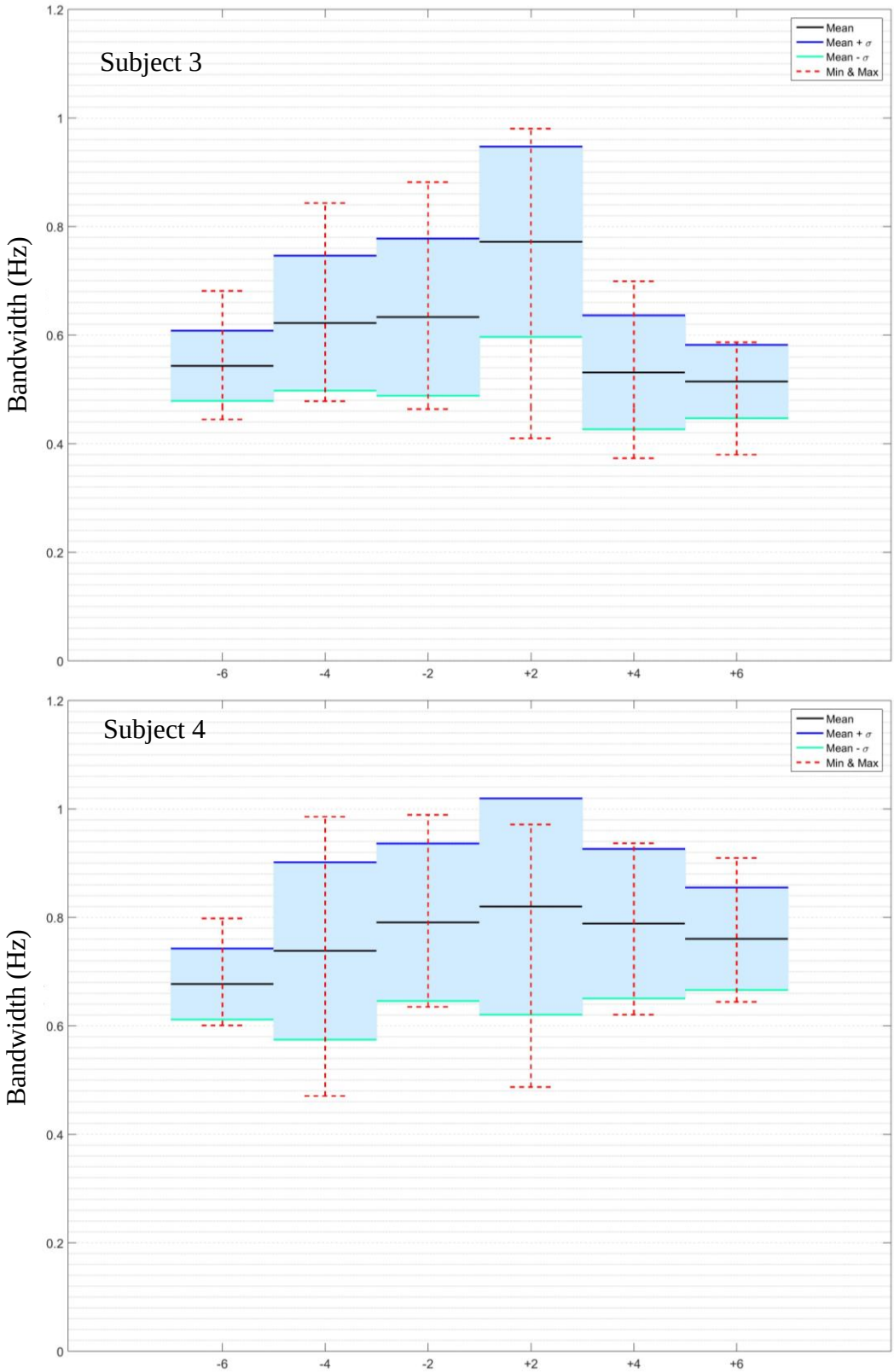

Figure 4.30 bandwidth in responses of subjects 3 and 4

CHAPTER 5 : CONCLUSION

Bandwidth may be a useful indicator to describe the capability of the human neuromuscular system. This is because bandwidth takes into account many different physical parameters and dynamic characteristics of the system. There are other characteristics which describe the quality of a control system's performance such as percentage of overshoot, settling time, and rise time. However, almost of them are determined independently. This means that none of them are calculated by an equation which includes all of the physical and mechanical properties of the dynamical system.

Although the results showed different values of bandwidth for different subjects and different targets, all of them ranged within a small interval. This interval was approximately [0.28,1.02] Hz. The small size of this interval, large number of trials and sufficient number of subjects who performed the experiment leds to the conclusion that the results for the bandwidth are reliable.

One interesting result was the correlation of bandwidth with time delay and settling time. For those subjects who had shorter time delay and settling time, a higher bandwidth was observed. That makes sense in terms of control systems' theory. A system which responds to the input command and reaches the steady state in a shorter time, is considered to be a system with high quality performance. Since bandwidth was introduced as an indicator of the quality and capability of a biofeedback control system, a system with shorter time delay and settling time is expected to have a larger bandwidth.

Based on the results of this study, bandwidth was also observed to be associated with the proportional gain of the controller. Neuromuscular control systems with higher bandwidth had a larger proportional gain. That also makes sense in classical control and dynamic, because a large

proportional gain causes a large change in the output for a given magnitude of error between the current position and the target location. A teribbly large proportional gain makes the system unstable and a insignificant gain makes the controller unresponsive and unable to correct the errors [56]. However, over a limited range, increasing the controller gain generally makes the performance of the controller better.

During the human motion tracking experiments a participants moving his/her torso in the sagittal plane. The bandwidth of the neuromuscular system for this particular motion is also associated with the moment of inertia of the body. Higher inertia makes the motion more challenging [57] requiring more torques to achieve the same movment. Hence, a system with a higher moment of inertia would not accelerate as quickly as a system with a lower moment of inertia. Increasing the controller gain may improve the performance of such a system. This behavior was observed in this study.

During motion, friction and viscosity cause a loss of energy and make movement more difficult. Hence, lower friction and viscosity are generally desirable in a controlled and dynamical system. However, in many cases, the dynamical system needs a damper to help control the velocity and dynamic of the motion [58]. If the damping ratio was too high, the system would not have moved at all. And if it was zero, it may be difficult to contol the oscillation. In our study, it was observed that higher bandwidth was associated with smaller values for the damping coefficient.

Future Work

In this study, the rotation movement of upper body in the sagittal plane was studied. As an extension to this study, additonal experiments including motion in other anatomical planes can be considered. In addtion, the bandwith of different body segments / joints can be calcualted under

various dynamic conditions. Moreover, bandwidth could be used to better understand people with low back pain and the capability of their neuromuscualar control system

The proposed mathematical model in this study was simple making understanding the system easier. A more comprehensive mathematical model could be developed. Also, due to the small magnitudes of motion, some approximations were applied in the mathematical model, such as Euler's approximation, for the function *sine* to make the system a linear. It may be possible to choose another mathematical model for the system and model it as a nonlinear system.

Another extension to this research is the modification of the controller. In this project, the controller only contained proportional gain and feedback. It was considered as simple as possible to make it easier to understand. For future work, more complex controllers may be applied in the system such as PID controllers, customized controllers with different numbers of zeros and poles in their transfer function or controllers with a sensor system in the feedback section.

The Trust-Region-Reflective algorithm was selected as the iteration method in the optimization and parameter estimation process. It was not evaluated and there may be other algorithms that make the optimization process more accurate and take less time and processing memory. There are many different methods, such as Quasi-Newton, gradient descent, reduced gradient method, etc. [59]. Thus, in future work, the iteration method in the parameter estimation could be modified and evaluated to determine what method is the best for these types of projects.

Parameters of *"k" , "b"* and *"G"* are characteristics of the human body that could not be measured as easily as the mass or height. In this project, an average value or a range was presented, based on the results for each of the parameters *"k" , "b"* and *"G".* However, the stiffness coefficient of the muscles, damping coefficient in the joints, and the gain of the human's neural system differ for each type of motion and body organ. It would be a good extension to work on

each parameter particularly in different dynamic conditions of different body organs, and present an average value or a range for each parameter.

Finally standard numerical value of bandwidth for healthy human subjects in different dynamic conditions should be devloped. This could lead to a better understanding of brain function which may be useful in human rehabilitation, optimization of sports performance, developemnt of human-inspired robotics, and other medical sciences.

Bibliography

[1] C. &. H. R. Phillips, Feedback control systems (4th ed.), Upper Saddle River, N.J.: Prentice Hall, 2000.

[2] B. Friedland, Control System Design (An introduction to state-space methods), Mineola: Dover Publications, 1986.

[3] D. B. a. M. Salanova, The neuromuscular system: from earth to space life science: neuromuscular cell signalling in disuse and exercise, New York: Springer, 2015.

[4] A. Tózeren, Human Body Dynamics (Clasical Mechanics and Human Movement), New York: Springer, 2000.

[5] P. G. R. A. Cholewicki J, "Postural control of trunk during unstable sitting," *Biomechanics,* vol. 33, pp. 1733-1737, 2000.

[6] G. K. Tanaka M.L., "Methods & Nonlinear Analysis for Measuring Torso Stability," in *ASCE 18th Engineering Mechanics Division*, Blacksburg, VA, 2007.

[7] E. Sontag, Mathematical Control Theory: Deterministic Finite Dimensional Systems, New York: Springer, 1998.

[8] E. Beltrami, An algorithmic approach to nonlinear analysis and optimization, New York: Academic Press, 1970.

[9] H. Hatze, "The complete optimization of a human motion," *Mathematical Biosciences,* vol. 28, no. 1-2, pp. 99-135, 1976.

[10] H. HATZE, "QUANTITATIVE ANALYSIS, SYNTHESIS AND OPTIMIZATIONOF HUMAN MOTION," *Human Movement Science,* vol. 3, pp. 5-25, 1984.

[11] "Wikipedia.org," Wikipedia, [Online]. Available: https://en.wikipedia.org/wiki/Biomechanics#cite_note-Humphrey-14. [Accessed 23 March 2016].

[12] B. Abernethy, V. Kippers, S. J. Hanrahan, M. G. Pandy, A. M. McManus and L. MacKinnon, Biophysical foundations of human movement (3rd ed.), Champaign, IL: Human Kinetics.

[13] S. Mason, A History of the Sciences, New York, NY: Collier Books, 1962.

[14] J. D. Humphrey, "Continuum biomechanics of soft biological tissues," *Proceedings of the Royal Society of London* , vol. 459, pp. 3-46, 2003.

[15] W. Baumann, Grundlagen der Biomechanik, Verlag Karl Hofman, 1989.

[16] D. A. Winter, Biomechanics in motor control of human movement, Hoboken, NJ: John Wiley & Sons, 2009.

[17] "Wikipedia.org," Wikipedia, [Online]. Available: https://en.wikipedia.org/wiki/Mathematical_model. [Accessed 22 March 2016].

[18] E. Hanavan, A mathematical model of the human body, DTIC document, 1964.

[19] K. Barin, "Evaluation of a generalized model of human postural dynamic and control in the sagittal plane," *Biological Cybernetics, Springer,* pp. 37-50, 1989.

[20] D. A. Winter, "Human balance and posture control during standing and walking," *Gait & Posture,* vol. 3, no. 4, pp. 193-214, 1995.

[21] A. J. G. H. J. G. Vaughan C. L., "Selection of body segment parameters by optimization methods," *Biomechanical Engineering,* vol. 104, no. 1, pp. 38-44, 1982.

[22] W. J. M. Zajac Felix E., "Modeling musculoskeletal movement systems: joint and body segmental dynamics, musculoskeletal actuation, and neuromuscular control," in *Multiple Muscle Systems*, New York, Springer, 1990, pp. 121-148.

[23] S. S. M., "Gauss and the invention of least squares," *The annals of statistics,* vol. 9, no. 3, pp. 465-474, 1981.

[24] C. R. Rao, H. Toutenburg, A. Fieger, C. Heumann, T. Nittner and S. Scheid, Least Squares and Alternatives, New York: Springer, 1999.

[25] R. H. CL Lawson, Solving least squares problems, Houston, Texas: SIAM, 1974.

[26] "Least Squares," Wikipedia, [Online]. Available: https://en.wikipedia.org/wiki/Least_squares. [Accessed 24 March 2016].

[27] K. C. T., Iterative methods for optimization, Raleigh: SIAM, 1999.

[28] "Curve Fitting," Wikipedia, [Online]. Available: https://en.wikipedia.org/wiki/Curve_fitting. [Accessed 24 March 2016].

[29] D. A. Rosenbaum, Human motor control, San Diego: Academic Press, 1991.

[30] C. E. P. R. E. H. A. M. W. H. R. L. HUSTON, "On Human Body Dynamics," *ANNALS OF BIOMEDICAL ENGINEERING,* vol. 4, pp. 25-43, 1976).

[31] M. A. Townsend, "Dynamics and coordination of torso motions in human locomotion," *Journal of Biomechanics,* vol. 14, no. 11, pp. 727-738, 1981.

[32] M. L. T. a. K. P. Granata, *Nonlinear Analysis of Low Back Stability,* Wake Forest: Virginia Tech, 2007.

[33] S. D. R. M. A. N. Martin L Tanaka, "Mathematical modeling and simulation of seated stability," *Journal of Biomechanics* , vol. 43, pp. 906-912, 2010.

[34] M. L. M. S. C. S. a. M. A. N. Bradley S. Davidson, "Neural Control of Posture During Small Magnitude Perturbations: Effects of Aging and Localized Muscle Fatigue," *IEEE TRANSACTIONS ON BIOMEDICAL ENGINEERING,* vol. 58, no. 6, pp. 1546-1554, 2011.

[35] J. M. P. J. M. C. P. J. C. J. C. C. J. R. N. Peter Reeves, "Reliability of assessing trunk motor control using position and force tracking and stabilization tasks," *Journal of Biomechanics,* vol. 47, no. 1, pp. 44-49, 2014.

[36] "Bandwidth (signal processing)," Wikipedia, [Online]. Available: https://en.wikipedia.org/wiki/Bandwidth_(signal_processing). [Accessed 24 March 2016].

[37] M. E. Van Valkenburg, Network Analysis, Upper Saddle River: Prentice-Hall, 1974.

[38] N. P. Reeves, "Limits in motor control bandwidth during stick balancing," *Journal of Neurophysiology,* vol. 109, no. 10, pp. 2523 - 2527, 2013.

[39] Shahab Karimi, Martin Tanaka, Peter Reeves, Sudhir Kaul, "UTILIZING BANDWIDTH TO QUANTIFY HUMAN TORSO MOTOR CONTROL CAPABILITY," in *Summer Biomechanics, Bioengineering and Biotransport Conference,* National Harbor, 2016.

[40] S. Broughton and K. Bryan, Discrete Fourier Analysis and Wavelets: Applications to Signal and Image Processing, New York: Wiley and sons, 2008.

[41] D. N. K. J. J. H. K. R. Rao, Fast Fourier Transform - Algorithms and Applications, Springer Netherlands, 2010.

[42] R. R. Seeley, T. D. Stephens and P. Tate, Anatomy & Physiology, New Tork: McGraw Hill, 1998.

[43] R. C. &. B. R. H. Dorf, Modern control systems, Upper Saddle River, NJ: Prentice Hall, 2001.

[44] C. S. M.S. Bazaraa, Nonlinear programming, New York: Wiley, 1979.

[45] R. B. S. a. G. A. S. Richard H. Byrd, "A Trust Region Algorithm for Nonlinearly Constrained Optimization," *SIAM Journal on Numerical Analysis,* vol. 24, no. 5, p. 1152–1170, 1987.

[46] T. Jia-de, "Nonlinear Curve Fitting Based on MATLAB," *Computer and Modernization,* vol. 06, 2008.

[47] M. Z.-j. WANG Ke, "Actualizing Least-squares Curve-fitting Based on Matlab," *Journal of Beijing Broadcasting Institute,* vol. 02, 2005.

[48] P. d. Leva, "Adjustments to Zatsiorsky-Seluyanov's segment inertia parameters," *Journal of Biomechanics,* vol. 29, no. 9, p. 1223–1230, 1996.

[49] S. E. F. &. A. T. Plagenhoef, "Anatomical data for analyzing human motion," *Research Quarterly for Exercise and Sport,* vol. 54, pp. 169-178, 1983.

[50] R. Bracewell, The Fourier Transform & Its Applications, Boston: McGraw Hill, 2000.

[51] D. Pedoe, Geometry: A comprehensive course, Dover, 1988.

[52] E. Solomentsev, Complex number, Hazewinkel: Springer, 2001.

[53] T. M. I. &. M. J. B. Tay, High performance control, Boston: Birkhäuser, 1998.

[54] W. &. F. O. Braune, Determination of the Moments of Inertia of the Human Body and Its Limbs, Springer, 1988.

[55] e. a. Charles E. Clauser, WEIGHT, VOLUME, AND CENTER OF MASS OF SEGMENTS OF THE HUMAN BODY, Ohio: Air Force Systems Command, 1969.

[56] K. Ogata, System Dynamics (4th ed.), Minnesota: Prentice Hall, 2005.

[57] A. M. E. translation, Newton's Principia : the mathematical principles of natural philosophy, New York: Daniel Adee, 1846.

[58] S. Bennett, "A brief history of automatic control," *IEEE Control Systems Magazine ,* vol. 16, no. 3, p. 17–25, 1996.

[59] "Wikipedia.org," Wikipedia, 23 March 2015. [Online]. Available: https://en.wikipedia.org/wiki/Mathematical_optimization.

[60] J. A. Simpson and E. Weiner, The Oxford English Dictionary, Oxford: Clarendon Press, 1989.

[61] K. D. B. Z. B. H. L. Y. &. S. M. King, "High magnitude cyclic load triggers inflammatory response in lumbar ligaments," *Clinical Biomechanics,* vol. 24, no. 10, pp. 792-798, 2009.

Appendix A: Average and standard deviation plot of estimated parameters for each subject's response to different targets (horizontal axis represents the target)

1) Moment of inertia

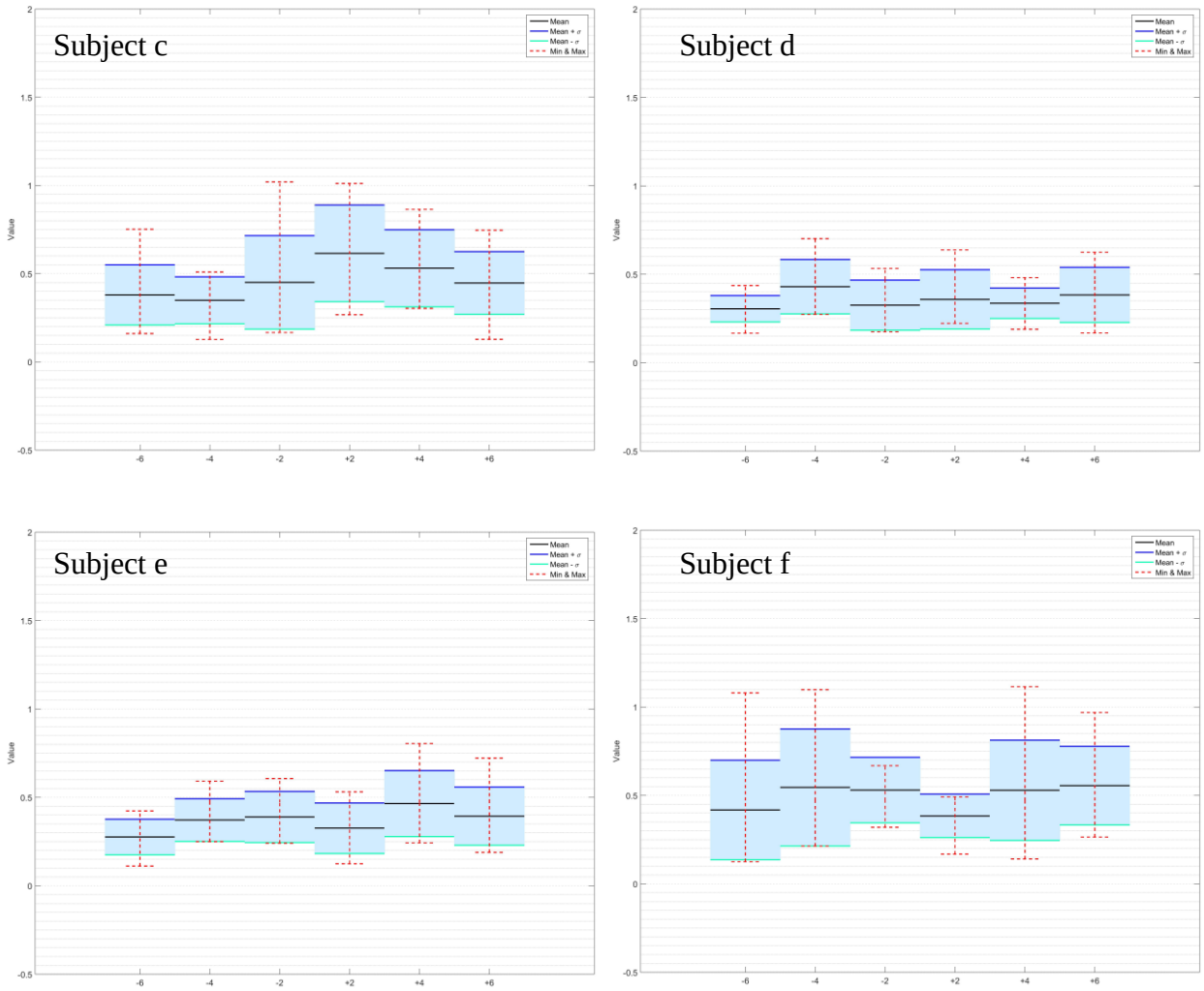

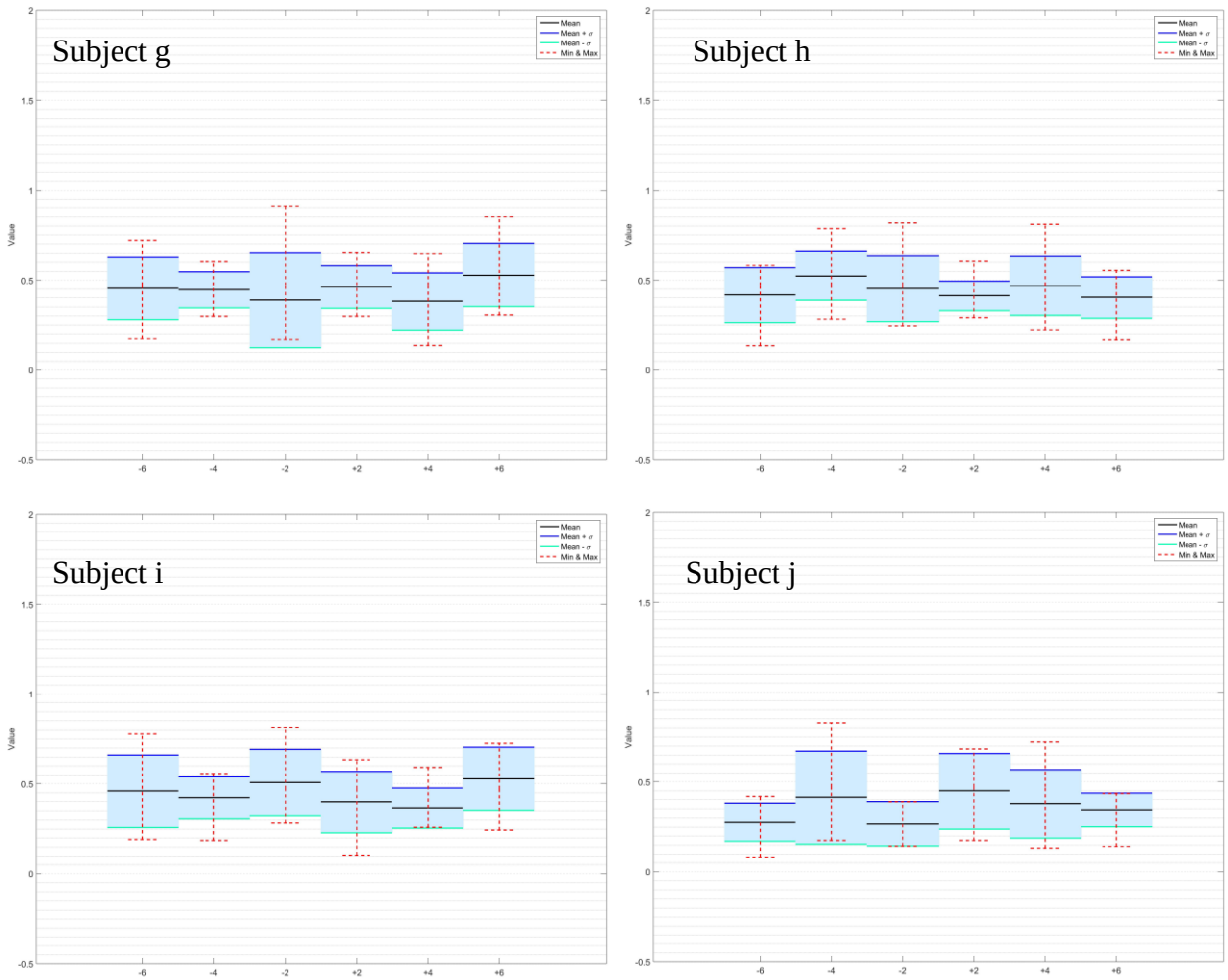

2) Rotating mass

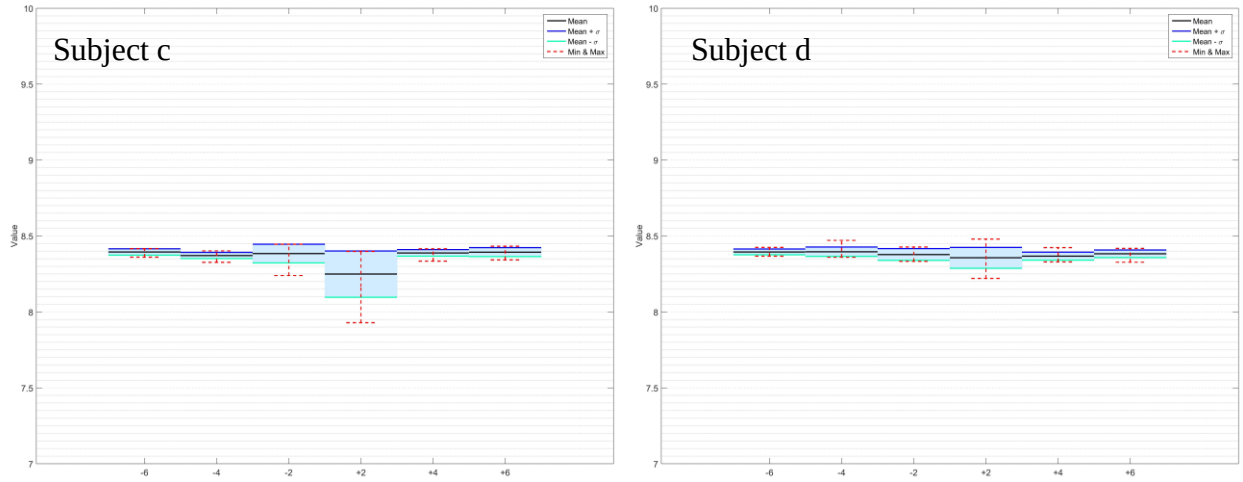

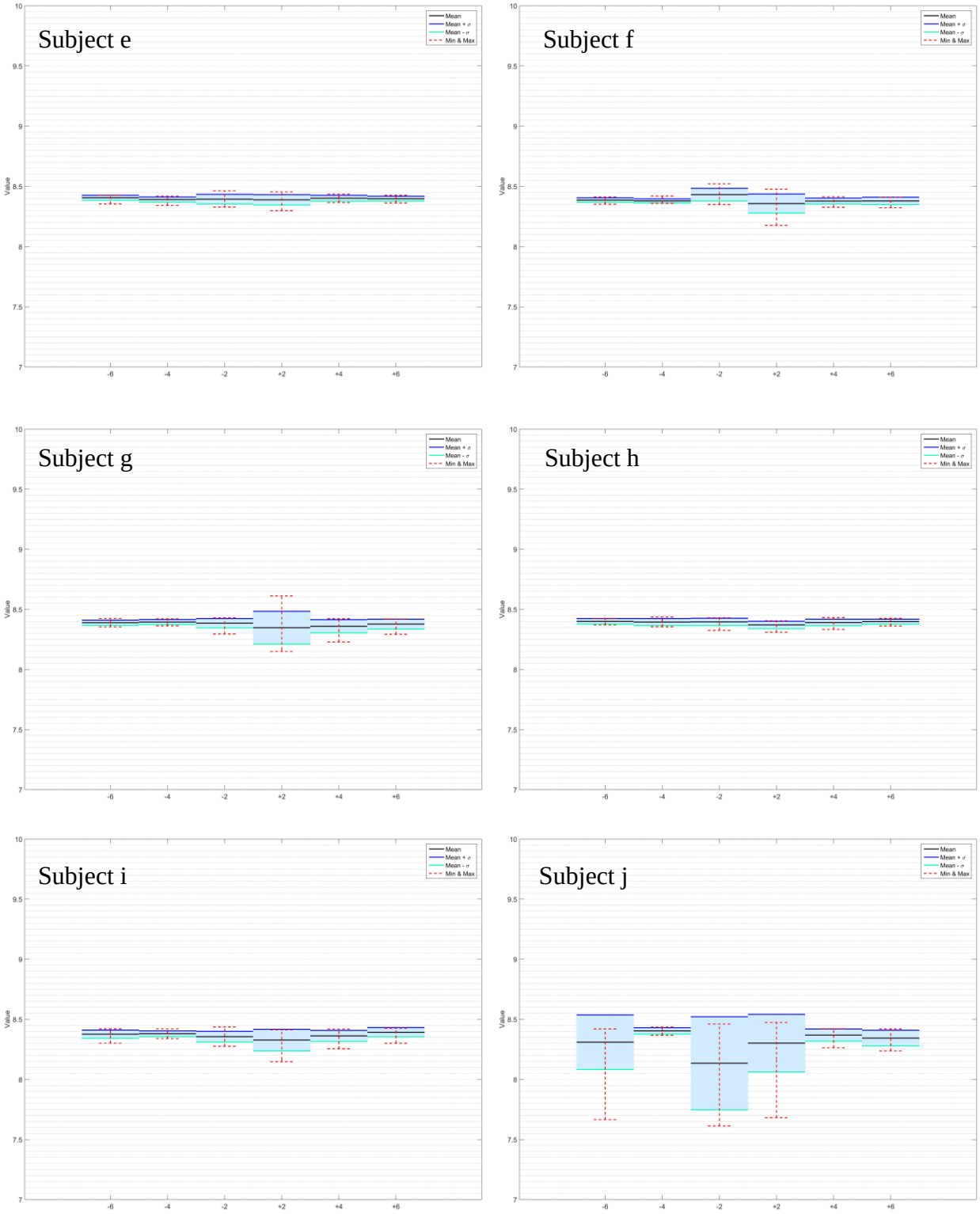
Subject e
Subject f
Subject g
Subject h
Subject i
Subject j
Mean
Mean + σ
Mean - σ
Min & Max
Value
10
9.5
9
8.5
8
7.5
7
-6
-4
-2
+2
+4
+6

3) Effective length

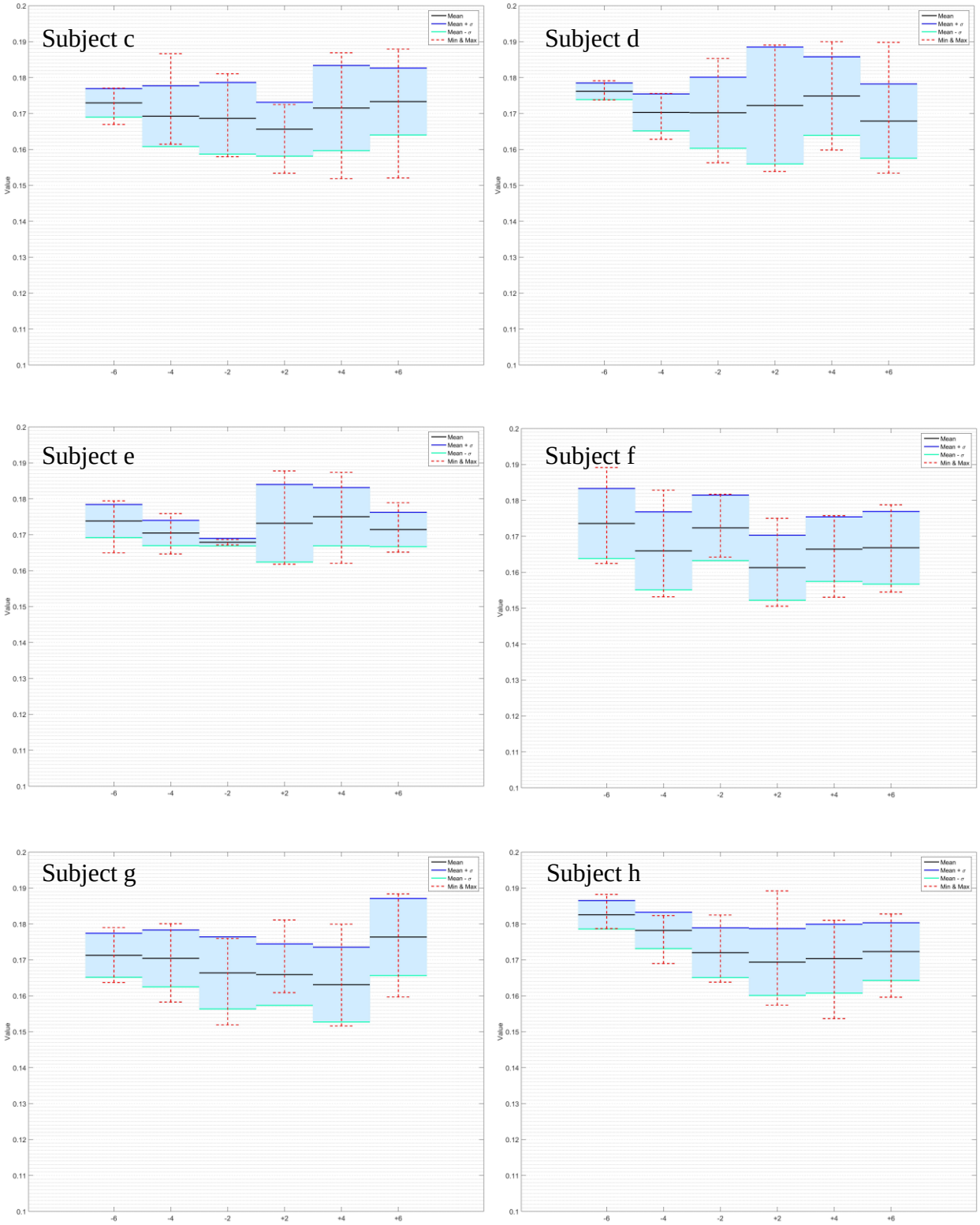

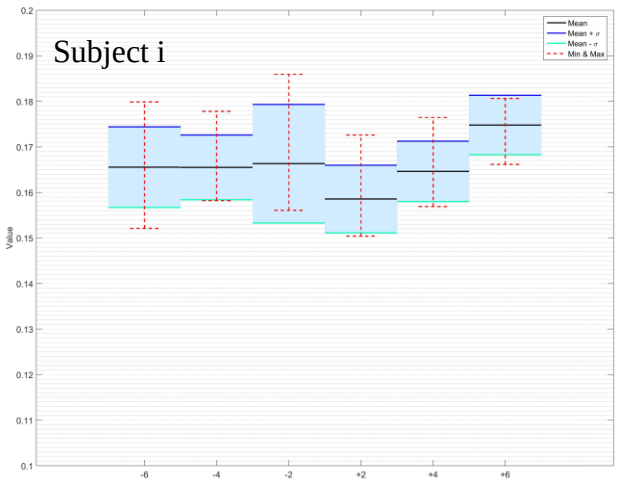
Subject i
Mean
Mean + σ
Mean - σ
Min & Max
Value

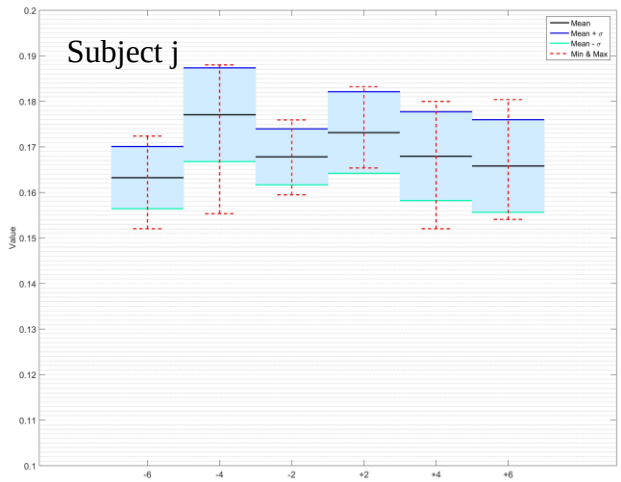
Subject j
Mean
Mean + σ
Mean - σ
Min & Max
Value

4) Delay

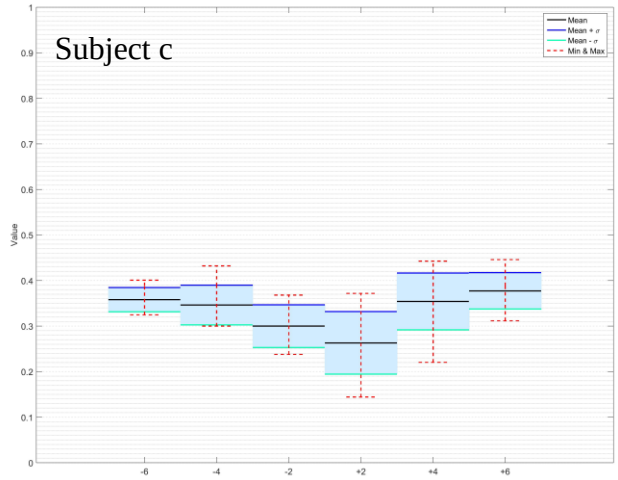
Subject c
Mean
Mean + σ
Mean - σ
Min & Max
Value

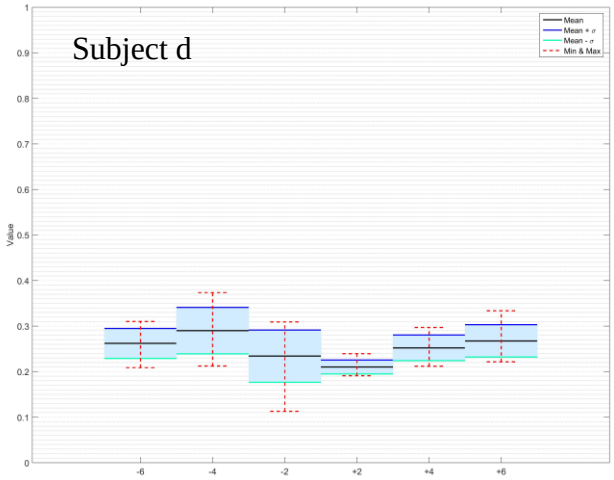
Subject d
Mean
Mean + σ
Mean - σ
Min & Max
Value

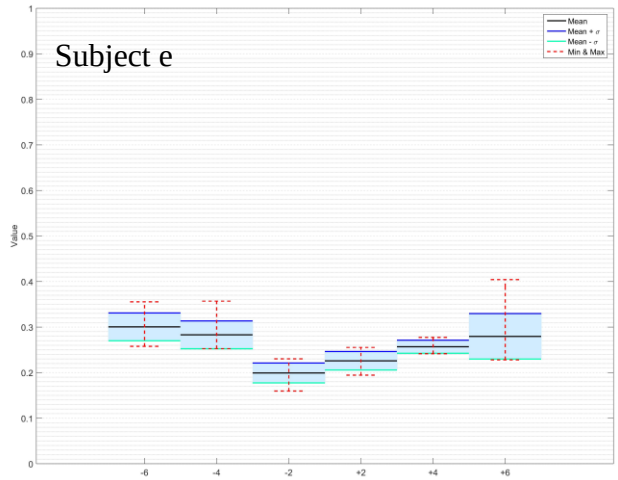
Subject e
Mean
Mean + σ
Mean - σ
Min & Max
Value

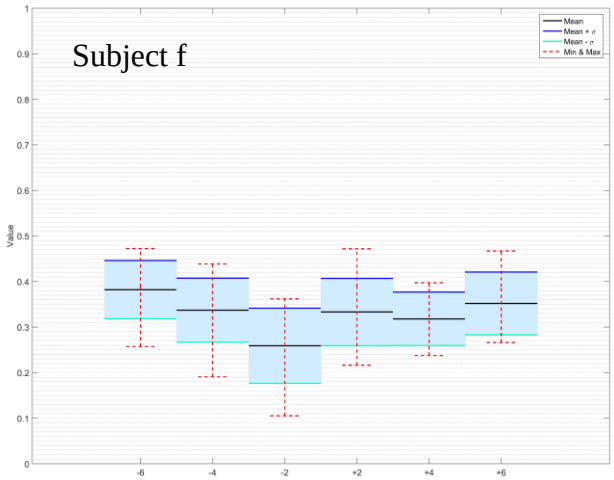
Subject f
Mean
Mean + σ
Mean - σ
Min & Max
Value

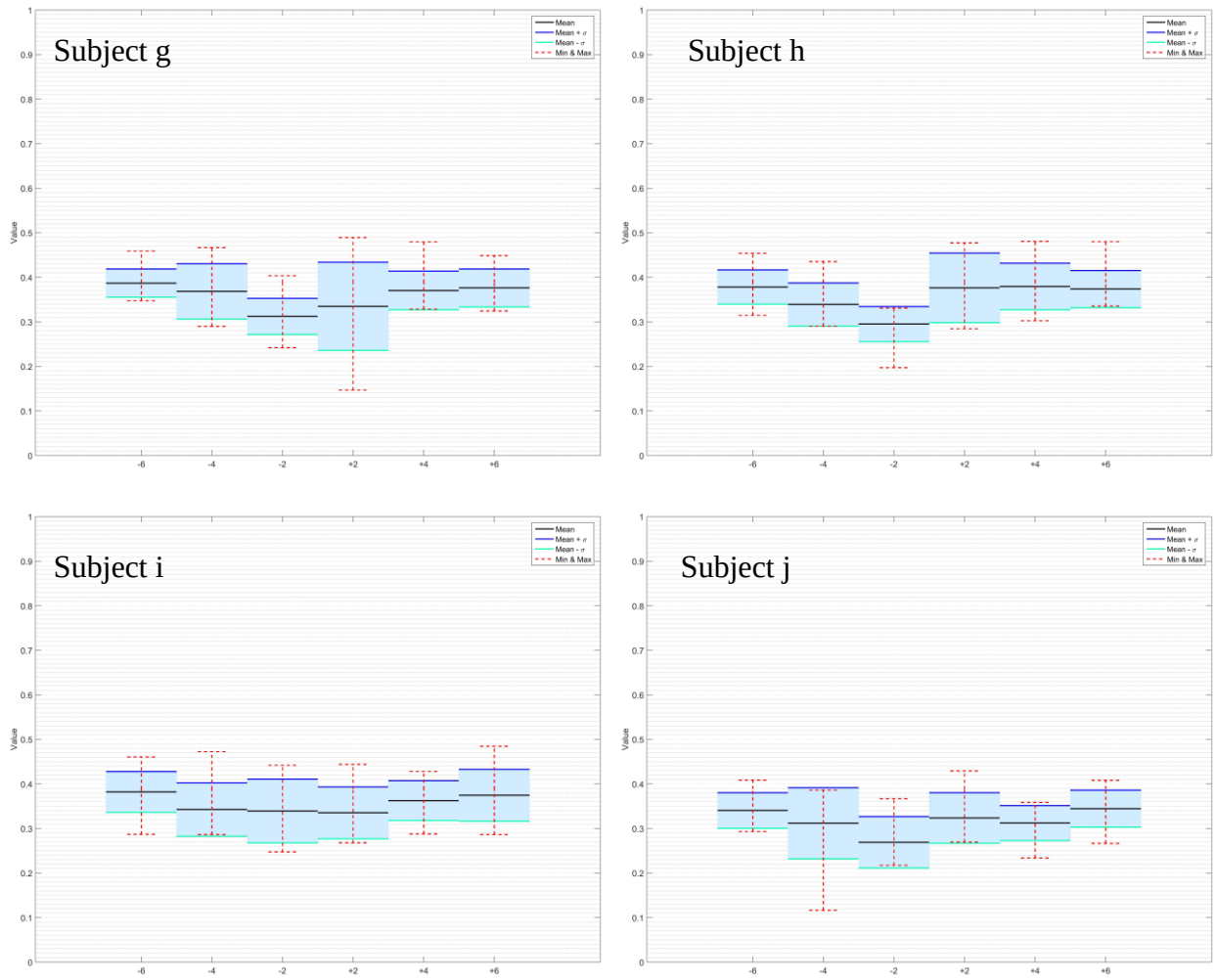

5) Stiffness coefficient

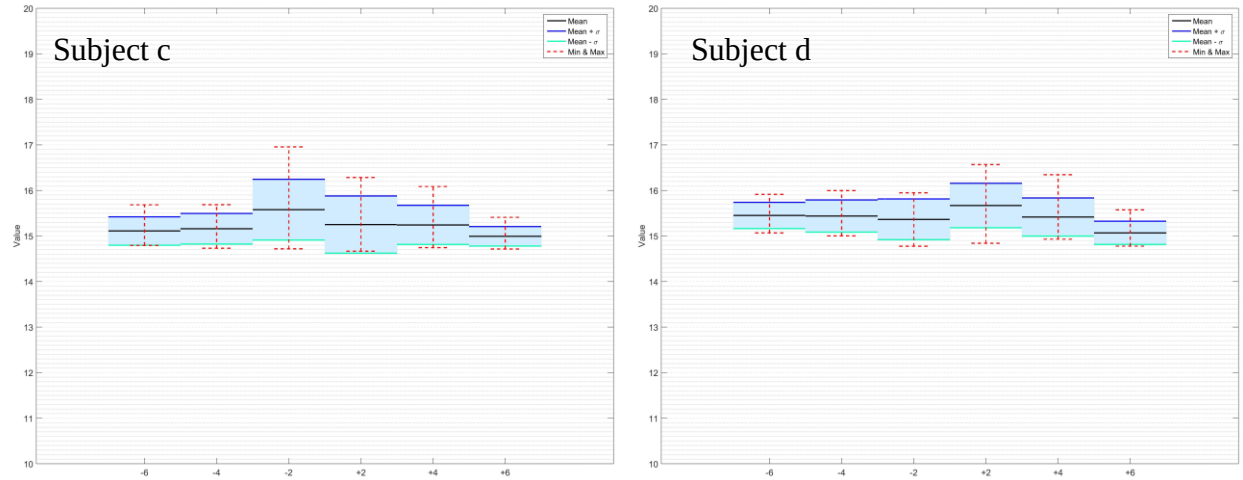

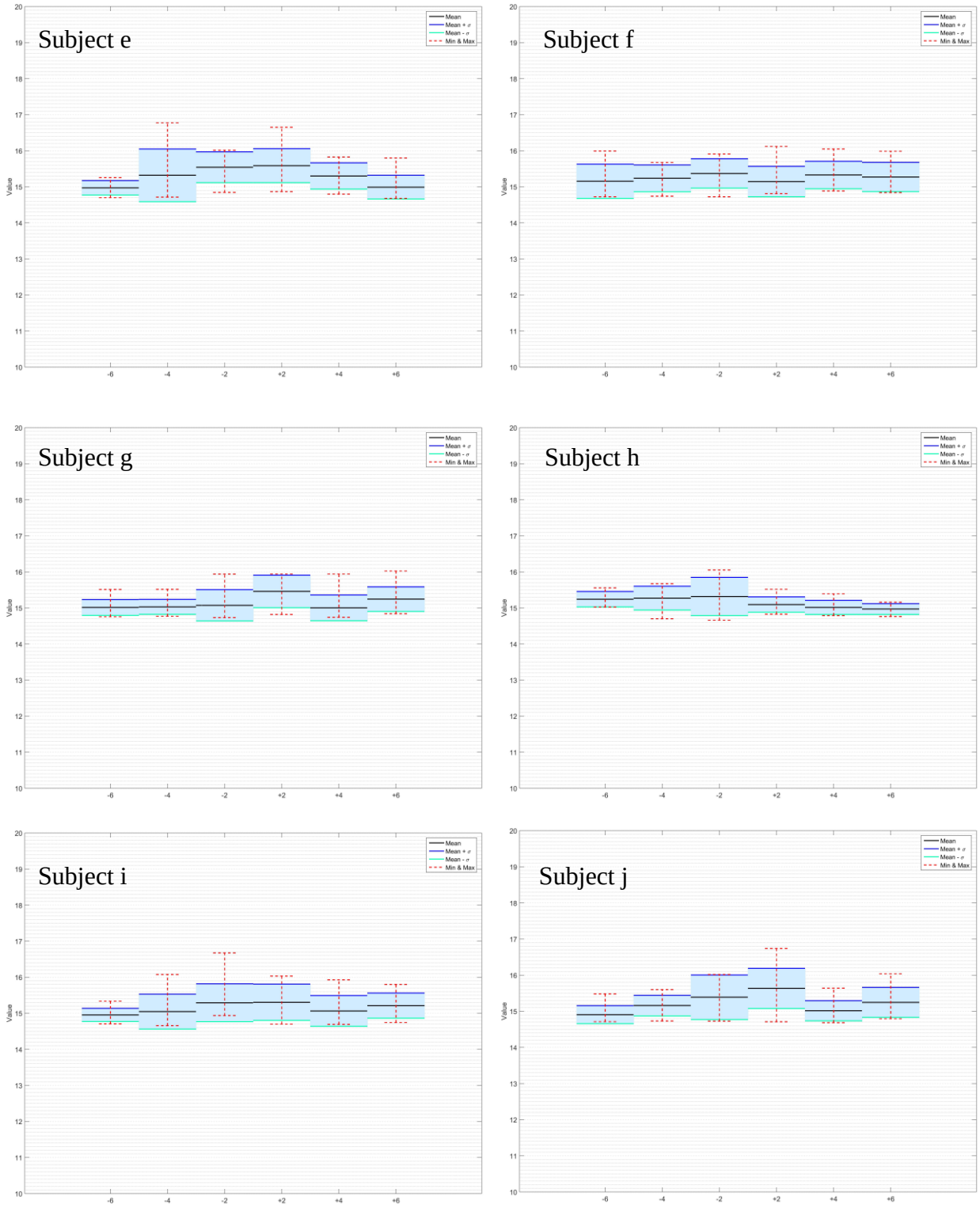
Subject e
Subject f
Subject g
Subject h
Subject i
Subject j
Mean
Mean + σ
Mean - σ
Min & Max
Value
20
19
18
17
16
15
14
13
12
11
10
-6
-4
-2
+2
+4
+6

6) Damping coefficient

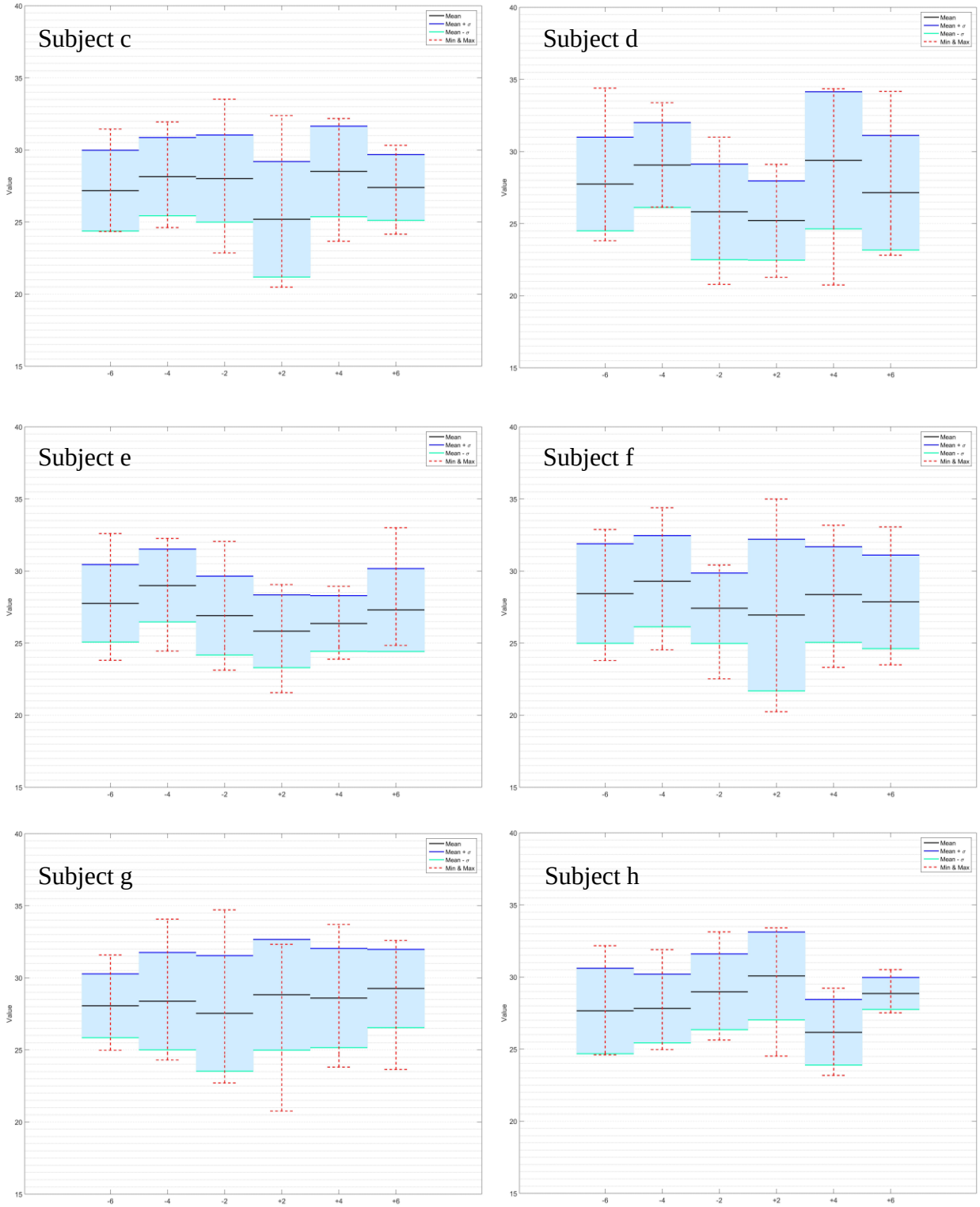

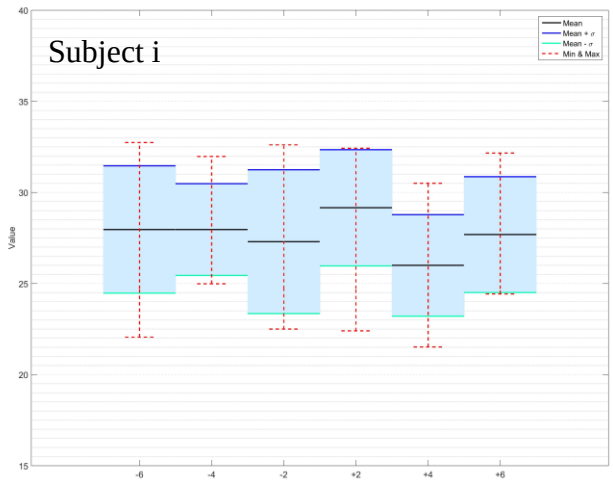

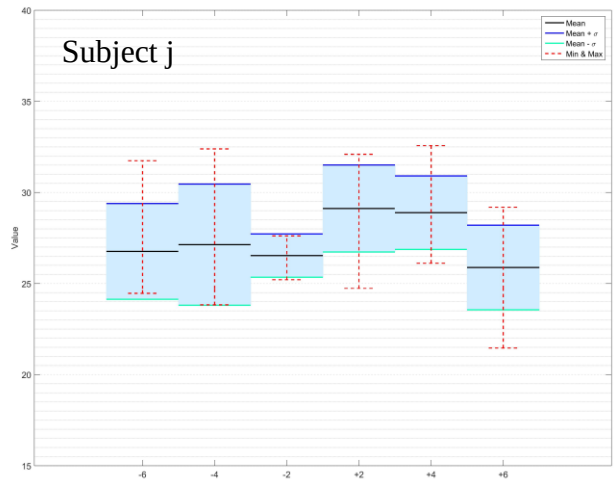

7) Proportional gain

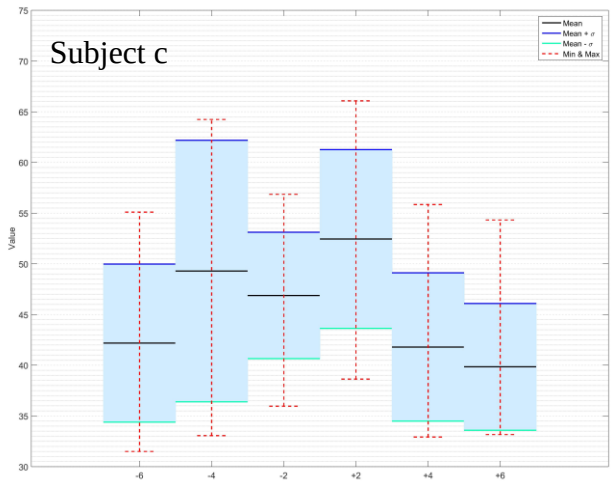

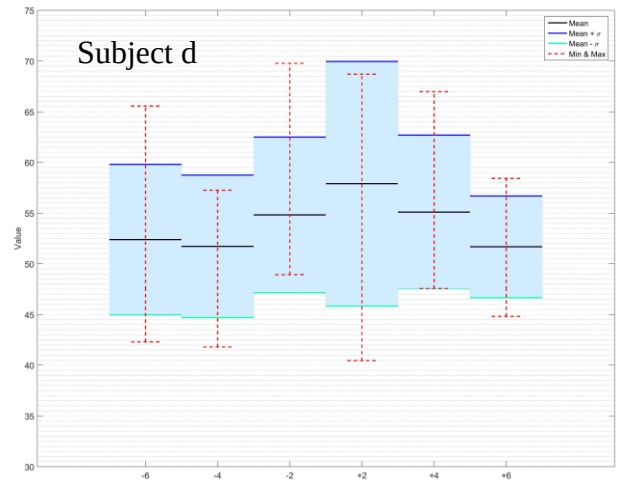

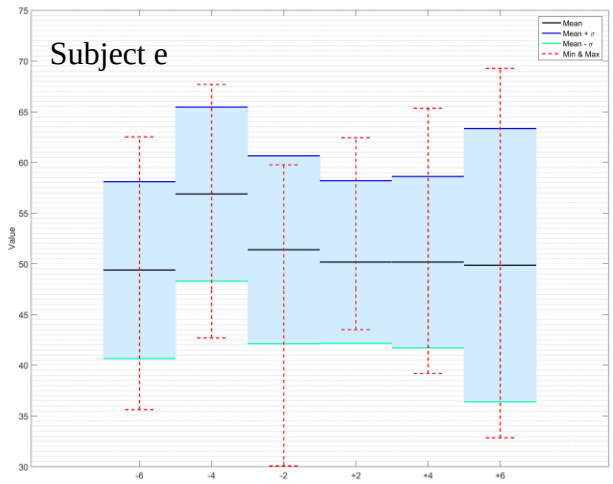

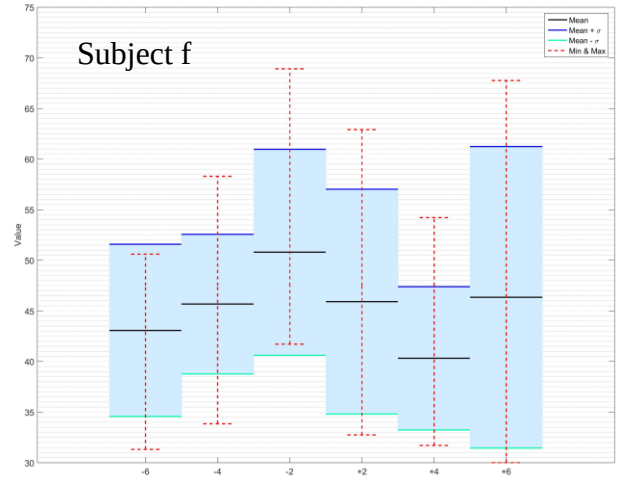

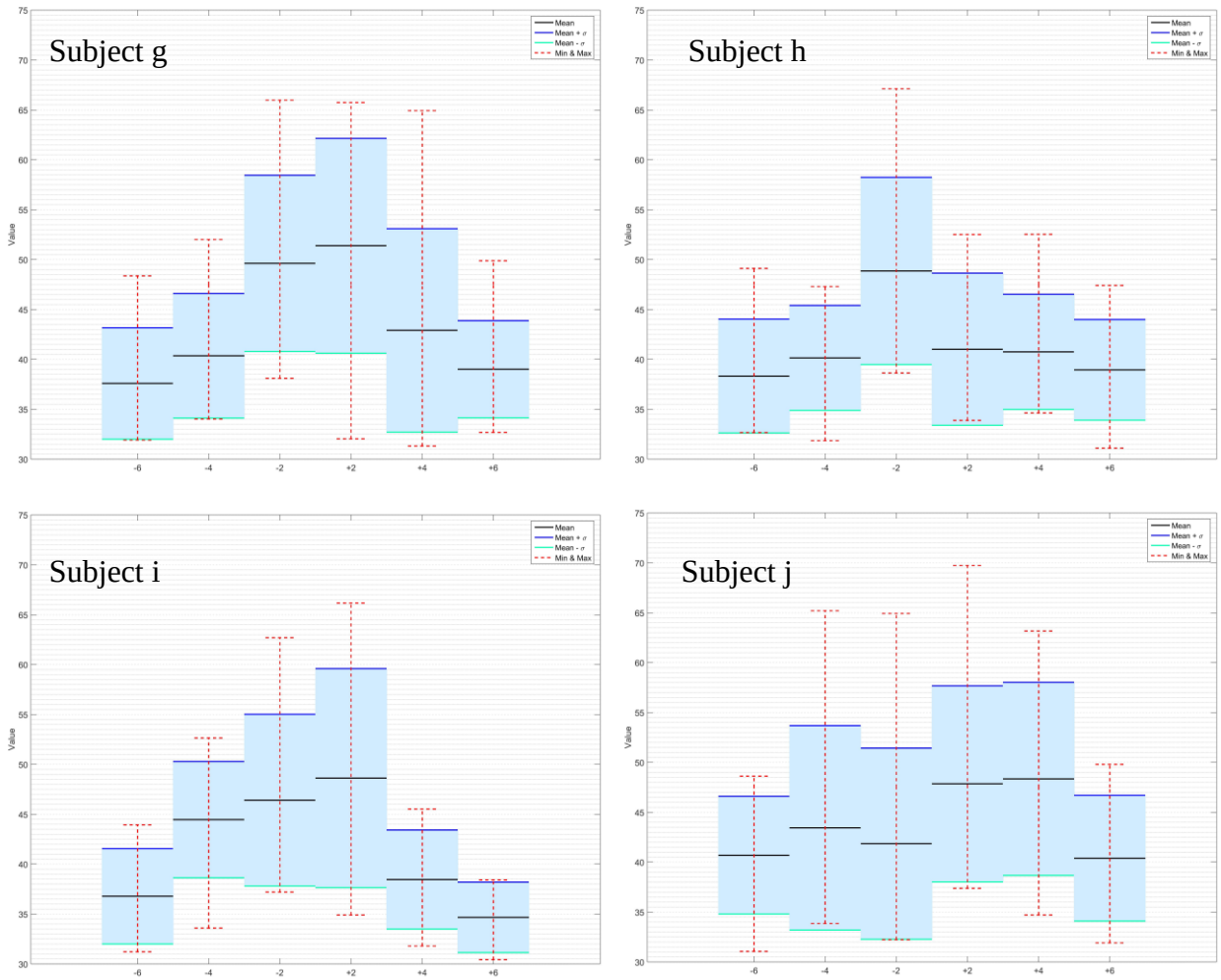
Subject g
Subject h
Subject i
Subject j
Mean
Mean + σ
Mean - σ
Min & Max
Value
75
70
65
60
55
50
45
40
35
30
-6
-4
-2
+2
+4
+6

Appendix B: Average and standard deviation plot of estimated parameters for all of subjects' responses to each target

1) Moment of inertia

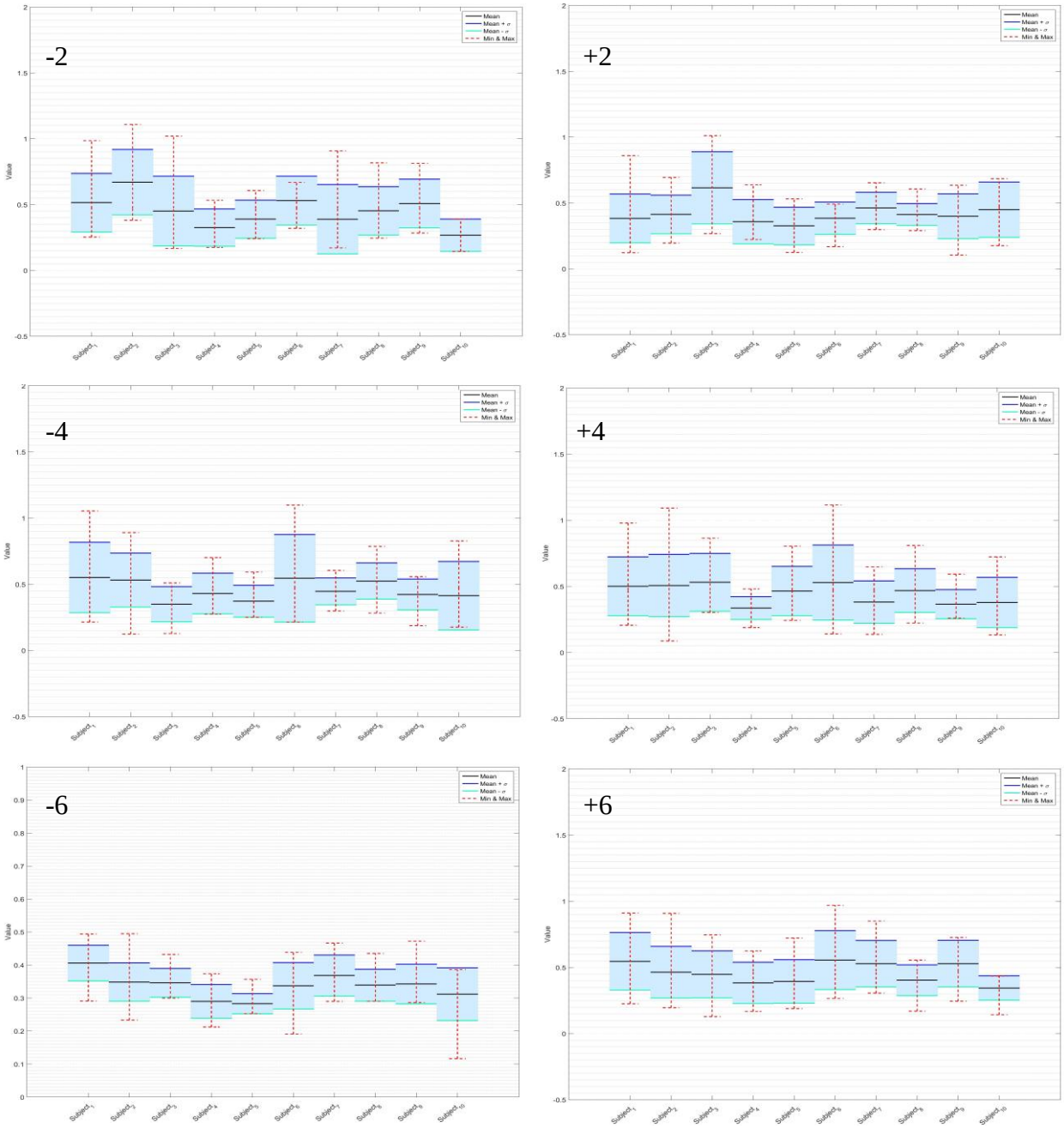

2) Rotating mass

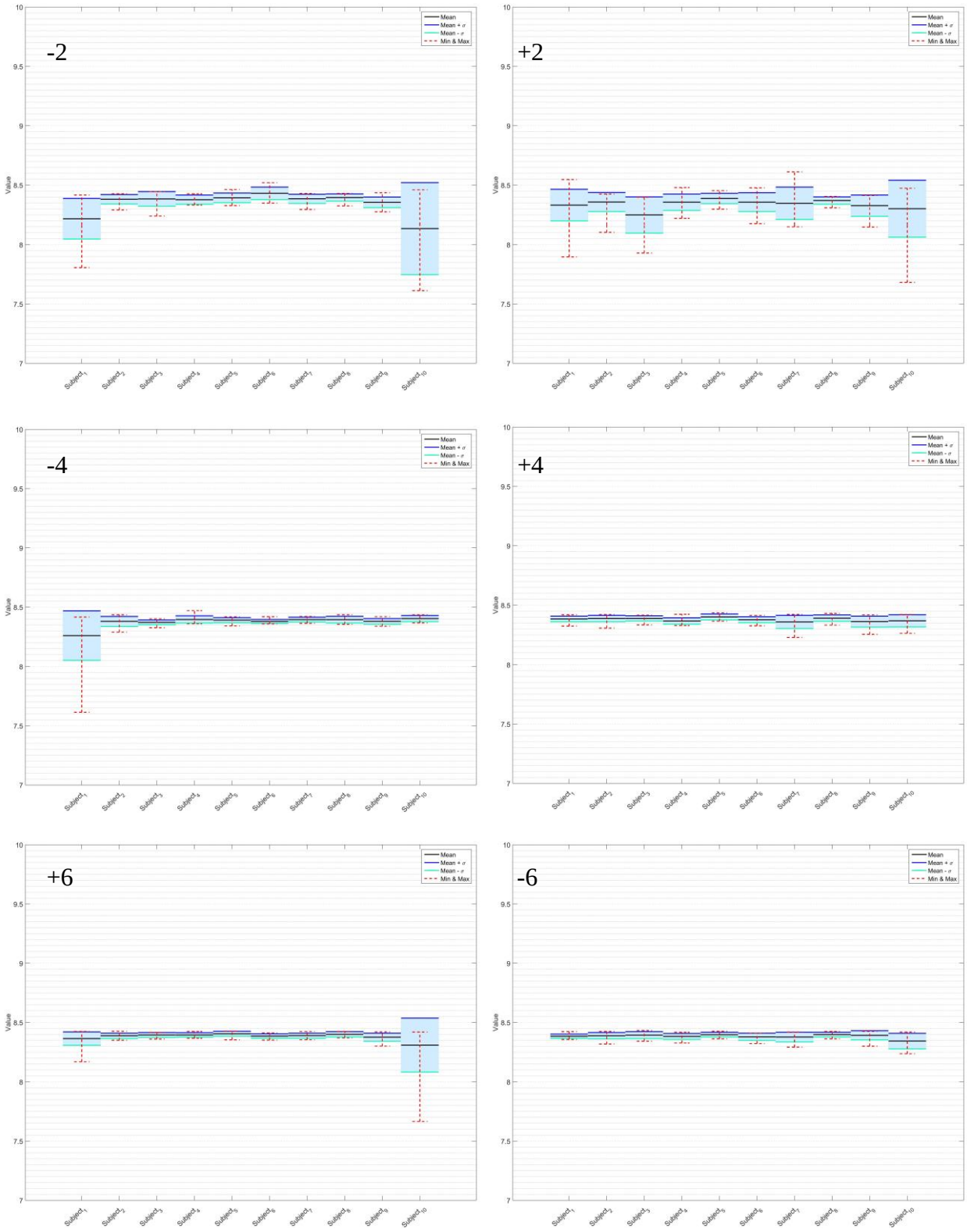

3) Effective length

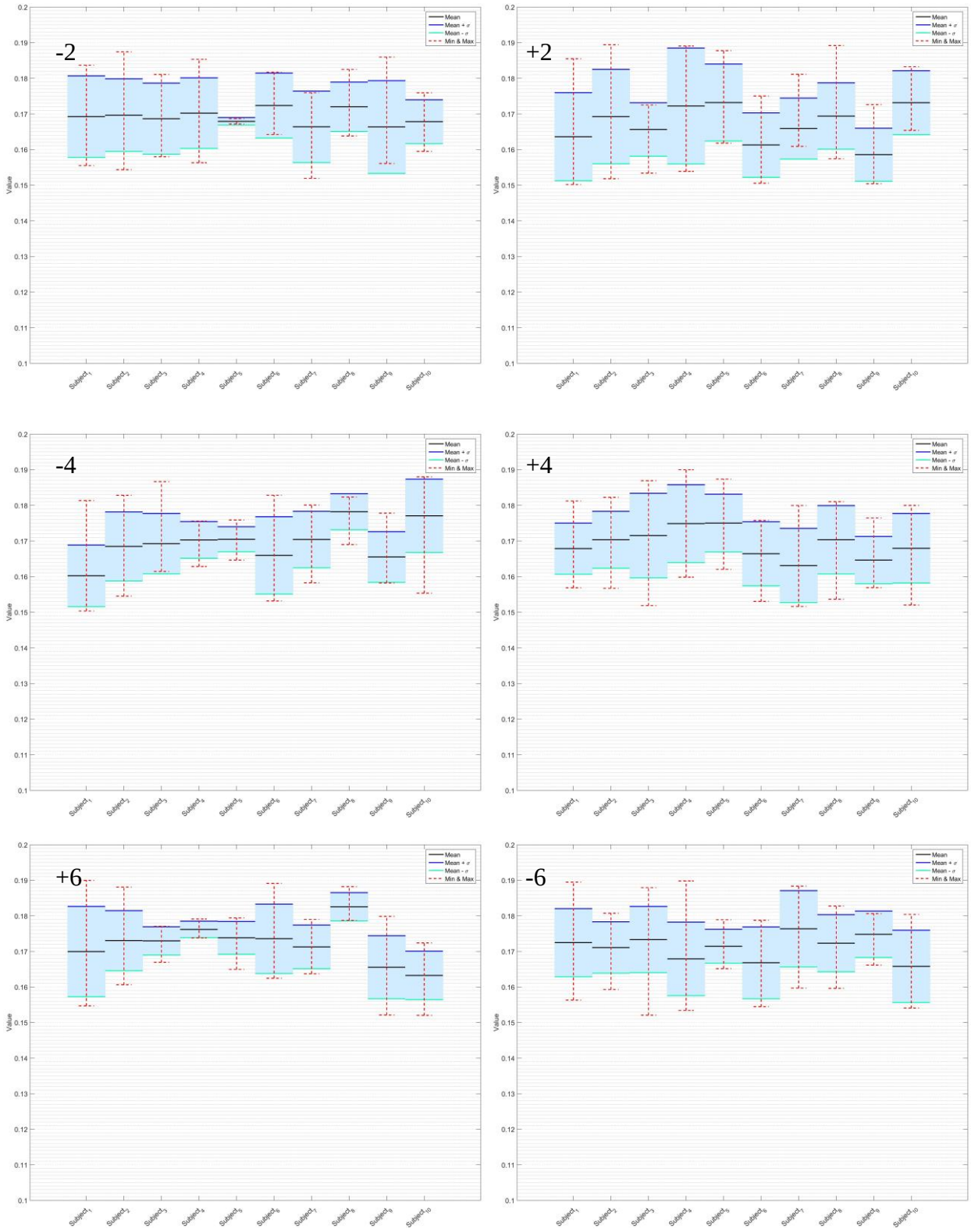

4) Delay

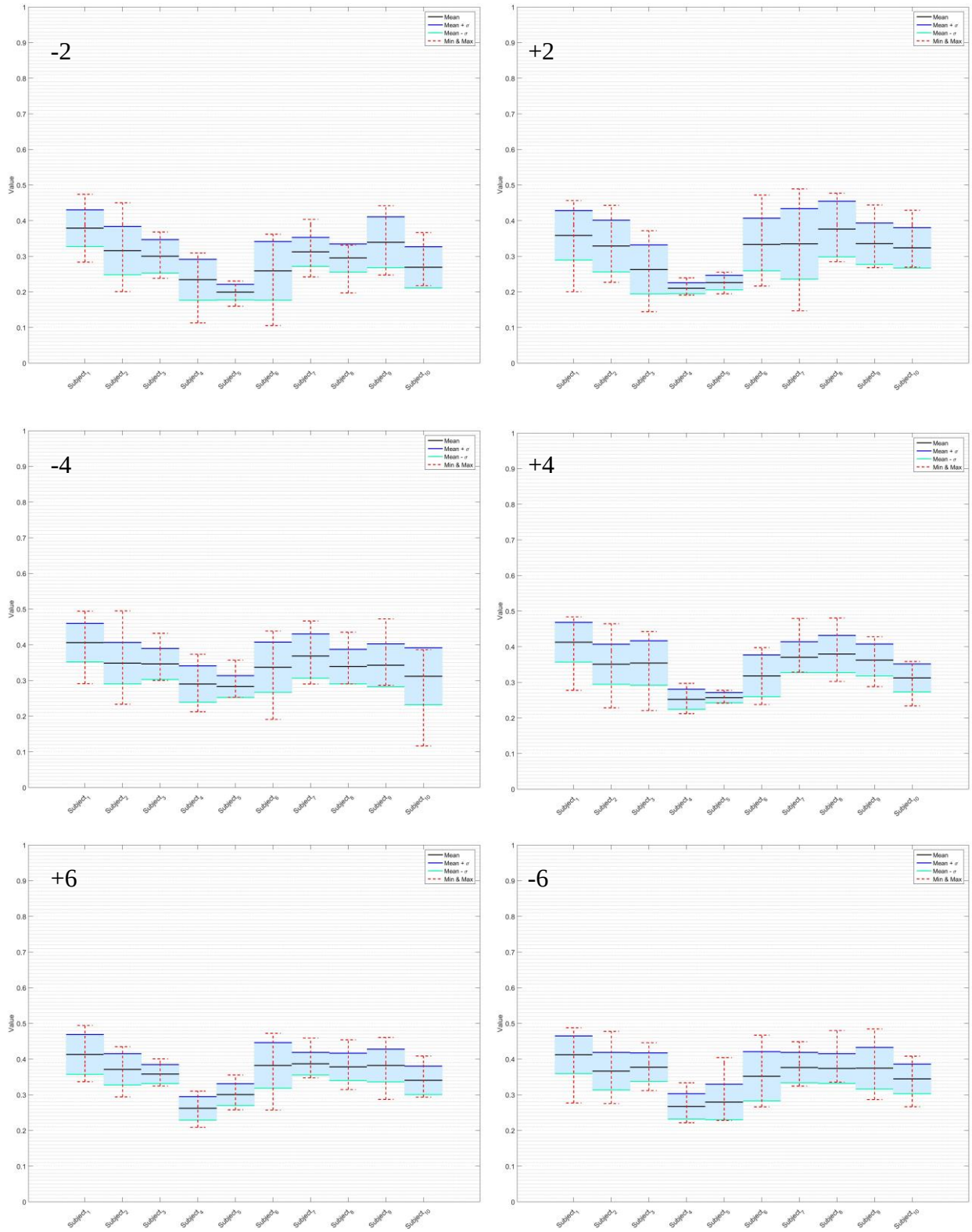
-2
+2
-4
+4
+6
-6
Mean
Mean + σ
Mean - σ
Min & Max
Value
Subject1
Subject2
Subject3
Subject4
Subject5
Subject6
Subject7
Subject8
Subject9
Subject10

5) Stiffness coefficient

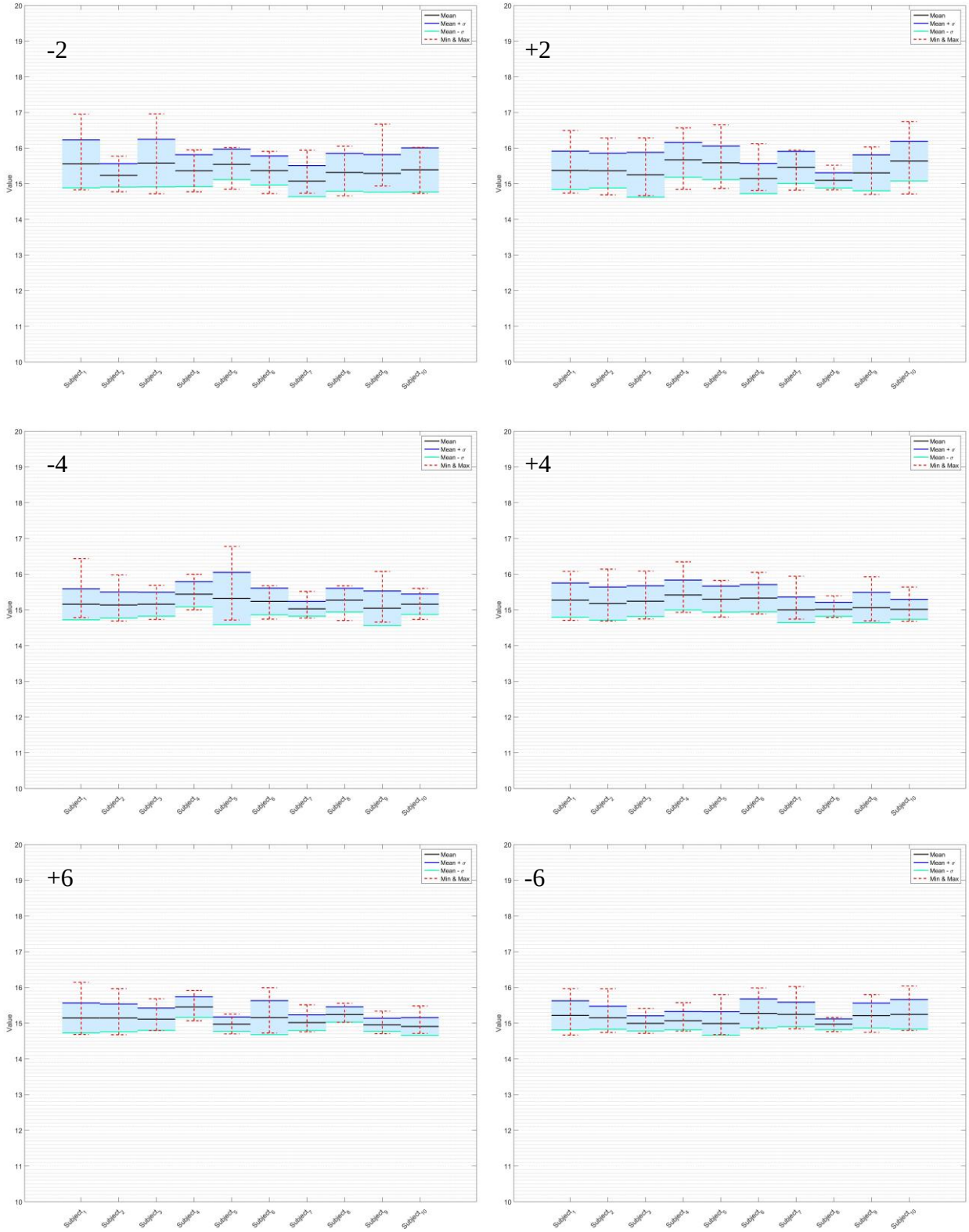

6) Damping coefficient

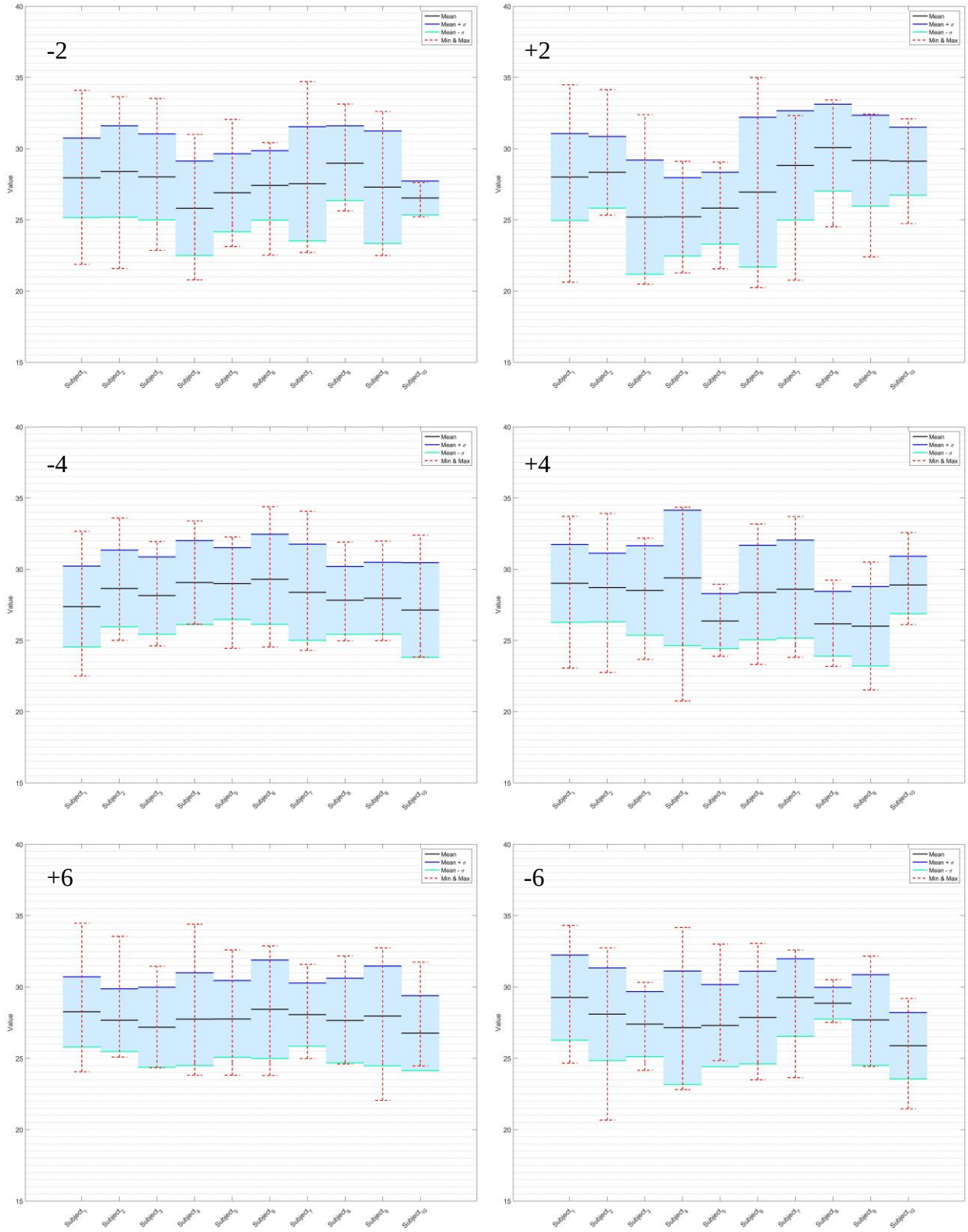

7) Proportional gain

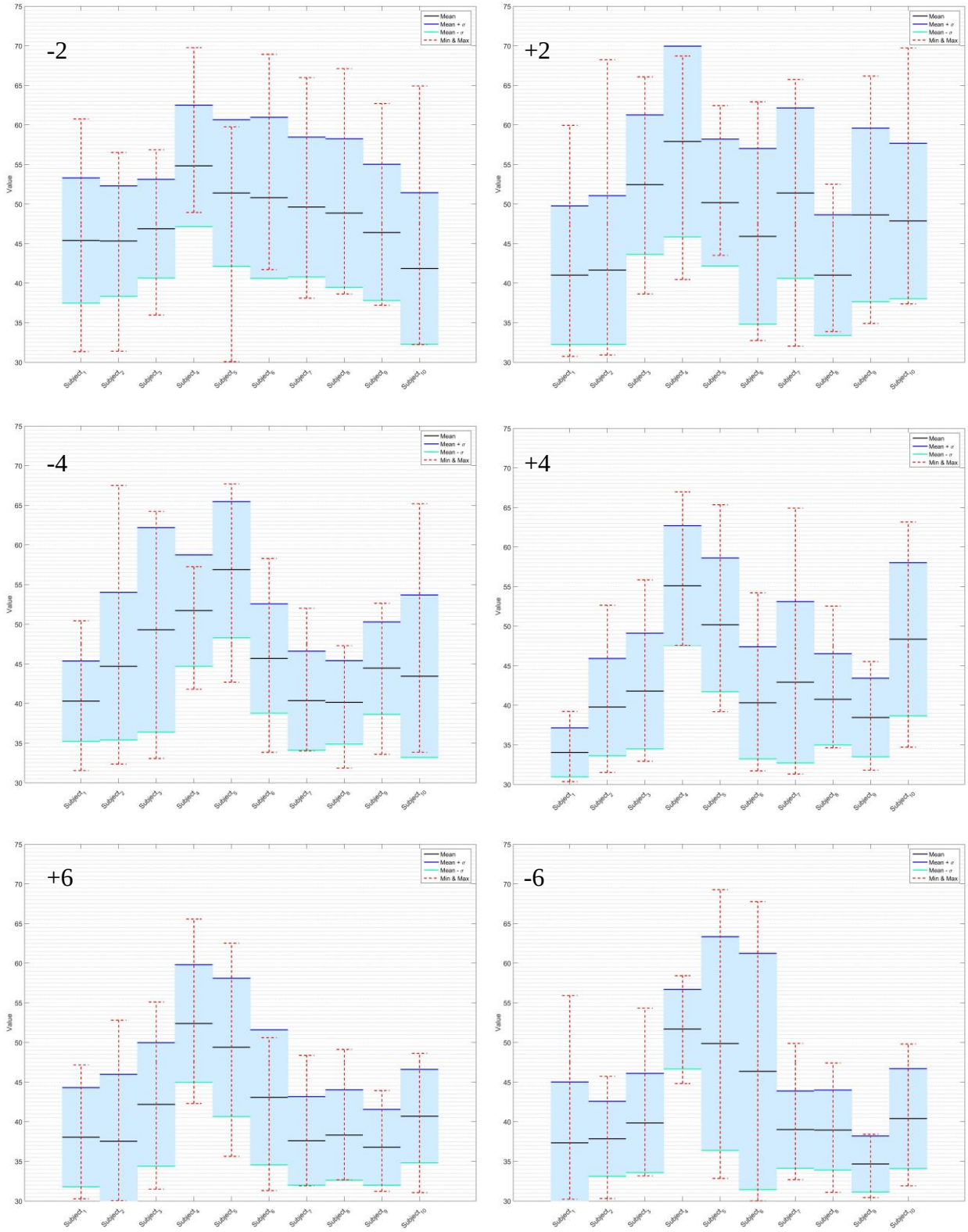

Appendix C: Average and standard deviation plot of estimated parameters for all of subjects' responses to each target

1) Percentage of overshoot

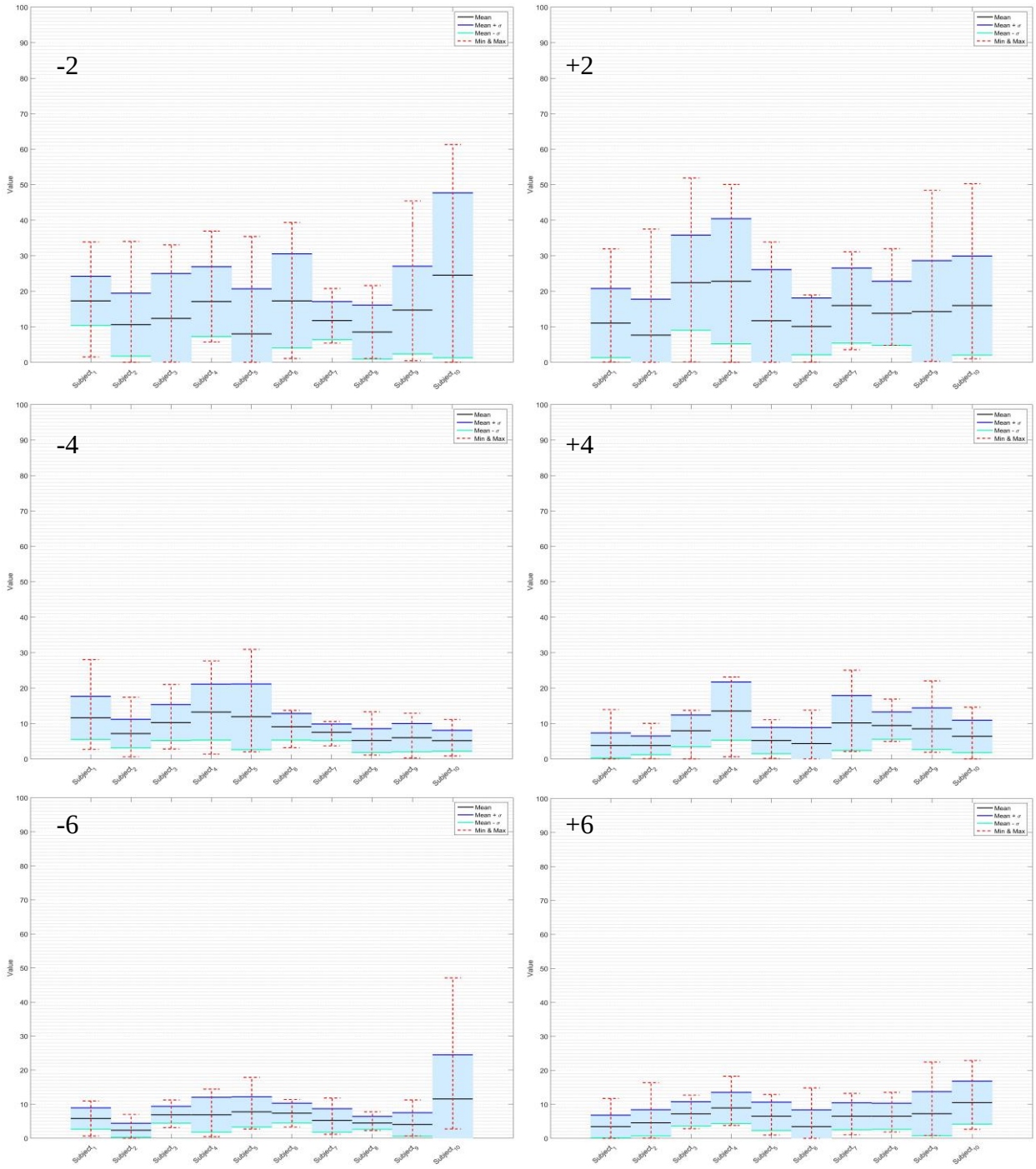

2) Settling time

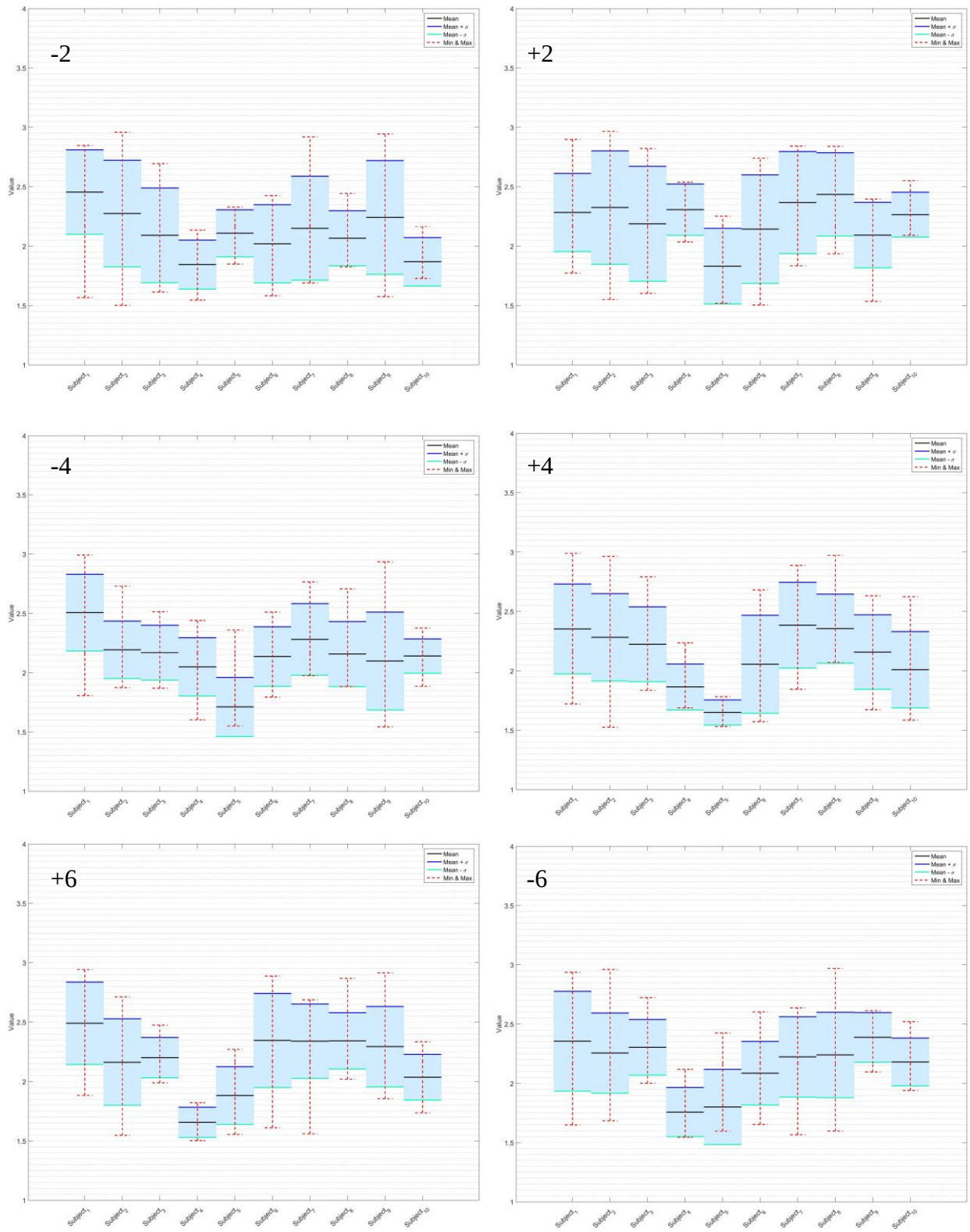

Appendix D: Average and standard deviation values of bandwdith of each subject's response to different targets

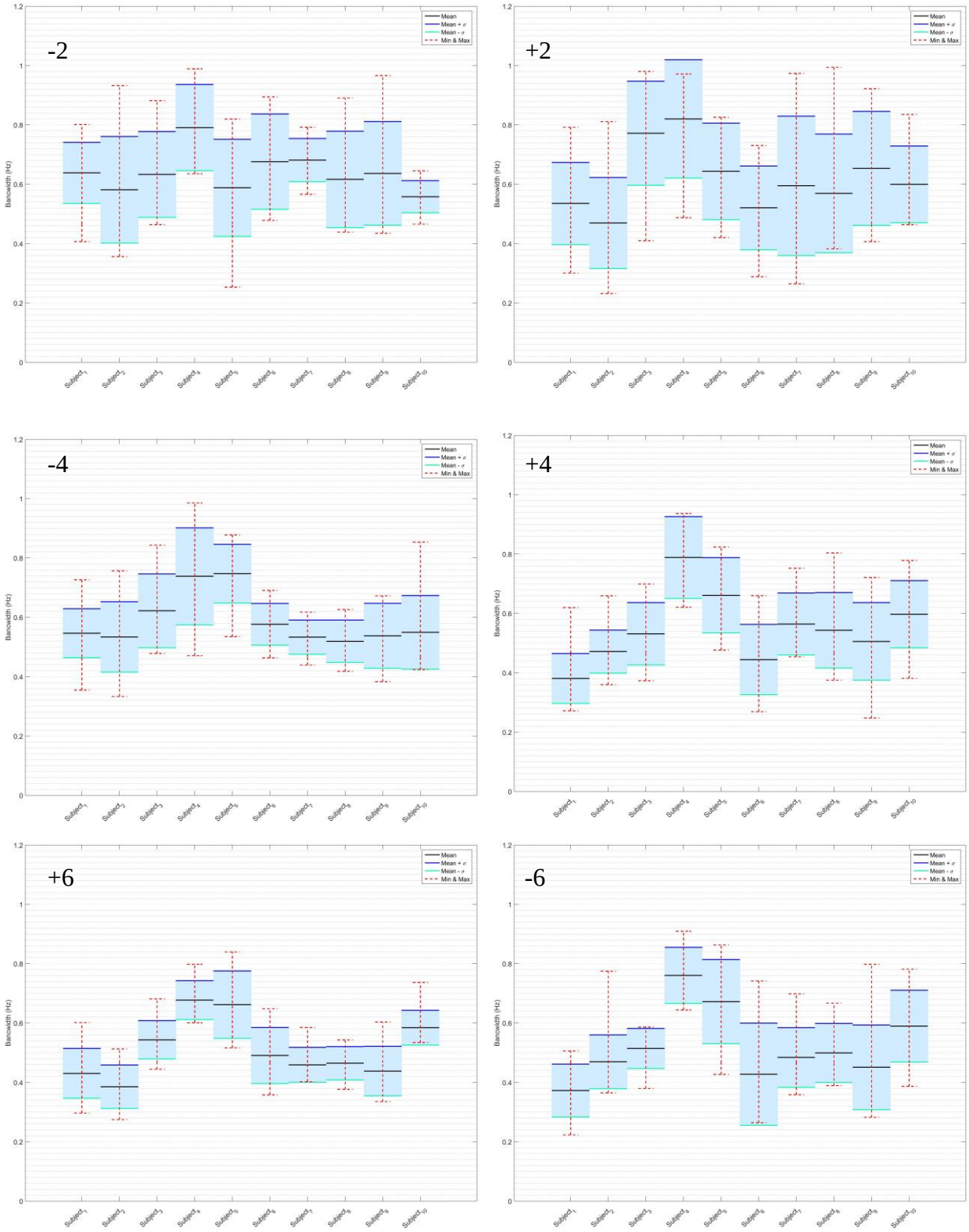

Appendix E: Mathematical model of responses of subjects 1 and 2 to different targets

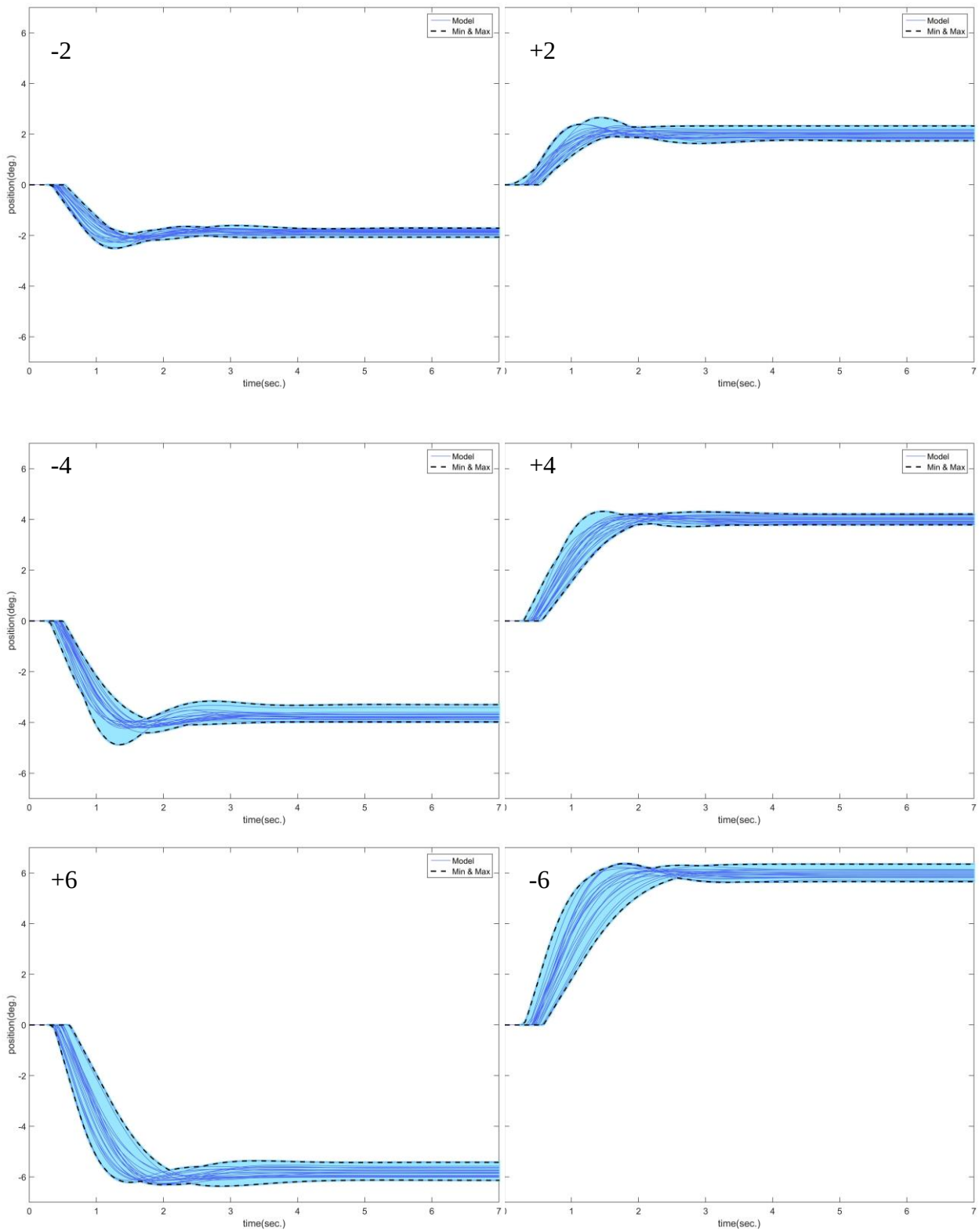

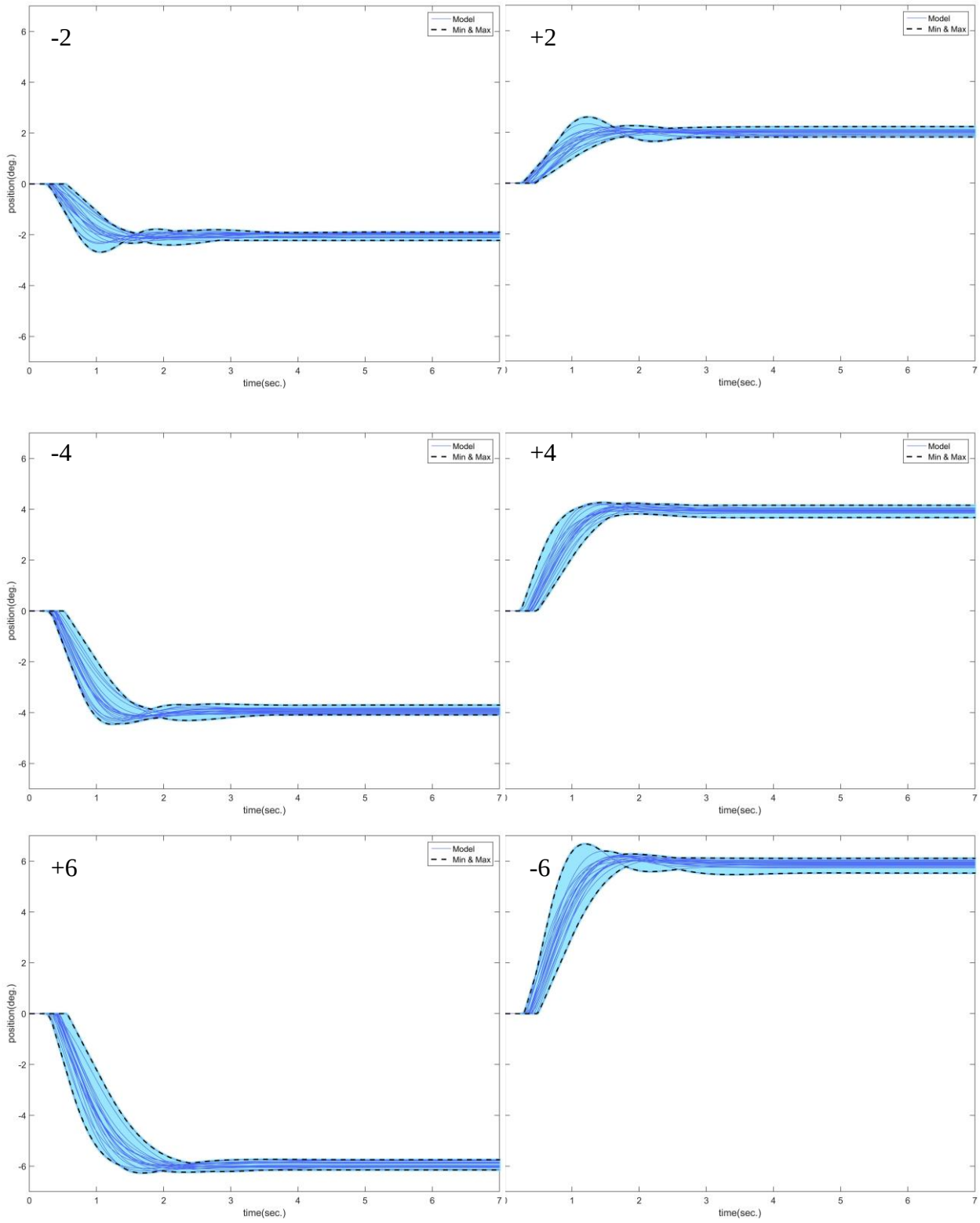
-2
+2
-4
+4
+6
-6
Model
Min & Max
position(deg.)
time(sec.)

Appendix F: One series of experimental and modeled response of each subject to different targets

Subject a

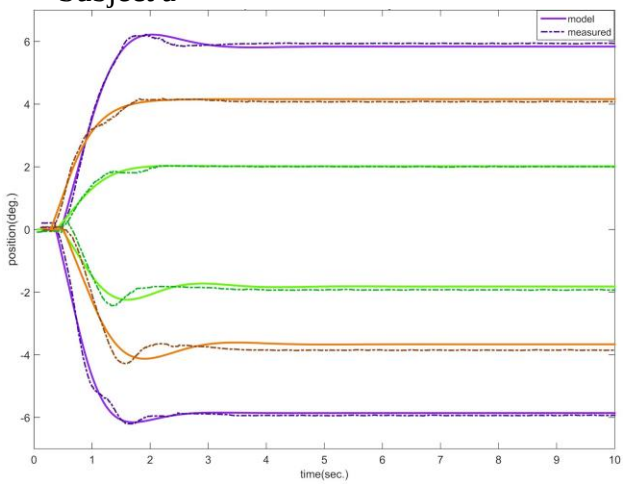

Subject b

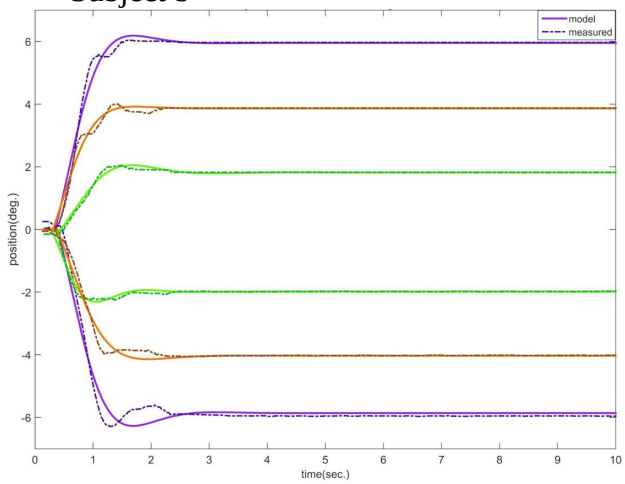

Subject c

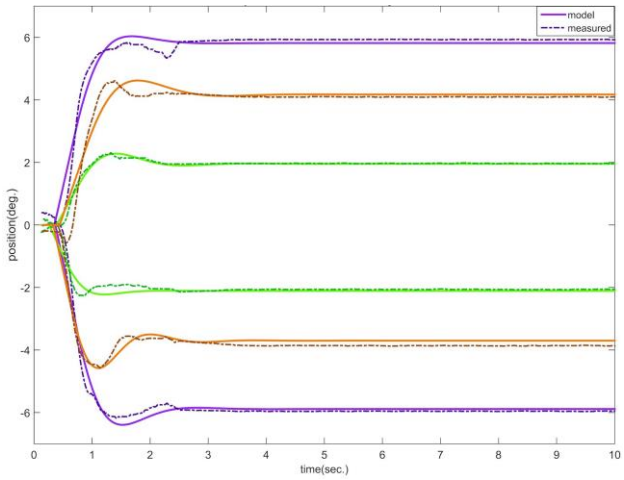

Subject d

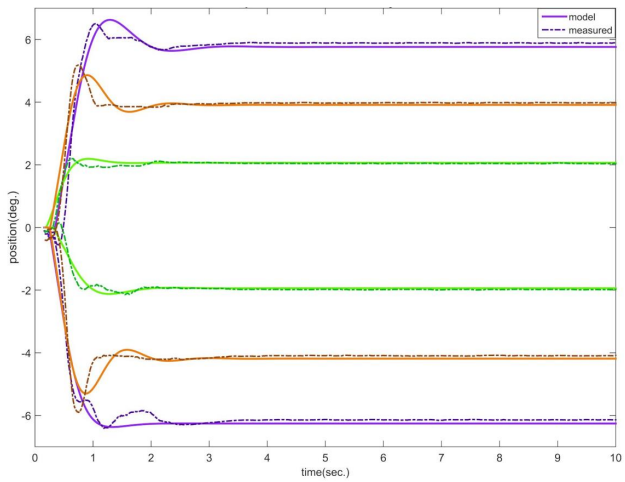

Subject e

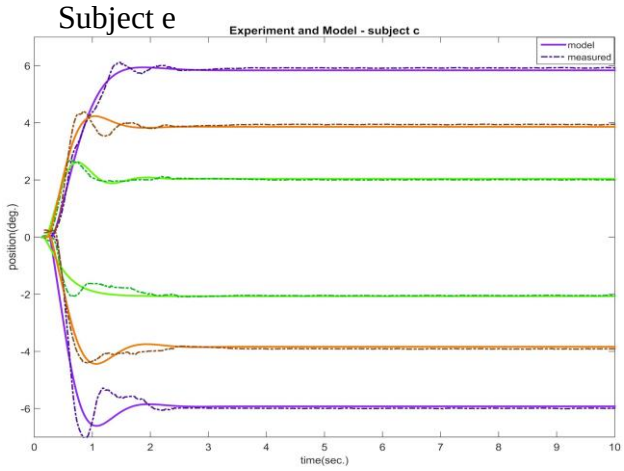

Subject f

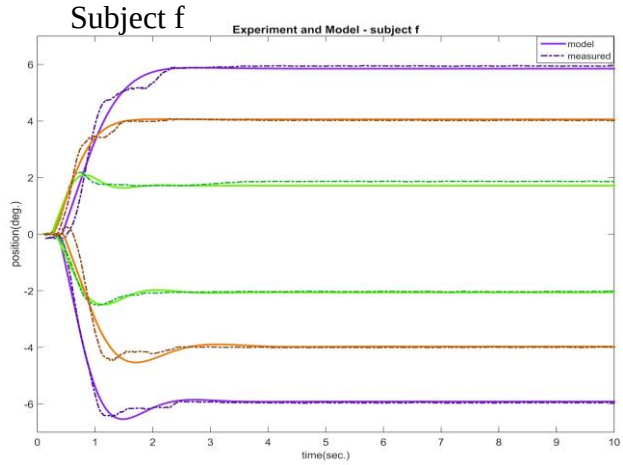

Subject g

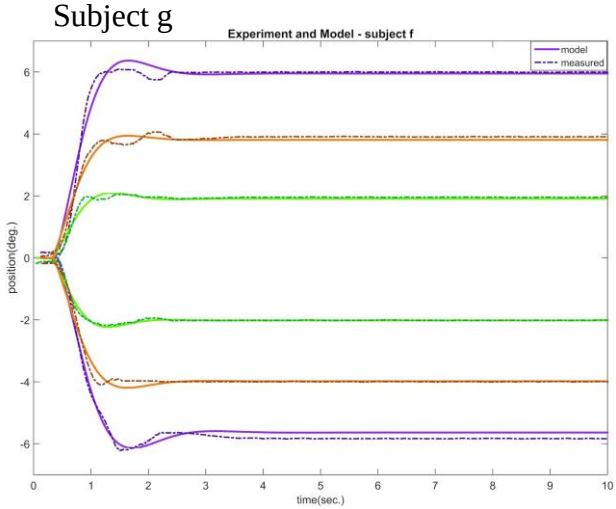

Subject h

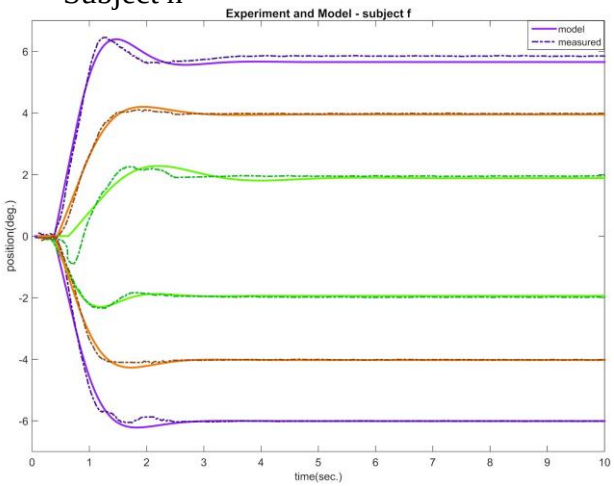

Subject i

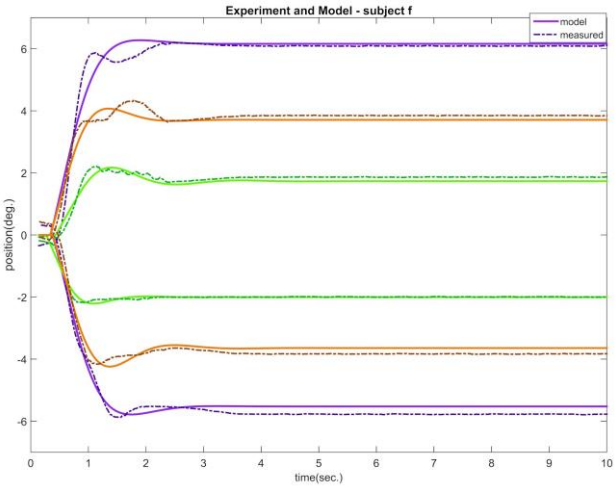

Subject j

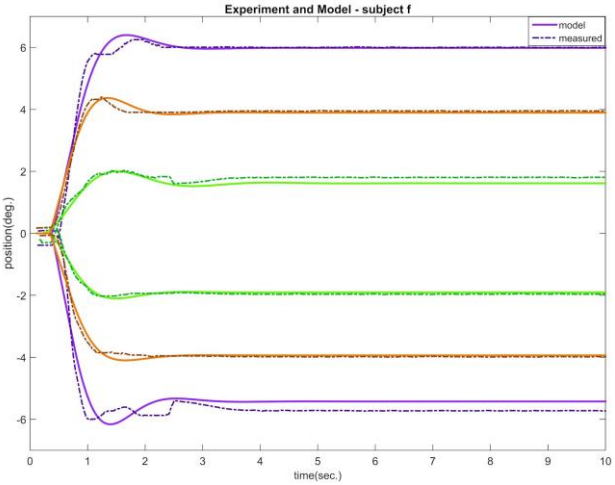

Appendix G: MATLAB codes

```
%For organizing experimental data%

for x = 1:9


clear('k')
clear('j')
clear('y')
clear('u')

Mag = [2 4 6];
k = 1;
j = 1;


while k<4

i = Mag(k);

   while j<41

y = eval([char(96+x) '_' num2str(i) '_n_' num2str(j) '.OutputData']);
u = eval([char(96+x) '_' num2str(i) '_n_' num2str(j) '.InputData']);
s = size(y);
s = s(1,1);
y(s+1:1000) = y(s);
u(s+1:1000) = u(s);
eval([char(96+x) '_' num2str(i) '_n_' num2str(j) '=iddata(y,u,0.01);']);

j = j+1;

   clear('u');
   clear('y');
   clear('s');

   end
j = 1;
   k= k+1;
end


clear('k')
clear('j')
clear('y')
clear('u')

Mag = [2 4 6];
k = 1;
j = 1;
```

```
while k<4

i = Mag(k);

   while j<41

y = eval([char(96+x) '_' num2str(i) '_p_' num2str(j) '.OutputData']);
u = eval([char(96+x) '_' num2str(i) '_p_' num2str(j) '.InputData']);
s = size(y);
s = s(1,1);
y(s+1:1000) = y(s);
u(s+1:1000) = u(s);
eval([char(96+x) '_' num2str(i) '_p_' num2str(j) '=iddata(y,u,0.01);']);

j = j+1;

   clear('u');
   clear('y');
   clear('s');

   end
j = 1;
   k= k+1;
end
x = x+1;
end


%Funtion of mathematical model%

function F = out_sim(x,t)

I = x(1);
b = x(2);
k = x(3);
T = x(4);
m = x(5);
L = x(6);
G = x(7);

myobj = sim('shahab','SrcWorkspace','Current', ...
          'StopTime','10');

      y = myobj.get('yout');

      i = t/0.01;

      F = y(1:1000);


End
```

```
%Extension of steady state for subject c , positive directions
i = 1;
j = 1;
MAG = [2 4 6];


for i = 1:3

 for j = 1:40


clear ('yf')
clear ('fc')
clear ('fcn')

c = linspace(-2,2,250);


fc = (4.5*c.*(c.^2))./((nthroot((2.5 +3*( c.^2)).^2, 3)).^2);
fc = fc/max(fc);


v_250 = eval(['c_' num2str(MAG(i)) '_p_' num2str(j) '.OutputData(250) ;']);
v_500 = eval(['c_' num2str(MAG(i)) '_p_' num2str(j) '.Inputdata(250) ;']);

delta = (v_500 - v_250);

delta = delta/2;
fc = delta*fc;
fc = fc';
mian = (v_250 + v_500)/2;
fc = fc+mian;

fcn = randi([0,100],270,1);

fcn = medfilt1(fcn,20);
fcn = fcn/2000;
fcn = fcn - 0.025;
o = fcn(11:260);
fcn = o;
fc = fc+fcn;

eval(['c_' num2str(MAG(i)) '_p_' num2str(j) '.OutputData(251:500) = fc;']);

yf = rand(520,1);
yf = medfilt1(yf,20);
yf = yf/10;
yf = yf-0.05;
o = yf(11:510);
yf = o;

yf = yf + eval(['c_' num2str(MAG(i)) '_p_' num2str(j) '.Inputdata(250) ;']);
eval(['c_' num2str(MAG(i)) '_p_' num2str(j) '.OutputData(501:1000) = yf;']);
```

```
eval([' yf(1:600,1) = c_' num2str(MAG(i)) '_p_' num2str(j) '.OutputData(400)
;']);

fcn = randi([0,100],620,1);
fcn = medfilt1(fcn,20);
fcn = fcn/2000;
fcn = fcn - 0.025;
o = fcn(11:610);
fcn = o;
yf = yf+fcn;

eval(['c_' num2str(MAG(i)) '_p_' num2str(j) '.OutputData(401:1000) = yf;']);


j = j+1;
 end




i = i+1;

end



%Parameter estimation and simulation for subject g , target -2%

rslt_g_2_n = [];
rslt_g_4_n = [];
rslt_g_6_n = [];

rslt_g_2_p = [];
rslt_g_4_p = [];
rslt_g_6_p = [];



j = 1;

shahab

set_param('shahab/Step','After','-2')

 while j < 21
clear
('tdata','ydata','g','in0','options','x','I','b','k','T','m','L','G','y','t',
's','u','data','sys','S','BW')
tdata = 0.01:0.01:10;
tdata = tdata';
eval(['ydata = g_2_n_' num2str(j) '.OutputData;']); %2 is magnitude, n is
negative direction
```

```
g = @(in,tdata)(out_sim(in,tdata));

in0 = [0.5 0.5 0.5 0.5 0.5 0.5 0.5];

options = optimoptions(@lsqcurvefit,'TolFun',10^-
4,'FinDiffRelStep',0.01,'TolX',10^-
4,'MaxFunEvals',1000,'MaxIter',1000,'PrecondBandWidth',0);

lb = [ 0 0 0 0.01 1 0.1 0];
ub = [ 1000 1000 1000 2 20 1 1000];

x = lsqcurvefit(g,in0,tdata,ydata,lb,ub,options); %parameter estimation

I = x(1);
b = x(2);
k = x(3);
T = x(4);
m = x(5);
L = x(6);
G = x(7);

myobj = sim('shahab','SrcWorkspace','Current', ...
          'StopTime','10');

      y = myobj.get('yout');
      t = myobj.get('tout');

      s = size(y);
      s = s(1,1);
      u = [];
      u(1:s,1) = a_2_n_1.InputData(1);
      data = iddata(y , u , 0.01);
      sys = tfest(data,20);

      S = stepinfo(y,t);
      BW = bandwidth(sys);

      %I b k T m L G OS Peak PeakTime RiseTime SettlingTime BW
      rslt_g_2_n(j,1:7) = x;
      rslt_g_2_n(j,8) = S.Overshoot;
      rslt_g_2_n(j,9) = S.Peak;
      rslt_g_2_n(j,10) = S.PeakTime;
      rslt_g_2_n(j,11) = S.RiseTime;
      rslt_g_2_n(j,12) = S.SettlingTime;
      rslt_g_2_n(j,13) = BW;

      j = j+1
 end



%Plot of statistical analysis
figure
```

```
MAG = [6 4 2];

j = 1;

i = 1;

y_1 = [];

y_2 = [];

y_3 = [];

y_4 = [];

y_5 = [];

y_6 = [];

y_7 = [];

y_8 = [];

y_9 = [];

y_10 = [];

y_1 = rslt_a_2_n(:,1);

y_2 = rslt_b_2_n(:,1);

y_3 = rslt_c_2_n(:,1);

y_4 = rslt_d_2_n(:,1);

y_5 = rslt_e_2_n(:,1);

y_6 = rslt_f_2_n(:,1);

y_7 = rslt_g_2_n(:,1);

y_8 = rslt_h_2_n(:,1);

y_9 = rslt_i_2_n(:,1);

y_10 = rslt_j_2_n(:,1);

for j = 1:10
```

```
A = [];

B = [];

eval(['Mean = mean(y_' num2str(j) ');']);

standard = eval(['std(y_' num2str(j) ');']);

mean_line((j-1)*20+1:j*20) = Mean;

high_line((j-1)*20+1:j*20) = Mean+standard;

low_line((j-1)*20+1:j*20) = Mean-standard;
t = linspace(j,j+1,20);

k = 1;
for k = 1:1000



    A = [j+k*0.001 ; j+k*0.001 ];

    B = [low_line(j*20) ; high_line(j*20)];

    plot(A , B , 'Color' , [209/255 236/255 255/255] , 'LineWidth' , 1);

    hold on

    k = k+1;

end
p1 = plot(t,mean_line((j-1)*20+1:j*20),'k' , 'LineWidth' , 2)

% hold on

p2 = plot(t,high_line((j-1)*20+1:j*20),'Color' , [4/255 0 1],'LineWidth' , 2)
% hold on

p3 = plot(t,low_line((j-1)*20+1:j*20),'Color' , [0/255 1 174/255],'LineWidth'
, 2)
% hold on
A = [];

B = [];
A = [(j+j+1)/2 , (j+j+1)/2];

eval([ 'B(1,1) = min(y_' num2str(j) ');' ]);

eval([ 'B(1,2) = max(y_' num2str(j) ');' ]);

p4 = plot(A,B,'r','LineWidth',1.5,'LineStyle','--');
```

```
% hold on
A = [];

B = [];

med = (j+j+1)/2;

A = linspace(med-0.2 , med+0.2 , 5);

eval([ 'B(1:5) = max(y_' num2str(j) ');' ]);

plot(A,B,'r','LineWidth',1.5,'LineStyle','--');

% hold on

A = [];

B = [];

med = (j+j+1)/2;

A = linspace(med-0.2 , med+0.2 , 5);

eval([ 'B(1:5) = min(y_' num2str(j) ');' ]);

plot(A,B,'r','LineWidth',1.5,'LineStyle','--');

% hold on
j = j+1;

end
legend([p1 p2 p3 p4],{'Mean','Mean + \sigma' , 'Mean - \sigma' , 'Min &
Max'});

xlim([0 12])

ylim([-.5 2])

% xlabel('                          -6                          -4
-2                    +2                    +4                          +6
' , 'FontSize' , 14);

ylabel('Value' , 'FontSize' , 14);

ax = gca;

ax.XTickLabelMode = 'manual'

ax.XTickMode = 'manual'

ax.XTick = [1.5 ; 2.5 ; 3.5 ; 4.5 ; 5.5 ; 6.5 ; 7.5 ; 8.5 ; 9.5 ; 10.5 ];
```

```
ax.XTickLabel = ['Subject_{1 }' ; 'Subject_{2 }' ; 'Subject_{3 }' ;
'Subject_{4 }' ; 'Subject_{5 }' ; 'Subject_{6 }' ; ...

    'Subject_{7 }' ; 'Subject_{8 }' ; 'Subject_{9 }' ; 'Subject_{10}'];

ax.FontSize = 14

ax.XTickLabelRotation = 45

ax.YGrid = 'on'

ax.YMinorGrid = 'on'

ax.GridLineStyle = '--'

set(gcf, 'PaperUnits', 'inches');
 x_width=25 ;y_width=18.75
 set(gcf, 'PaperPosition', [0 0 x_width y_width]); %
 saveas(gcf,'2n1.jpg')

hold off

%Table of statistical analysis
load ('only_result')
x = 1;
y = 1;
z= 1;
for x = 1:10
    for y = 1:3
        for z = 1:2

i = 1;
j = [];
k = 1;

s = eval(['size(rslt_' char(96+x) '_' num2str(y*2) '_' char(109+2*z-1)
');']);
s = s(1,1);

for i = 1:s
    if eval(['rslt_' char(96+x) '_' num2str(2*y) '_' char(109+2*z-1)
'(i,1)>1.2'])
      j(k) = i;
      k = k+1;
      i = i+1;
    else
        i = i+1;
    end
end
eval(['rslt_' char(96+x) '_' num2str(2*y) '_' char(109+2*z-1) '=
removerows(rslt_' char(96+x) '_' num2str(2*y) '_' char(109+2*z-1)
',''ind'',j);']);
z = z+1;
        end
```

```
    z = 1;
    y = y+1;
    end
y = 1;
x = x+1;
end


i = 1;
j = 1;
k = 1;


for i = 1:3
    for j = 1:2
D = [];
SD = [];

eval(['y_1 = rslt_a_' num2str(2*i) '_' char(109+(2*j-1)) '(:,1);']);
eval(['y_2 = rslt_b_' num2str(2*i) '_' char(109+(2*j-1)) '(:,1);']);
eval(['y_3 = rslt_c_' num2str(2*i) '_' char(109+(2*j-1)) '(:,1);']);
eval(['y_4 = rslt_d_' num2str(2*i) '_' char(109+(2*j-1)) '(:,1);']);
eval(['y_5 = rslt_e_' num2str(2*i) '_' char(109+(2*j-1)) '(:,1);']);
eval(['y_6 = rslt_f_' num2str(2*i) '_' char(109+(2*j-1)) '(:,1);']);
eval(['y_7 = rslt_g_' num2str(2*i) '_' char(109+(2*j-1)) '(:,1);']);
eval(['y_8 = rslt_h_' num2str(2*i) '_' char(109+(2*j-1)) '(:,1);']);
eval(['y_9 = rslt_i_' num2str(2*i) '_' char(109+(2*j-1)) '(:,1);']);
eval(['y_10 = rslt_j_' num2str(2*i) '_' char(109+(2*j-1)) '(:,1);']);

m = 1;
for m = 1:10
D(m,1) = eval(['mean(y_' num2str(m) ');']);
D(m,1) = round(D(m,1),3);
m = m+1;
end
m = 1;
for m = 1:10
SD(m,1) = eval(['std(y_' num2str(m) ');']);
SD(m,1) = round(SD(m,1),3);
m = m+1;
end

p_1 = [num2str(D(1),'%#-4.2f'),'  (',num2str(SD(1),'%#-4.2f'),')'];
p_2 = [num2str(D(02),'%#-4.2f'),'  (',num2str(SD(02),'%#-4.2f'),')'];
p_3 = [num2str(D(03),'%#-4.2f'),'  (',num2str(SD(03),'%#-4.2f'),')'];
p_4 = [num2str(D(04),'%#-4.2f'),'  (',num2str(SD(04),'%#-4.2f'),')'];
p_5 = [num2str(D(05),'%#-4.2f'),'  (',num2str(SD(05),'%#-4.2f'),')'];
p_6 = [num2str(D(06),'%#-4.2f'),'  (',num2str(SD(06),'%#-4.2f'),')'];
p_7 = [num2str(D(7),'%#-4.2f'),'  (',num2str(SD(07),'%#-4.2f'),')'];
p_8 = [num2str(D(08),'%#-4.2f'),'  (',num2str(SD(08),'%#-4.2f'),')'];
p_9 = [num2str(D(09),'%#-4.2f'),'  (',num2str(SD(09),'%#-4.2f'),')'];
p_10 = [num2str(D(10),'%#-4.2f'),'  (',num2str(SD(10),'%#-4.2f'),')'];

eval(['P_' num2str(2*i) '_' char(109+(2*j-1))
'_I=[p_1;p_2;p_3;p_4;p_5;p_6;p_7;p_8;p_9;p_10]';]);
```

```
j = j+1;
    end
    i = i+1;
end

%plot of experimental and modeled data

x = rslt_j_6_n(4,1:7);

I = x(1);
b = x(2);
k = x(3);
T = x(4);
m = x(5);
L = x(6);
G = x(7);

set_param('shahab/Step','After','-6')
myobj = sim('shahab','SrcWorkspace','Current', ...
          'StopTime','10');

      y_model = myobj.get('yout');
      t = myobj.get('tout');

      y_measured = j_6_n_4.OutputData;


      plot(t,y_model,'Color' , [143/255 45/255 240/255],'LineWidth',2.5);
      hold on
      plot(t,y_measured,'Color' , [77/255 3/255 152/255],'LineStyle' , '-.'
,'LineWidth',2);
      hold on
      xlim([0 10]);
      ylim([-7 7]);
      xlabel('time(sec.)' , 'FontSize' , 14);
ylabel('position(deg.)');
title('Experiment and Model - subject f')



%%%%%%%%%%%%%%%%%%%%%%%%%%%%%%%%%%%%%%%%%%%%%%%%%%%%%%%%%%%%%%%%%%%%%%%%%%%%

x = rslt_j_6_p(4,1:7);

I = x(1);
b = x(2);
k = x(3);
T = x(4);
m = x(5);
L = x(6);
G = x(7);

set_param('shahab/Step','After','+6')
myobj = sim('shahab','SrcWorkspace','Current', ...
```

```
        'StopTime','10');

    y_model = myobj.get('yout');
    t = myobj.get('tout');

    y_measured = j_6_p_4.OutputData;


    plot(t,y_model,'Color' , [143/255 45/255 240/255],'LineWidth',2.5);
    hold on
    plot(t,y_measured,'Color' , [77/255 3/255 152/255],'LineStyle' , '-.'
,'LineWidth',2);
    hold on

    xlim([0 10]);
    ylim([-7 7]);
    xlabel('time(sec.)');
ylabel('position(deg.)');

legend('model', 'measured')

%%%%%%%%%%%%%%%%%%%%%%%%%%%%%%%%%%%%%%%%%%%%%%%%%%%%%%%%%%%%%%%%%%%%%%%%%%%%%%%%
%%%%%%




x = rslt_j_2_n(4,1:7);

I = x(1);
b = x(2);
k = x(3);
T = x(4);
m = x(5);
L = x(6);
G = x(7);

set_param('shahab/Step','After','-2')
myobj = sim('shahab','SrcWorkspace','Current', ...
        'StopTime','10');

    y_model = myobj.get('yout');
    t = myobj.get('tout');

    y_measured = j_2_n_4.OutputData;


    plot(t,y_model,'Color' , [103/255 246/255 7/255],'LineWidth',2.5);
    hold on
    plot(t,y_measured,'Color' , [0/255 181/255 36/255],'LineStyle' , '-.'
,'LineWidth',2);
    hold on
    xlim([0 10]);
```

```
      ylim([-7 7]);


%%%%%%%%%%%%%%%%%%%%%%%%%%%%%%%%%%%%%%%%%%%%%%%%%%%%%%%%%%%%%%%%%%%%%%

x = rslt_j_2_p(4,1:7);

I = x(1);
b = x(2);
k = x(3);
T = x(4);
m = x(5);
L = x(6);
G = x(7);

set_param('shahab/Step','After','+2')
myobj = sim('shahab','SrcWorkspace','Current', ...
          'StopTime','10');

      y_model = myobj.get('yout');
      t = myobj.get('tout');

      y_measured = j_2_p_4.OutputData;


      plot(t,y_model,'Color' , [103/255 246/255 7/255],'LineWidth',2.5);
      hold on
      plot(t,y_measured,'Color' , [0/255 181/255 36/255],'LineStyle' , '-.'
,'LineWidth',2);
      hold on
      xlim([0 10]);
      ylim([-7 7]);

%%%%%%%%%%%%%%%%%%%%%%%%%%%%%%%%%%%%%%%%%%%%%%%%%%%%%%%%%%%%%%%%%%%%%%%%%%%%%%%
%%%%%%%%%

x = rslt_j_4_n(4,1:7);

I = x(1);
b = x(2);
k = x(3);
T = x(4);
m = x(5);
L = x(6);
G = x(7);

set_param('shahab/Step','After','-4')
myobj = sim('shahab','SrcWorkspace','Current', ...
          'StopTime','10');

      y_model = myobj.get('yout');
      t = myobj.get('tout');

      y_measured = j_4_n_4.OutputData;
```

```
      plot(t,y_model,'Color' , [236/255 125/255 13/255],'LineWidth',2.5);
      hold on
      plot(t,y_measured,'Color' , [148/255 73/255 16/255],'LineStyle' , '-.'
,'LineWidth',2);
      hold on
      xlim([0 10]);
      ylim([-7 7]);
      xlabel('time(sec.)');
ylabel('position(deg.)');




%%%%%%%%%%%%%%%%%%%%%%%%%%%%%%%%%%%%%%%%%%%%%%%%%%%%%%%%%%%%%%%%%%%%%%

x = rslt_j_4_p(4,1:7);

I = x(1);
b = x(2);
k = x(3);
T = x(4);
m = x(5);
L = x(6);
G = x(7);

set_param('shahab/Step','After','4')
myobj = sim('shahab','SrcWorkspace','Current', ...
          'StopTime','10');

      y_model = myobj.get('yout');
      t = myobj.get('tout');

      y_measured = j_4_p_4.OutputData;


      plot(t,y_model,'Color' , [236/255 125/255 13/255],'LineWidth',2.5);
      hold on
      plot(t,y_measured,'Color' , [148/255 73/255 16/255],'LineStyle' , '-.'
,'LineWidth',2);
      hold off
      xlim([0 10]);
      ylim([-7 7]);
      xlabel('time(sec.)' , 'FontSize' , 14);
      ax = gca;
      ax.FontSize = 14;
ylabel('position(deg.)');

legend('model', 'measured')
```